Angewandte Chemie
Eine Zeitschrift der Gesellschaft Deutscher Chemiker

Supporting Information

Light-Induced Mechanistic Divergence in Gold(I) Catalysis: Revisiting the Reactivity of Diazonium Salts

Svenja Taschinski, René Döpp, Martin Ackermann, Frank Rominger, Folkert de Vries, Maximilian F. S. J. Menger, Matthias Rudolph, A. Stephen K. Hashmi, and Johannes E. M. N. Klein**

anie_201908268_sm_miscellaneous_information.pdf

Table of contents

1) Experimental Section

1.1) General Remarks

Chemicals and Solvents

Chemicals and solvents were purchased from commercial suppliers (ABCR, Acros, Alfa Aesar, Chempur, Fluka, Fluorochem, Merck, Euriso-Top, BOOM and Sigma Aldrich) or obtained from the chemical store at the University of Heidelberg and the University of Groningen and used as delivered. Dry solvents were dispensed from a solvent purification system MB SPS-800 or obtained by using drying columns.[1]

Reactions

Reactions requiring inert conditions were carried out in heat-gun dried glassware under an atmosphere of nitrogen using standard Schlenk-techniques. For some reactions degassed solvents were used by sparging them with nitrogen for at least one hour.

NMR Spectroscopy (NMR)

NMR spectra were, if not mentioned otherwise, recorded at room temperature at the chemistry department of the University of Heidelberg on the following spectrometers: Bruker Avance-III-300, Bruker Avance DRX-300, Bruker Avance-III-500 and Bruker Avance-III-600 and at the University of Groningen on the following spectrometers: Varian Oxford 300, AgilentTech 400/54 Premium Shielded, Varian Oxford 500, Bruker Avance-Neo 600. Chemical shifts are given in ppm and coupling constants in Hz. ^{1}H and ^{13}C spectra were calibrated in relation to deuterated solvents, namely $CDCl_3$ (7.26 ppm; 77.16 ppm), CD_2Cl_2 (5.32 ppm; 53.84 ppm), DMSO-d^{6} (2.50 ppm; 39.52 ppm), CD_3CN (1.94 ppm; 118.26 ppm), $(CD_3)CO$ (2.05 ppm; 206.26 ppm).[2] ^{31}P spectra were calibrated in relation to the reference measurement of phosphoric acid (0.00 ppm). ^{19}F spectra were calibrated in relation to the reference measurement of 1,2-difluorobenzene (-139 ppm). The following abbreviations were used for ^{1}H NMR spectra to indicate the signal multiplicity: s (singlet), bs (broad singlet), d (doublet), t (triplet), q (quartet) and m (multiplet) as well as combinations of them. When combinations of multiplicities are given the first character noted refers to the biggest coupling constant. All ^{13}C NMR spectra were measured with ^{1}H-decoupling. The nature of the observed C atoms in these spectra is indicated as follows: [s (quaternary carbon), d (CH-group), t (CH_2-group), q (CH_3-group)] and were determined by DEPT135 spectra.

Mass Spectrometry (MS and HRMS)

Mass spectra were determined at the MS department of the University of Heidelberg and the Microanalytical Department of the University of Groningen.

Infrared Spectroscopy (IR)

Infrared spectra were recorded on an FT-IR spectrometer named Bruker LUMOS (Heidelberg) and JASCO FT/IR-4700 (Groningen). The method is denoted in brackets. For the most significant bands the wave number $\tilde{\nu}$ (cm^{-1}) is given.

Gas Chromatography / Mass Spectrometry (GC/MS)

GC/MS spectra were measured on the following hardware system:
Schimadzu GCMS-QP2010 Ultra Mass Selective Detector, coupled with a Schimadzu GC-2010 Plus gas chromatograph. As capillary column, an Agilent HP-5MS ((5%-Phenyl)-methylpolysiloxane, 30 m x 0.25 mm, 0.25 µm) was employed and helium was used as carrier gas.

Melting Points

Melting points were measured in open glass capillaries in a Büchi melting point apparatus and were not corrected.

Flash Column Chromatography

Flash column chromatography was accomplished using Silica gel 60 (0.04 - 0.063 mm/ 230 - 400 mesh ASTM) purchased from Macherey-Nagel, SiliaFlash® P60 (0.04 - 0.063 mm/ 230 - 400 mesh) purchased from Silicycle UltraPure Silica gels and aluminium oxide (activated, neutral, Brockmann Activity I) from Fluka. As eluents mixtures of petroleum ether (PE) and ethyl acetate (EA) or diethylether were used.

Analytical Thin Layer Chromatography (TLC)

Analytical Thin Layer Chromatography was carried out on precoated Merck TLC Silica Gel 60 F_{254} aluminium sheets or Merck TLC Aluminium oxide 60 F_{254} aluminium sheets. Components were visualized by observation under UV-light (λ = 254 nm or 366 nm) or by treatment with an acidic solution of anisaldehyde, basic solution of vanilin or an aqueous solution of $KMnO_4$.

Photo Reactor

The photo reactor has been designed according to a previously published standardized procedure.[3]

NMR Irradiation

The irradiation inside the NMR Spectrometer was done with a THORLABS M405FP1 Fiber-Coupled LED, with the nominal wavelength of 405 nm, bandwidth of 12 nm, minimum output 19.3 mW, 1400 mA and 3.45 V.

1.2) General Procedures

1.2.1) General Procedure A, Sonogashira-Coupling (GP A)

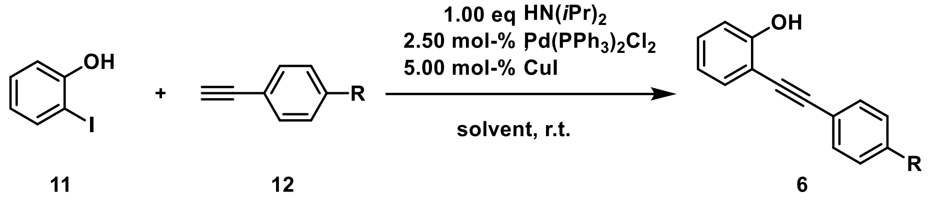

Sonogashira-coupling products were synthesized according to a modified procedure previously reported by Wegner and co-workers.[4]

To a heat-gun dried Schlenk tube under an atmosphere of nitrogen, 1.00 eq 2-iodophenol **11**, 5.00 mol-% copper(I) iodide, 2.50 mol-% $Pd(PPh_3)_2Cl_2$ and were dissolved in freshly degassed solvent. A small excess (1.20 eq) of alkyne **12** was added and the resulting mixture was stirred at room temperature until complete conversion was detected by TLC. The mixture was diluted with water and the phases were separated. The aqueous layer was extracted three times with ethylacetate, the combined organic layers were separated, dried over sodium sulfate and evaporated onto Celite®. The crude products **6** were purified by flash column chromatography.

1.2.2) General Procedure B, Synthesis of Diazonium Salts (GP B)

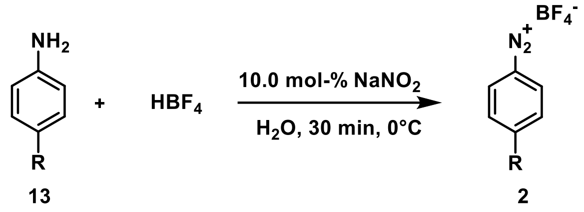

Diazonium salts were synthesized according to a modified procedure previously reported by Tóth and co-workers.[5]

Tetrafluoroboronic acid (48% in water, 2.60 eq) was dissolved in 4.00 mL water, aniline **13** (1.00 eq) was added at 0 °C and stirred for 30 minutes. A solution of sodium nitrite (1.00 eq) in 1.50 mL water was added dropwise and the resulting mixture was stirred for 30 minutes. The mixture was filtered and the residue was dissolved in a minimum amount of acetone and precipitated with diethylether. The products **2** were collected by filtration and washed with diethylether.

1.2.3) General Procedure C, Synthesis of Azobenzofurans (GP C)

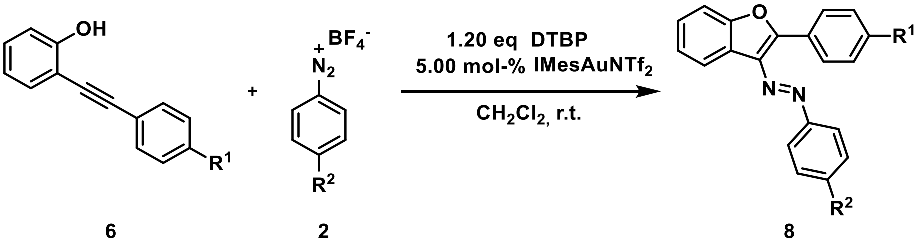

IMesAuNTf$_2$ (5.00 mol-%) and 2,6-di*tert*butylpyridine (1.20 eq) were dissolved in dichloromethane and stirred for ten minutes. Aryldiazonium tetrafluoroborate **2** (3.00 eq), molecular sieves (3 Å) and *o*-alkynylphenol **6** (1.00 eq) were added and the mixture was stirred for the mentioned time at room temperature. The mixture was evaporated onto Celite® and purified by flash column chromatography.

1.3) Synthesis of Substrates

1.3.1.1) 2-(4-Tolylethynyl)phenol

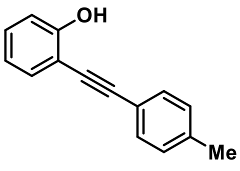

$\mathbf{6_{Me}}$

According to **GP A**: 2-Iodophenol **11** (2.00 g, 9.09 mmol, 1.00 eq) was dissolved in 50 mL THF, bis(triphenylphosphine)palladium(II) dichloride (160 mg, 227 µmol, 2.50 mol-%), copper iodide (86.6 mg, 455 µmol, 5.00 mol-%), diisopropylamine (1.28 mL, 920 mg, 9.09 mmol, 1.00 eq) and 1-ethynyl-4-methylbenzene $\mathbf{12_{Me}}$ (1.38 mL, 1.27 mg, 10.9 mmol, 1.20 eq) were added and the mixture was stirred at room temperature for 16 hours. Purification by flash column chromatography (SiO_2, PE/EA, 100:1) yielded the product $\mathbf{6_{Me}}$ (1.77 g, 8.50 mmol, 93%) as a light brown, crystalline solid.

R$_f$ (SiO_2, PE/EA, 10:1) = 0.42; ^{1}H NMR (299.95 MHz, CD_2Cl_2): δ = 2.38 (s, 3 H), 5.89 (s, 1 H), 6.88-6.99 (m, 2 H), 7.17-7.27 (m, 3 H), 7.40-7.48 (m, 3 H) ppm. The spectroscopic data matches previously reported data.[6]

1.3.1.2) 2-((4-Methoxyphenyl)ethynyl)phenol

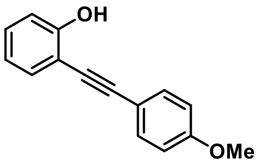

$\mathbf{6_{OMe}}$

According to **GP A**: 2-Iodophenol **11** (2.27 g, 10.3 mmol, 1.00 eq) was dissolved in 20 mL toluene, bis(triphenylphosphine)palladium(II) dichloride (181 mg, 258 µmol, 2.50 mol-%), copper iodide (98.3 mg, 516 µmol, 5.00 mol-%), diisopropylamine (1.46 mL, 1.04 g, 10.3 mmol, 1.00 eq) and 1-ethynyl-4-methoxybenzene $\mathbf{12_{OMe}}$ (1.47 mL, 1.50 g, 11.4 mmol, 1.10 eq) were added and the mixture was stirred at room temperature for four hours. Purification by flash column chromatography (SiO_2, PE/EA, 50:1) yielded the product $\mathbf{6_{OMe}}$ (1.67 g, 7.45 mmol, 72%) as a light yellow solid.

R$_f$ (SiO_2, PE/EA, 10:1) = 0.26; ^{1}H NMR (300.51 MHz, CD_2Cl_2): δ = 3.83 (s, 3 H), 5.87 (bs, 1 H), 6.88-6.97 (m, 4 H), 7.23-7.29 (m, 1 H), 7.41 (dd, *J* = 7.68 Hz, *J* = 1.46 Hz, 1 H), 7.50 (dt, *J* = 8.93 Hz, *J* = 2.16 Hz, 2 H) ppm. The spectroscopic data matches previously reported data.[7]

1.3.1.3) 2-(Phenylethynyl)phenol

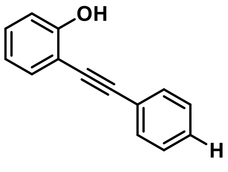

6_H

According to **GP A**: 2-Iodophenol **11** (2.27 g, 10.3 mmol, 1.00 eq) was dissolved in 20 mL toluene, bis(triphenylphosphine)palladium(II) dichloride (181 mg, 258 µmol, 2.50 mol-%), copper iodide (98.3 mg, 516 µmol, 5.00 mol-%), diisopropylamine (1.46 mL, 1.04 mg, 10.3 mmol, 1.00 eq) and phenylactelylene **12_H** (1.18 mL, 1.16 g, 11.4 mmol, 1.10 eq) were added and the mixture was stirred at room temperature for four hours. Purification by flash column chromatography (SiO_2, PE/EA, 100:1 -> 50:1) yielded the product **6_H** (1.95 g, 10.0 mmol, 97%) as a light yellow solid.

R_f (SiO_2, PE/EA, 10:1) = 0.44; ^1H NMR (300.51 MHz, CD_2Cl_2): δ = 5.88 (s, 1 H), 6.90-6.99 (m, 2 H), 7.25-7.32 (m, 1 H), 7.36-7.46 (m, 4 H), 7.53-7.60 (m, 2 H) ppm. The spectroscopic data matches previously reported data.[8]

1.3.1.4) 2-((4-Fluorophenyl)ethynyl)phenol

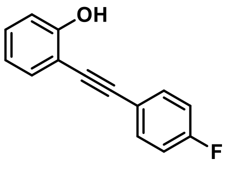

6_F

According to **GP A**: 2-Iodophenol **11** (1.20 g, 5.45 mmol, 1.00 eq) was dissolved in 20 mL toluene, bis(triphenylphosphine)palladium(II) dichloride (95.7 mg, 136 µmol, 2.50 mol-%), copper iodide (51.9 mg, 273 µmol, 5.00 mol-%), diisopropylamine (770 µL, 552 mg, 5.45 mmol, 1.00 eq) and 1-ethynyl-4-fluorobenzene **12_F** (688 µL, 721 mg, 6.00 mmol, 1.10 eq) were added and the mixture was stirred at room temperature for three hours. Purification by flash column chromatography (SiO_2, PE/EA, 50:1) yielded the product **6_F** (902 mg, 4.25 mmol, 78%) as a light brown, crystalline solid.

R_f (SiO_2, PE/EA, 4:1) = 0.57; ^1H NMR (300.51 MHz, $CDCl_3$): δ = 5.76 (s, 1 H), 6.91 (dt, J = 7.62 Hz, J = 1.05 Hz, 1 H), 6.97 (dd, J = 7.62 Hz, J = 0.66 Hz, 1 H), 7.08 (tt, J = 8.71 Hz, J = 2.79 Hz, 2 H), 7.25-7.31 (m, 1 H), 7.41 (dd, J = 7.62 Hz, J = 1.59 Hz, 1 H), 7.50-7.57 (m, 2 H) ppm; ^{19}F NMR (282.76 MHz, $CDCl_3$): δ = -109.89 (s) ppm. The spectroscopic data matches previously reported data.[4]

1.3.1.5) Benzenediazonium tetrafluoroborate

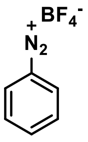

$\mathbf{2_H}$

According to **GP B**: Tetrafluoroboronic acid (48% in water, 5.55 mL, 7.66 g, 41.9 mmol, 2.60 eq) was dissolved in 10.0 mL water, aniline $\mathbf{13_H}$ (1.47 mL, 1.50 g, 16.1 mmol, 1.00 eq) was added at 0 °C and stirred for 60 minutes. A solution of sodium nitrite (1.11 g, 16.1 mmol, 1.00 eq) in 2.00 mL water was added dropwise and the resulting mixture was stirred for 60 minutes. The product $\mathbf{2_H}$ (2.35 g, 12.3 mmol, 76%) was isolated as a colorless solid.

^{1}H NMR (299.95 MHz, CD_3CN): δ = 7.90-7.99 (m, 2 H), 8.40 (tt, *J* = 8.08 Hz, *J* = 1.22 Hz, 1 H), 8.44-8.51 (m, 2 H) ppm; ^{19}F NMR (282.21 MHz, CD_3CN): δ = -151.73 (s, 4 F) ppm. The spectroscopic data matches previously reported data.[5]

1.3.1.6) 4-Methylbenzenediazonium tetrafluoroborate

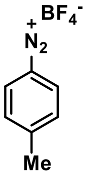

$\mathbf{2_{Me}}$

According to **GP B**: Tetrafluoroboronic acid (48% in water, 3.45 mL, 4.76 g, 26.0 mmol, 2.60 eq), 4-methylaniline $\mathbf{13_{Me}}$ (1.07 g, 10.0 mmol, 1.00 eq), sodium nitrite (690 mg, 10.0 mmol, 1.00 eq). The product $\mathbf{2_{Me}}$ (342 mg, 1.66 mmol, 17%) was isolated as a light purple crystalline solid.

^{1}H NMR (399.82 MHz, DMSO-d^6): δ = 2.58 (s, 3 H), 7.80 (d, *J* = 8.34 Hz, 2 H), 8.55 (d, *J* = 8.34 Hz, 2 H) ppm; ^{19}F NMR (376.17 MHz, DMSO-d^6): δ = -148.32 (s, 4 F) ppm. The spectroscopic data matches previously reported data.[9]

1.3.1.7) 4-Methoxybenzenediazonium tetrafluoroborate

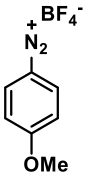

$\mathbf{2_{OMe}}$

According to **GP B**: Tetrafluoroboronic acid (48% in water, 3.45 mL, 4.76 g, 26.0 mmol, 2.60eq), 4-methoxyaniline $\mathbf{13_{OMe}}$ (1.23 g, 10.0 mmol, 1.00 eq), sodium nitrite (690 mg, 10.0 mmol, 1.00 eq). The product $\mathbf{2_{OMe}}$ (745 mg, 3.36 mmol, 34%) was isolated as a light purple, crystalline solid.

^{1}H NMR (399.82 MHz, DMSO-d^6): δ = 4.04 (d, *J* = 1.14 Hz, 3 H), 7.48 (dd, *J* = 9.25 Hz, *J* = 1.21 Hz, 2 H), 8.58-8.64 (m, 2 H) ppm; ^{19}F NMR (376.17 MHz, DMSO-d^6): δ = -148.33 (s, 4 F) ppm. The spectroscopic data matches previously reported data.[9]

1.3.1.8) 4-Fluorobenzenediazonium tetrafluoroborate

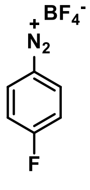

2_F

According to **GP B**: Tetrafluoroboronic acid (48% in water, 3.50 mL, 4.76 g, 26.0 mmol, 2.60 eq), 4-fluoroaniline **13_F** (1.11 g, 10.0 mmol, 1.00 eq), sodium nitrite (690 mg, 10.0 mmol, 1.00 eq). The product **2_F** (416 mg, 1.98 mmol, 20%) was collected by filtration as a light yellow, crystalline solid.

^{1}H NMR (300.51 MHz, $(CD_3)_2CO$): δ = 7.88-7.94 (m, 2 H), 8.99-9.03 (m, 2 H) ppm; ^{19}F NMR (282.76 MHz, $(CD_3)_2CO$): δ = -86.63 (s, 1 F), -151.09 (s, 4 F) ppm. The spectroscopic data matches previously reported data.[10]

1.3.1.9) 4-Nitrobenzenediazonium tetrafluoroborate

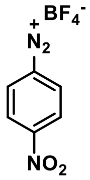

2_{NO_2}

According to **GP B**: Tetrafluoroboronic acid (48% in water, 3.50 mL, 4.76 g, 26.0 mmol, 2.60 eq), 4-nitroaniline **13_{NO_2}** (1.11 g, 10.0 mmol, 1.00 eq), sodium nitrite (690 mg, 10.0 mmol, 1.00 eq). The product **2_{NO_2}** (1.37 g, 5.78 mmol, 58%) was collected by filtration as a light yellow, crystalline solid.

^{1}H NMR (399.82 MHz, DMSO-d^6): δ = 8.72 (d, J = 8.89 Hz, 2 H), 8.93 (d, J = 8.89, 2 H) ppm; ^{19}F NMR (376.17 MHz, DMSO-d^6): δ = -148.32 (s, 4 F) ppm. The spectroscopic data matches previously reported data.[11]

1.4) Gold-Catalyzed Reactions

1.4.1) General Procedure for Reaction Screening, Arylated Benzofuran

The formation of substituted benzofuran **7**$_{\mathbf{Me}}$ was determined *via* GC MS analysis, according to the following procedure using hexamethylbenzene as internal standard.

Base (200 µmol), diazonium salt (200 µmol) and hexamethylbenzene (100 µmol) were dissolved in 500 µL stock solution of alkyne (200 µmol/mL), 100 µL of a stock solution of catalyst (10.0 µmol/mL in dichloromethane) and 400 µL addition solvent were added. The mixture was stirred at room temperature under irradiation with blue LED (450 nm) for two hours. The mixture was filled up to 5.00 mL and an aliquot was taken for GC MS analysis. The yields were determined *via* internal standard and the response factor was determined with an external five-point calibration curve. All reactions were carried out in duplicate and the averages are given unless specified.

Entry	Catalyst Base	Yield **7**$_{\mathbf{Me}}$ [%] Irradiation with blue-LED		
	Solvent	MeCN	MeCN	MeCN
		A	B	Average
1	Ph$_3$PAuCl NaHCO$_3$	44(a)	48(a)	46(b)
2	Ph$_3$PAuNTf$_2$ NaHCO$_3$	55(a)	53(a)	54(c)
3	Ph$_3$PAuCl DTBP	4	4	4
4	Ph$_3$PAuNTf$_2$ DTBP	8	13	11

(a) Full conversion of starting material. (b) Average yield side-product **10**: 7%. (c) Average yield side-product **10**: 25%.

1.4.2) General Procedure for Reaction Screening, Azobenzofuran

The formation of azobenzofuran $\mathbf{8_{Me}}$ was determined and quantified by ^{1}H NMR spectroscopy, according to the following procedure using benzylacetate as internal standard.

Base (100 µmol) and diazonium salt (100 µmol) were dissolved in 100 µL of a stock solution of catalyst (25.0 µmol/mL in dichloromethane) and molecular sieves (3 Å) was added. 400 µL stock solution of alkyne (125 µmol/mL) was added and the mixture was stirred for 24 hours at room temperature. The solvents were evaporated and the crude product was dried at the Schlenk line. The solid was dissolved in 600 µL $CDCl_3$ and treated with 7.00 µL of benzylacetate. The yields were determinated *via* ^{1}H NMR spectroscopy. If not mentioned otherwise, all reactions were carried out in duplicate and the averages are given unless specified.

Entry	Catalyst Base	Yield $\mathbf{8_{Me}}$ [%] No irradiation					
	Solvent	CH_2Cl_2			MeCN		
		A	**B**	**Average**	**A**	**B**	**Average**
1	Ph_3PAuCl $NaHCO_3$	5	5	5	6	9	7
2	$Ph_3PAuNTf_2$ $NaHCO_3$	22$^{(a)}$	23$^{(a)}$	22	12	10	11
3	Ph_3PAuCl DTBP	Not observed	Not observed	Not observed	Not observed	Not observed	Not observed
4	$Ph_3PAuNTf_2$ DTBP	15	23	19	21	26	23
5	$IMesAuNTf_2$ 2.00 eq $NaHCO_3$	10$^{(a)}$	10$^{(a)}$	10	20	25	22
6	$IMesAuNTf_2$ 2.00 eq DTBP	66	70	68	16	19	17
7	$IMesAuNTf_2$ 1.20 eq DTBP	59$^{(b)}$	67$^{(b)}$	63	-	-	-
8	$IMesAuNTf_2$ 1.20 eq DTBP	64$^{(c)}$	67$^{(d)}$	-	-	-	-

(a) Full conversion of starting material. (b) Full conversion of starting material after 48 hours. (c) Single run, 150 µmol (3 equiv.) $\mathbf{2_H}$ were used. (d) Single run, 200 µmol (4 equiv.) $\mathbf{2_H}$ were used.

1.4.3) Gold-Catalyzed Reactions, Scope of Reaction

1.4.3.1) (*E*)-1-(2-(4-Methoxyphenyl)benzofuran-3-yl)-2-phenyldiazene

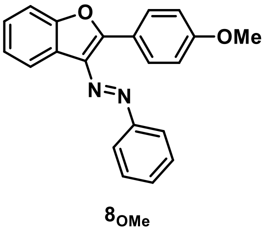
8$_{OMe}$

According to **GP C**, 2-((4-methoxyphenyl)ethynyl)phenol **6$_{OMe}$** (56.1 mg, 250 µmol, 1.00 eq) and 2,6-di*tert*butylpyridine (67.4 µL, 57.4 mg, 300 µmol, 1.20 eq) were dissolved in 2.00 mL dichloromethane and stirred at room temperature for ten minutes. Benzenediazonium tetrafluoroborate **2$_H$** (144 mg, 750 µmol, 3.00 eq) and IMesAuNTf$_2$ (9.77 mg, 12.5 µmol, 5.00 mol-%) were added and the mixture was stirred at room temperature for 16 hours. The mixture was evaporated onto Celite® and purification by flash column chromatography (Al$_2$O$_3$, PE/Et$_2$O 200:1) yielded the product **8$_{OMe}$** (72.3 mg, 220 µmol, 88%) as an orange, crystalline solid.

M.p.: 149 °C; R_f (SiO$_2$, PE/EA, 10:1) = 0.40; IR(ATR): $\tilde{\nu}$ = 686, 745, 770, 783, 836, 934, 1010, 1022, 1075, 1105, 1175, 1205, 1247, 1304, 1411, 1422, 1448, 1502, 1580, 1604, 1742, 1938, 2033, 2839, 2965, 3030, 3065, 3083 cm^{-1}; UV (λ = 242 nm in CH$_2$Cl$_2$): log ε = 3.87; ^{1}H NMR (300.51 MHz, CDCl$_3$): δ = 3.92 (s, 3 H), 7.08 (td, *J* = 9.07 Hz, *J* = 2.10 Hz, 2 H), 7.33-7.39 (m, 2 H), 7.43-7.47 (m, 1 H), 7.51-7.56 (m, 3 H), 7.93-7.96 (m, 2 H), 8.40 (td, *J* = 9.07 Hz, *J* = 2.10 Hz, 2 H), 8.44-8.48 (m, 1 H) ppm; ^{13}C NMR (100.66 MHz, CDCl$_3$): δ = 55.59 (q), 111.09 (d), 114.49 (d, 2 C), 121.58 (s), 122.64 (d, 2 C), 122.66 (s), 124.01 (d), 124.81 (d), 125.84 (d), 129.25 (d, 2 C), 130.16 (d), 130.46 (d, 2 C), 133.79 (s), 153.79 (s), 154.01 (s), 157.74 (s), 161.43 (s) ppm; HR-DART (+) C$_{21}$H$_{17}$N$_2$O$_2$ [M+H]$^+$: calcd. 329.1276, found 329.1285.

1.4.3.2) (*E*)-1-Phenyl-2-(2-(*p*-tolyl)benzofuran-3-yl)diazene

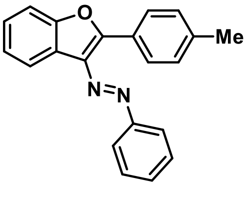
8$_{Me}$

According to **GP C**, 2-(*p*-tolylethynyl)phenol **6$_{Me}$** (52.1 mg, 250 µmol, 1.00 eq) and 2,6-di*tert*butylpyridine (67.4 µL, 57.4 mg, 300 µmol, 1.20 eq) were dissolved in 2.00 mL dichloromethane and stirred at room temperature for ten minutes. Benzenediazonium tetrafluoroborate **2$_H$** (144 mg, 750 µmol, 3.00 eq) and IMesAuNTf$_2$ (9.77 mg, 12.5 µmol, 5.00 mol-%) were added and the mixture was stirred at room temperature for 27 hours. The mixture was evaporated onto Celite® and purification by flash column chromatography (Al$_2$O$_3$, PE/Et$_2$O, 200:1) yielded the desired product **8$_{Me}$** (60.9 mg, 195 µmol, 78%) as an orange, crystalline solid.

M.p.: 137 °C; R_f (SiO$_2$, PE/EA, 10:1) = 0.73; IR(ATR): $\tilde{\nu}$ = 609, 617, 634, 670, 689, 716, 743, 774, 825, 874, 934, 1017, 1077, 1145, 1201, 1252, 1289, 1304, 1347, 1372, 1410, 1450, 1475, 1504, 1552, 1577, 1608, 1784, 1898, 1921, 2855, 2924, 3032, 3065 cm^{-1}; UV (λ = 295 nm in CH_2Cl_2): log ε = 4.43; ^{1}H NMR (300.51 MHz, $CDCl_3$): δ = 2.46 (bs, 3 H), 7.34-7.41 (m, 4 H), 7.44-7.48 (m, 1 H), 7.53-7.57 (m, 3 H), 7.95-7.97 (m, 2 H), 8.32-8.34 (m, 2 H), 8.46-8.48 (m, 1 H) ppm; ^{13}C NMR (100.66 MHz, $CDCl_3$): δ = 21.73 (q), 111.22 (d), 121.47 (s), 122.71 (d, 2 C), 124.13 (d), 124.85 (d), 126.03 (d), 127.17 (s), 128.76 (d, 2 C), 129.26 (d, 2 C), 129.65 (d, 2 C), 130.30 (d), 134.32 (s), 140.52 (s), 153.89 (s), 153.96 (s), 157.77 (s) ppm; HRMS (EI (+), 70 eV) $C_{21}H_{16}N_2O$ $[M]^+$: calcd. 312.12571, found 312.12462.

1.4.3.3) (*E*)-1-Phenyl-2-(2-phenylbenzofuran-3-yl)diazene

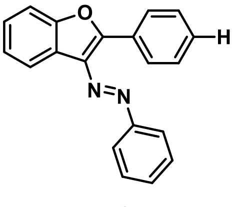

8$_H$

According to **GP C**, 2-(phenylethynyl)phenol **6$_H$** (48.6 mg, 250 µmol, 1.00 eq) and 2,6-di*tert*butylpyridine (67.4 µL, 57.4 mg, 300 µmol, 1.20 eq) were dissolved in 2.00 mL dichloromethane and stirred at room temperature for ten minutes. Benzenediazonium tetrafluoroborate **2$_H$** (144 mg, 750 µmol, 3.00 eq) and IMesAuNTf$_2$ (9.77 mg, 12.5 µmol, 5.00 mol-%) were added and the mixture was stirred at room temperature for 168 hours. The mixture was evaporated onto Celite® and purification by flash column chromatography (Al_2O_3, PE/Et_2O, 200:1) yielded the desired product **8$_H$** (16.5 mg, 55.3 µmol, 22%) as an orange, crystalline solid.

M.p.: 121 °C; R_f (SiO$_2$, PE/EA, 10:1) = 0.76; IR(ATR): $\tilde{\nu}$ = 620, 663, 689, 745, 773, 934, 1029, 1070, 1109, 1141, 1204, 1288, 1343, 1372, 1412, 1439, 1455, 1475, 1490, 1552 cm^{-1}; UV (λ = 294 nm in CH_2Cl_2): log ε = 4.36; ^{1}H NMR (300.51 MHz, $CDCl_3$): δ = 7.39 (dt, *J* = 7.51 Hz, *J* = 1.92 Hz, 2 H), 7.45-7.51 (m, 2 H), 7.54-7.58 (m, 5 H), 7.96-7.99 (m, 2 H), 8.42-8.49 (m, 3 H) ppm; ^{13}C NMR (100.66 MHz, $CDCl_3$): δ = 111.28 (d), 121.38 (s), 122.76 (d, 2 C), 124.26 (d), 124.93 (d), 126.23 (d), 128.80 (d, 2 C), 128.86 (d, 2 C), 129.29 (d, 2 C), 129.94 (s), 130.08 (d), 130.47 (d), 134.72 (s), 153.91 (s), 153.98 (s), 157.30 (s) ppm; HRMS (EI (+), 70 eV) $C_{20}H_{14}N_2O$ $[M]^+$: calcd. 298.11006, found 298.11001.

1.4.3.4) (*E*)-1-(2-(4-Fluorophenyl)benzofuran-3-yl)-2-phenyldiazene

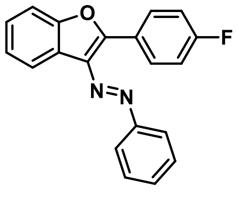

8$_{\mathrm{F}}$

According to **GP C**, 2-((4-fluorophenyl)ethynyl)phenol **6**$_{\mathrm{F}}$ (53.1 mg, 250 µmol, 1.00 eq) and 2,6-di*tert*butylpyridine (67.4 µL, 57.4 mg, 300 µmol, 1.20 eq) were dissolved in 2.00 mL dichloromethane and stirred at room temperature for ten minutes. Benzenediazonium tetrafluoroborate **2**$_{\mathrm{F}}$ (144 mg, 750 µmol, 3.00 eq) and IMesAuNTf$_2$ (9.77 mg, 12.5 µmol, 5.00 mol-%) were added and the mixture was stirred at room temperature for 21 days. The mixture was evaporated onto Celite® and purification by flash column chromatography (Al_2O_3, PE/Et_2O, 200:1) yielded the desired product **8**$_{\mathrm{F}}$ (26.0 mg, 82.2 µmol, 33%) as an orange, crystalline solid.

M.p.: 142 °C; R$_f$ (SiO_2, PE/EA, 10:1) = 0.71; IR(ATR): $\tilde{\nu}$ = 689, 746, 771, 797, 839, 936, 1017, 1076, 1102, 1160, 1201, 1232, 1286, 1370, 1411, 1450, 1477, 1500, 1556, 1598 cm^{-1}; UV (λ = 292 nm in CH_2Cl_2): log ε = 4.42; ^{1}H NMR (300.51 MHz, $CDCl_3$): δ = 7.24-7.26 (m, 2 H), 7.37 (dt, *J* = 7.56 Hz, *J* = 0.93 Hz, 1 H), 7.40 (dt, *J* = 7.56 Hz, *J* = 0.93 Hz, 1 H), 7.46-7.49 (m, 1 H), 7.54-7.57 (m, 3 H), 7.94-7.96 (m, 2 H), 8.43-8.48 (m, 3 H) ppm; ^{13}C NMR (150.93 MHz, $CDCl_3$): δ = 111.24 (d), 116.12 (d, d, *J* = 22.0 Hz, 2 C), 121.29 (s), 122.70 (d, 2 C), 124.22 (d), 125.02 (d), 126.22 (s, d, *J* = 22.0 Hz), 126.28 (d), 129.23 (d, 2 C), 130.56 (d), 130.77 (d, d, *J* = 8.45 Hz, 2 C), 134.40 (s, d, *J* = 1.31 Hz), 153.83 (s, d, *J* = 7.12 Hz), 156.35 (s), 164.03 (s, d, *J* = 252 Hz) ppm; ^{19}F NMR (282.76 MHz, $CDCl_3$): δ = -109.80 (s) ppm; HRMS (EI (+), 70 eV) $C_{20}H_{13}N_2OF$ [M]$^+$: calcd. 316.10064, found 316.10073.

1.4.3.5) (*E*)-1-(4-Methoxyphenyl)-2-(2-(*p*-tolyl)benzofuran-3-yl)diazene

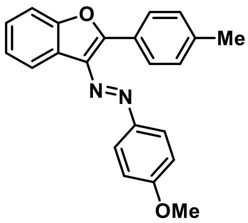

8$_{\mathrm{Me,OMe}}$

According to **GP C**, 2-(*p*-tolylethynyl)phenol **6**$_{\mathrm{Me}}$ (52.1 mg, 250 µmol, 1.00 eq) and 2,6-di*tert*butylpyridine (67.4 µL, 57.4 mg, 300 µmol, 1.20 eq) were dissolved in 2.00 mL dichloromethane and stirred at room temperature for ten minutes. *p*-Methoxybenzenediazonium tetrafluoroborate **2**$_{\mathrm{OMe}}$ (166 mg, 750 µmol, 3.00 eq) and IMesAuNTf$_2$ (9.77 mg, 12.5 µmol, 5.00 mol-%) were added and the mixture was stirred at room temperature for 48 hours. The mixture was evaporated onto Celite® and purification by flash column chromatography (Al_2O_3, PE/Et_2O, 100:1) yielded the desired product **8**$_{\mathrm{Me,OMe}}$ (33.0 mg, 96.4 µmol, 39%) as an orange, crystalline solid.

M.p.: 144 °C; R_f (SiO$_2$, PE/EA, 10:1) = 0.57; IR(ATR): $\tilde{\nu}$ = 608, 618, 639, 661, 715, 744, 758, 799, 820, 836, 933, 970, 1007, 1023, 1075, 1101, 1135, 1155, 1182, 1202, 1245, 1286, 1292, 1310, 1320, 1339, 1346, 1375, 1400, 1413, 1436, 1446, 1458, 1472, 1496, 1551, 1578, 1601, 2835, 2852, 2921, 2960, 3002, 3022, 3045, 3077 cm^{-1}; ^{1}H NMR (600.13 MHz, CDCl$_3$): δ = 2.46 (s, 3 H), 3.92 (s, 3 H), 7.01-7.08 (m, 2 H), 7.31-7.39 (m, 4 H), 7.53 (dt, J = 8.19 Hz, J = 0.84 Hz, 1 H), 7.91-7.98 (m, 2 H), 8.29-8.34 (m, 2 H), 8.44-8.48 (m, 1 H) ppm; ^{13}C NMR (150.91 MHz, CDCl$_3$): δ = 21.71 (q), 55.75 (q), 111.17 (d), 114.44 (d, 2 C), 121.74 (s), 124.14 (d), 124.40 (d, 2 C), 124.63 (d), 125.87 (d), 127.37 (s), 128.57 (d, 2 C), 129.60 (d, 2 C), 134.13 (s), 140.17 (s), 148.38 (s), 153.87 (s), 156.62 (s), 161.62 (s) ppm; HRMS (ESI (+) $C_{22}H_{19}N_2O_2$ [M+H]$^+$: calcd. 343.14410, found 343.14438.

1.4.3.6) (*E*)-1-(*p*-Tolyl)-2-(2-(*p*-tolyl)benzofuran-3-yl)diazene

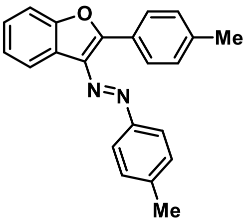

8$_{\mathbf{Me,Me}}$

According to **GP C**, 2-(*p*-tolylethynyl)phenol **6$_{\mathbf{Me}}$** (52.1 mg, 250 µmol, 1.00 eq) and 2,6-di*tert*butylpyridine (67.4 µL, 57.4 mg, 300 µmol, 1.20 eq) were dissolved in 2.00 mL dichloromethane and stirred at room temperature for ten minutes. *p*-Tolyldiazonium tetrafluoroborate **2$_{\mathbf{Me}}$** (154 mg, 750 µmol, 3.00 eq) and IMesAuNTf$_2$ (9.77 mg, 12.5 µmol, 5.00 mol-%) were added and the mixture was stirred at room temperature for 27 hours. The mixture was evaporated onto Celite® and purification by flash column chromatography (Al$_2$O$_3$, PE/Et$_2$O, 200:1) yielded the desired product **8$_{\mathbf{Me,Me}}$** (56.3 mg, 172 µmol, 69%) as an orange, crystalline solid.

M.p.: 135 °C; R_f (SiO$_2$, PE/EA, 10:1) = 0.66; IR(ATR): $\tilde{\nu}$ = 609, 662, 741, 757, 819, 875, 934, 1011, 1021, 1036, 1075, 1104, 1141, 1160, 1186, 1203, 1253, 1289, 1372, 1449, 1474, 1504, 1552, 1577, 1601, 2919, 3037, 3059, 3081 cm^{-1}; UV (λ = 298 nm in CH$_2$Cl$_2$): log ε =4.59; ^{1}H NMR (300.51 MHz, CDCl$_3$): δ = 2.46 (bs, 6 H), 7.32-7.40 (m, 6 H), 7.52-7.55 (m, 1 H), 7.87 (td, J = 8.29 Hz, J = 1.82 Hz, 2 H), 8.32 (td, J = 8.29 Hz, J = 1.82 Hz, 2 H), 8.45-8.48 (m, 1 H) ppm; ^{13}C NMR (100.66 MHz, CDCl$_3$): δ = 21.65 (q), 21.72 (q), 111.17 (d), 121.61 (s), 122.67 (d, 2 C), 124.13 (d), 124.74 (d), 125.95 (d), 127.29 (s), 128.68 (d, 2 C), 129.62 (d, 2 C), 129.93 (d, 2 C), 134.24 (s), 140.35 (s), 140.77 (s), 152.10 (s), 153.89 (s), 157.23 (s) ppm; HRMS (EI (+), 70 eV) $C_{22}H_{18}N_2O$ [M]$^+$: calcd. 326.14136, found 326.13978.

1.4.3.7) (*E*)-1-(4-Fluorophenyl)-2-(2-(*p*-tolyl)benzofuran-3-yl)diazene

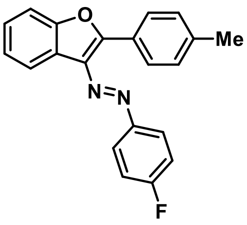

8$_{\mathrm{Me,F}}$

According to **GP C**, 2-(*p*-tolylethynyl)phenol **6$_{\mathrm{Me}}$** (52.1 mg, 250 µmol, 1.00 eq) and 2,6-di*tert*butylpyridine (67.4 µL, 57.4 mg, 300 µmol, 1.20 eq) were dissolved in 2.00 mL dichloromethane and stirred at room temperature for ten minutes. *p*-Fluorobenzenediazonium tetrafluoroborate **2$_{\mathrm{F}}$** (157 mg, 750 µmol, 3.00 eq) and IMesAuNTf$_2$ (9.77 mg, 12.5 µmol, 5.00 mol-%) were added and the mixture was stirred at room temperature for 48 hours. The mixture was evaporated onto Celite® and purification by flash column chromatography (Al_2O_3, PE/Et_2O, 200:1) yielded the desired product **8$_{\mathrm{Me,F}}$** (48.7 mg, 147 µmol, 59%) as an orange, crystalline solid.

M.p.: 156 °C; R$_f$ (SiO_2, PE/EA, 10:1) = 0.66; IR(ATR): $\tilde{\nu}$ = 609, 636, 663, 746, 820, 839, 875, 935, 1007, 1023, 1076, 1090, 1105, 1135, 1151, 1192, 1205, 1226, 1287, 1342, 1375, 1434, 1449, 1474, 1494, 1553, 1578, 1591, 1738, 1897, 2921, 3037 cm^{-1}; UV (λ = 296 nm in CH_2Cl_2): log ε = 4.40; ^{1}H NMR (300.51 MHz, $CDCl_3$): δ = 2.46 (bs, 3 H), 7.19-7.25 (m, 2 H), 7.33-7.41 (m, 4 H), 7.53-7.56 (m, 1 H), 7.93-7.98 (m, 2 H), 8.43 (td, *J* = 8.37 Hz, *J* = 1.60 Hz, 2 H), 8.42-8.44 (m, 1 H) ppm; ^{13}C NMR (100.66 MHz, $CDCl_3$): δ = 21.73 (q), 111.25 (d), 116.09 (d), 116.31 (d), 121.42 (s), 124.04 (d), 124.45 (d), 124.70 (d, d, *J* = 40.6 Hz, 2 C), 126.10 (d), 127.12 (s), 128.74 (d, 2 C), 129.68 (d, 2 C), 134.17 (s), 140.61 (s), 150.52 (s, d, *J* = 3.17 Hz), 153.89 (s), 157.80 (s), 164.04 (s, d, *J* = 251 Hz) ppm; ^{19}F NMR (282.76 MHz, $CDCl_3$): δ = -110.70 (s) ppm; HRMS (EI (+), 70 eV) $C_{21}H_{15}FN_2O$ [M]$^+$: calcd. 330.11629, found 330.11684.

1.4.3.8) 3-Phenyl-2-(*p*-tolyl)benzofuran

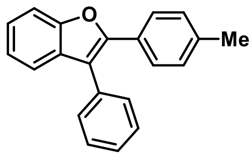

7$_{\mathrm{Me}}$

Ph_3PAuCl (9.89 mg, 20.0 µmol, 10.0 mol-%), $NaHCO_3$ (33.6 mg, 400 µmol, 2.00 eq), benzenediazonium tetrafluoroborate **2$_{\mathrm{H}}$** (76.8 mg, 400 µmol, 2.00 eq) and *o*-(*p*-tolylethynyl)phenol **6$_{\mathrm{Me}}$** (41.7 mg, 200 µmol, 1.00 eq) were dissolved in 2.00 mL acetonitrile and the mixture was stirred for two hours under blue-LED irradiation (450 nm) at room temperature. The mixture was evaporated onto Celite® and purification by flash column chromatography (SiO_2, PE) yielded the product **7$_{\mathrm{Me}}$** (36.5 mg, 128 µmol, 64%) as a colorless solid (5.00 mol% catalyst: 29.0 mg, 102 µmol, 51%).

R$_f$ (SiO_2, PE) = 0.30; ^{1}H NMR (399.82 MHz, $CDCl_3$): δ = 2.35 (s, 3 H), 7.13 (d, *J* = 7.97 Hz, 2 H), 7.23 (td, *J* = 7.46 Hz, *J* = 1.06 Hz, 1 H), 7.29-7.35 (m, 1 H), 7.37-7.57 (m, 9 H) ppm. Its spectroscopic data matches with previously reported data.[12]

1.4.3.9) 2,3-Di-*p*-tolylbenzofuran

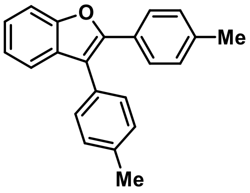

$\mathbf{7_{Me,Me}}$

Ph_3PAuCl (5.0 mg, 10.1 µmol, 5.05 mol-%), $NaHCO_3$ (33.5 mg, 399 µmol, 1.99 eq), 4-tolyldiazonium tetrafluoroborate $\mathbf{2_{Me}}$ (82.4 mg, 400 µmol, 2.00 eq) and *o*-(*p*-tolylethynyl)phenol $\mathbf{6_{Me}}$ (41.7 mg, 200 µmol, 1.00 eq) were dissolved in 1.00 mL acetonitrile and the mixture was stirred for two hours under blue-LED irradiation (450 nm) at room temperature. Reaction control *via* TLC-plate showed starting material left. Therefore the mixture was again irradiated with 450 nm blue LED for two hours at room temperature. The mixture was evaporated onto Celite® and purification by flash column chromatography (SiO_2, PE) yielded the product $\mathbf{7_{Me,Me}}$ (27.6 mg, 92.5 µmol, 46%) as a colorless solid.

R_f (SiO_2, PE) = 0.24; ^{1}H NMR (399.82 MHz, $CDCl_3$): δ = 2.33 (s, 3 H), 2.42 (s, 3 H), 7.11 (d, *J* = 7.95 Hz, 2 H), 7.16-7.33 (m, 4 H), 7.34-7.40 (m, 2 H, 7.43-7.49 (m, 1 H), 7.50-7.58 (m, 3 H) ppm. Its spectroscopic data matches with previously reported data.[13]

1.4.3.10) 3-(4-Fluorophenyl)-2-(*p*-tolyl)benzofuran

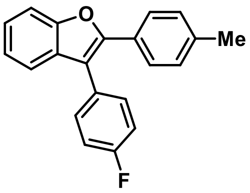

$\mathbf{8_{Me,F}}$

Ph_3PAuCl (5.0 mg, 10.1 µmol, 5.05 mol-%), $NaHCO_3$ (33.5 mg, 399 µmol, 1.99 eq), 4-fluorobenzenediazonium tetrafluoroborate $\mathbf{2_{F}}$ (82.4 mg, 393 µmol, 1.96 eq) and *o*-(*p*-tolylethynyl)phenol $\mathbf{6_{Me}}$ (41.6 mg, 200 µmol, 1.00 eq) were dissolved in 1.00 mL acetonitrile and the mixture was stirred for two hours under blue-LED irradiation (450 nm) at room temperature. The mixture was evaporated onto Celite® and purification by flash column chromatography (SiO_2, PE) yielded the product $\mathbf{8_{Me,F}}$ (31.8 mg, 105 µmol, 53%) as a colorless solid.

R_f (SiO_2, PE) = 0.33; ^{1}H NMR (399.82 MHz, $CDCl_3$): δ = 2.36 (s, 3 H), 7.12-7.19 (m, 4 H), 7.22-7.26 (m, 1 H), 7.33 (ddd, *J* = 8.26 Hz, *J* = 7.20 Hz, *J* = 1.35 Hz, 1 H), 7.42-7.50 (m, 3 H), 7.50-7.57 (m, 3 H) ppm; ^{19}F NMR (376.17 MHz, $CDCl_3$): δ = -114.45 (s) ppm. Its spectroscopic data matches with previously reported data.[14]

1.4.3.11) 3-(4-Nitrophenyl)-2-(*p*-tolyl)benzofuran

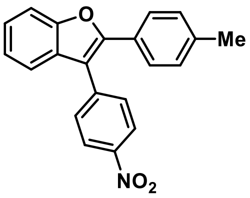

$\mathbf{8_{Me,NO_2}}$

Ph_3PAuCl (5.0 mg, 10.1 µmol, 5.05 mol-%), $NaHCO_3$ (33.5 mg, 399 µmol, 1.99 eq), 4-nitrobenzenediazonium tetrafluoroborate $\mathbf{2_{NO_2}}$ (94.9 mg, 401 µmol, 1.00 eq) and *o*-(*p*-tolylethynyl)phenol $\mathbf{6_{Me}}$ (41.7 mg, 200 µmol, 1.00 eq) were dissolved in 1.00 mL acetonitrile and the mixture was stirred for two hours under blue-LED irradiation (450 nm) at room temperature.

The mixture was evaporated onto Celite®. Purification by flash column chromatography (SiO_2, PE/EA 250:1) yielded the product **8**$_{\mathbf{Me,NO_2}}$ (21.4 mg, 65.0 µmol, 32%) as a yellow, crystalline solid (reaction time 30 min: 22.5 mg, 68.3 µmol, 34%).

R_f (SiO_2, PE/EA, 100/1) = 0.43; ^{1}H NMR (399.82 MHz, $CDCl_3$): δ = 2.37 (s, 3 H), 7.17 (d, J = 7.91 Hz, 2 H), 7.26-7.33 (m, 1 H), 7.37 (ddd, J = 8.14 Hz, J = 7.15 Hz, J = 1.22 Hz, 1 H), 7.50 (dd, J = 7.93 Hz, J = 5.59 Hz, 3 H), 7.58 (dt, J = 8.08 Hz, J = 0.94 Hz, 1 H), 7.65-7.73 (m, 2 H), 8.28-8.35 (m, 2 H) ppm. Its spectroscopic data matches with previously reported data.[15]

1.4.3.12) Irradiation of 3-(4-Nitrophenyl)-2-(*p*-tolyl)benzofuran with diazonium salt

Due to the low yields of arylation, we dissolved 3-(4-Nitrophenyl)-2-(*p*-tolyl)benzofuran **8**$_{\mathbf{Me,NO_2}}$ (10.6 mg, 32.2 µmol, 1.00 eq) and 4-nitrobenzenediazonium tetrafluoroborate **2**$_{\mathbf{NO_2}}$ (8.4 mg, 35.4 µmol, 1.10 eq) in 400 µL CD_3CN and the mixture was irradiated for two hours with blue-LED (450 nm). The solution turned form yellow before to dark brown after irradiation (see **Figure S 1**). The ^{1}H NMR spectrum shows that the excess of diazonium salt leads to consumption of benzofuran **8**$_{\mathbf{Me,NO_2}}$, which might result in further arylation processes and/or in the decomposition of **8**$_{\mathbf{Me,NO_2}}$.

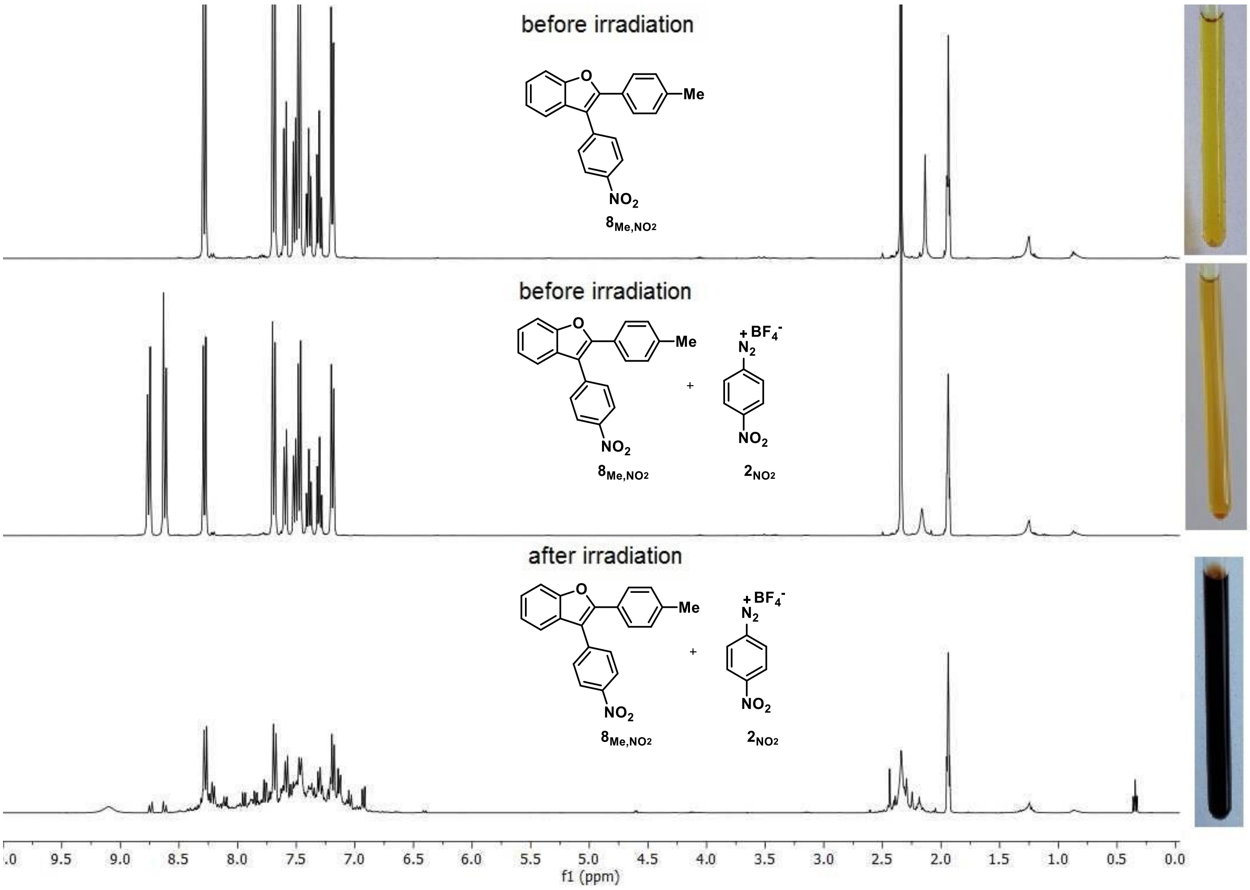

Figure S 1: ^{1}H NMR (399.82 MHz, CD_3CN) of **8**$_{\mathbf{Me,NO_2}}$.

1.5) Control Experiments

1.5.1) Arylated Benzofuran

Starting material (100 µmol), catalyst (5.00 mol-%), base (200 µmol), diazonium salt (200 µmol) and hexamethylbenzene (100 µmol) were dissolved in 1.00 mL acetonitrile. The mixture was stirred at room temperature under irradiation with blue LED (450 nm) for two hours. The mixture was filled up to 5.00 mL and an aliquot was taken for GC MS analysis. The yields were determined *via* internal standard and the response factor was determined with an external five-point calibration curve.

Table S 1: Control experiments for the formation of arylated benzofurans.

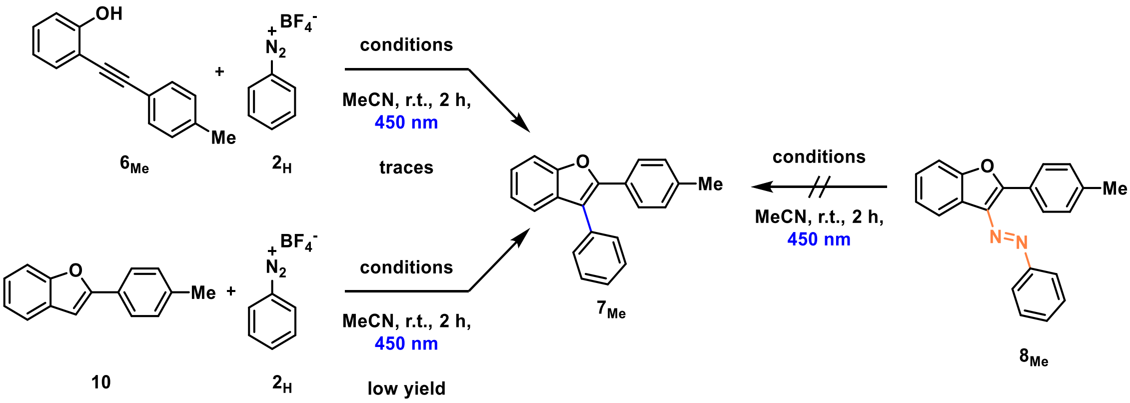

Entry	Starting Material	Catalyst	Base	Yield **7_{Me}** [%] Irradiation
1	**6_{Me}**	No	No	Not observed
2	**6_{Me}**	No	$NaHCO_3$	< 5
3	**10**	No	No	5
4	**10**	No	$NaHCO_3$	17
5	**10**	$Ph_3PAuNTf_2$	$NaHCO_3$	15
6	**6_{Me}**	HBF_4(a)	No	< 5
7	**6_{Me}**	$AgNTf_2$(b)	$NaHCO_3$	< 5
8	**8_{Me}** (c)	No	No	Not observed
9	**8_{Me}** (d)	$Ph_3PAuNTf_2$	$NaHCO_3$	Not observed

(a) 7.7 mol-% HBF_4. (b) 6.2 mol-% $AgNTf_2$. (c) 30 µmol in 200 µL MeCN. (d) 50 µmol in 500 µL MeCN, 100 µmol base, no diazonium salt added.

Without catalyst, the arylation did not take place by simply adding diazonium salt (entry 1), but is observed in traces (<5%) by adding base (entry 2). If benzofuran **10** is used as starting material, small amounts of the arylated product **7_{Me}** were observed by simply adding diazoniumsalt (entry 3). Low yields of product were formed with adding $NaHCO_3$ (entry 4), additionally adding $Ph_3PAuNTf_2$ (entry 5) did not affect the yield. Product **7_{Me}** was formed in traces using $AgNTf_2$ (entry 7) and HBF_4 as catalyst (entry 6). No product could be observed irradiating solely azobenzofuran **8_{Me}** and azobenzofuran **8_{Me}** under reaction conditions (entry 8 and 9).

1.5.2) Azocompound

Starting material (50.0 µmol), base (100 µmol) and diazonium salt (100 µmol) were dissolved in 100 µL of a stock solution of catalyst (25.0 µmol/mL in dichloromethane) and molecular sieves (3 Å) was added. 400 µL Dichloromethane was added and the mixture was stirred for 24 hours at room temperature. The solvents were evaporated and the crude product was dried at the Schlenk line. The solid was recorded in 600 µL $CDCl_3$ and treated with 7.00 µL benzylacetate. The yields were determined *via* ^1H NMR spectroscopy.

Table S 2: Control experiments for the formation of azobenzofurans.

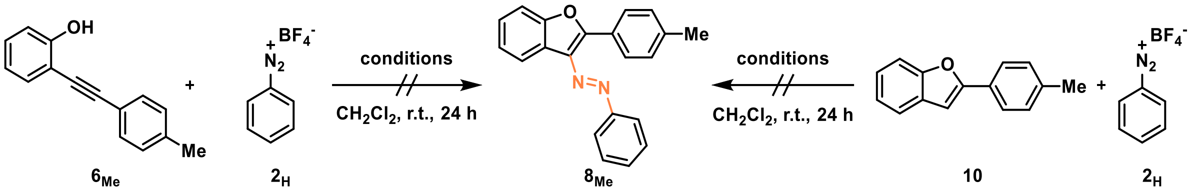

Entry	Starting Material	Catalyst	Base	Yield $\mathbf{8}_{Me}$ [%] No irradiation
1	$\mathbf{6}_{Me}$	No	No	Not observed
2	$\mathbf{6}_{Me}$	No	DTBP	Not observed$^{(a)}$
3	**10**	No	DTBP	Not observed
4	**10**	$Ph_3PAuNTf_2$	DTBP	Not observed
5	$\mathbf{6}_{Me}$	$HBF_4^{(b,c)}$	No	Not observed
6	$\mathbf{6}_{Me}$	$AgNTf_2^{(b,d)}$	DTBP	Not observed

(a) Different substituted azocompound observed (see 1.5.2.1)), (b) 4 eq of $\mathbf{2}_H$. (c) 15.3 mol-% HBF_4. (d) 6.7 mol-% $AgNTf_2$.

Azocompound $\mathbf{8}_{Me}$ could not be obtained if the reaction was carried out in the absence of a catalyst and base (entry 1). No product formation took place when using 2-(*p*-tolyl)benzofuran **10** as substrate with or without a catalyst (entries 3 and 4). If the reaction was carried out with DTBP using no catalyst, a different substituted azobenzofuran **14** could be isolated in low yield after 19 days of reaction time (~23%, entry 2, see 1.5.2.1)). No product was formed using neither $AgNTf_2$ (entry 6), nor HBF_4 (entry 5) as catalysts.

1.5.2.1) (*E*)-4-(Phenyldiazenyl)-2-(*p*-tolylethynyl)phenol

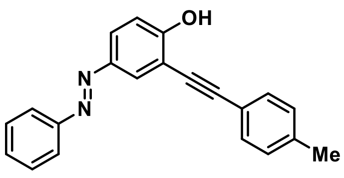

14

According to **GP C**, 2-(*p*-tolylethynyl)phenol **6**$_{\mathbf{Me}}$ (52.2 mg, 250 µmol, 1.00 eq) and 2,6-di*tert*butylpyridine (113 µL, 95.7 mg, 500 µmol, 2.00 eq) were dissolved in 2.00 mL dichloromethane and stirred at room temperature for ten minutes. Benzenediazonium tetrafluoroborate **2**$_{\mathbf{H}}$ (96.2 mg, 501 µmol, 2.00 eq) was added and the mixture was stirred at room temperature for 19 days and stopped. The mixture was evaporated onto Celite® and purification by flash column chromatography (SiO_2, PE/EA, 100:1 => 10/1) yielded the product **14** (17.6 mg, 56.3 µmol, 23%) as a moderately pure, orange solid.

R_f (SiO_2, PE/EA, 10:1) = 0.23; ^{1}H NMR (299.95 MHz, $CDCl_3$): δ = 2.39 (s, 3 H), 6.17 (bs, 1 H), 7.09-7.14 (m, 1 H), 7.19-7.23 (m, 2 H), 7.43-7.56 (m, 5 H), 7.88-7.94 (m, 3 H), 8.06 (d, *J* = 2.36 Hz, 1 H) ppm.

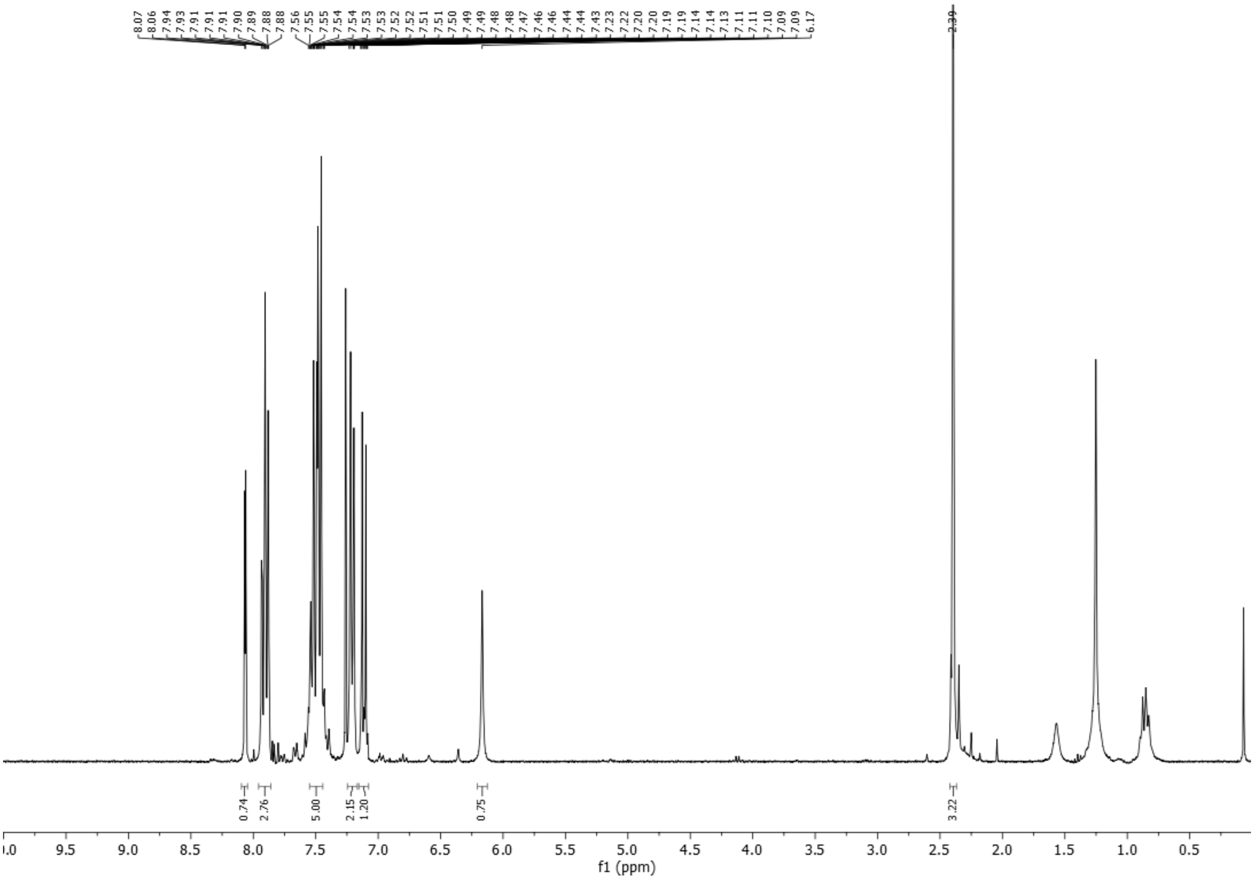

Figure S 2: ^{1}H NMR spectrum (299.95 MHz, $CDCl_3$) of **14**.

1.6) Synthesis of Gold(I) Complex

1.6.1.1) (2-(*p*-Tolyl)benzofuran-3-yl)(triphenyl-λ^5-phosphanyl) gold(I)

Vinyl gold(I)complex **9** was synthesized according to a modified procedure previously reported by Hashmi and co-workers.[16]

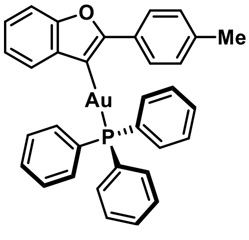

9

In a heat-gun dried Schlenk tube under an atmosphere of nitrogen, Ph_3PAuCl (146 mg, 294 µmol, 1.00 eq) and AgOTs (82.1 mg, 294 µmol, 1.00 eq) were dissolved in 50.0 mL THF and stirred for one hour at room temperature. Triethylamine (297µL, 208 mg, 2.08 mmol, 7.00 eq) and 2-((4-methylphenyl)ethynyl)phenol **6_{Me}** (62.5 mg, 300 µmol, 1.02 eq) were added and the mixture was stirred for 19 hours under exclusion of light. The mixture was filtered through a pad of neutral Al_2O_3 and evaporated at room temperature. The crude solid was recrystallized from dichloromethane/pentane, filtered, washed with pentane and yielded the product **9** (166 mg, 249 µmol, 85%) as a colorless, crystalline solid.

M.p.: decomp >181 °C; IR(ATR): $\tilde{\nu}$ = 693, 710, 741, 748, 822, 886, 920, 969, 997, 1012, 1029, 1069, 1100, 1158, 1180, 1200, 1251, 1264, 1281, 1308, 1331, 1338, 1433, 1447, 1465, 1479, 1490, 2918, 3014, 3046, 3067 cm^{-1}; ^1H NMR (600.13 MHz, CD_2Cl_2): δ = 2.37 (s, 3 H), 7.09-7.19 (m, 4 H), 7.46 (d, *J* = 7.95 Hz, 1 H), 7.49-7.59 (m, 9 H), 7.64-7.70 (m, 6 H), 7.73-7.79 (m, 1 H), 8.33 (d, *J* = 7.97 Hz, 2 H) ppm; ^{13}C NMR (150.92 MHz, CD_2Cl_2): δ = 21.42 (q), 110.57 (d), 121.79 (d), 123.50 (d), 124.78 (d), 125.71 (d, 2 C), 129.25 (d, 2 C), 129.57 (d, 3 C), 129.64 (d, 3 C), 131.13 (s, d, *J* = 52.0 Hz), 131.74 (s), 131.83 (d, d, *J* = 2.42 Hz, 3 C), 134.54 (s), 134.72 (d, 3 C), 134.81 (d, 3 C), 137.57 (s), 139.74 (s, 3 C), 155.38 (s, d, *J* = 3.86 Hz), 161.43 (s, d, *J* = 8.54 Hz) ppm; ^{31}P NMR (242.92 MHz, CD_2Cl_2): δ = 45.22 ppm; HR-DART (+) $C_{33}H_{26}AuOP$ $[M]^+$: calcd. 666.1381, found 666.1374.

1.6.2) Reactions of Vinyl Gold(I) Complex

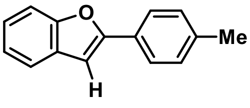

10

Vinyl gold(I) complex **9** (20.0 mg, 30.0 µmol, 1.00 eq) was dissolved in 500 µL CD_2Cl_2 and 2-((4-methylphenyl)ethynyl)phenol **6$_{Me}$** (6.9 mg, 33.0 µmol, 1.10 eq) was added. The solution was mixed constantly by a rotating machine for 30 hours. 4 µL Benzylacetate was added as internal standard and the ^{1}H NMR spectrum was recorded. Product **10** was formed with 16% conversion.

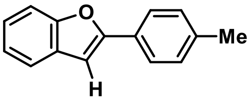

10

Vinyl gold(I) complex **9** (20.2 mg, 30.3 µmol, 1.01 eq) was dissolved in 500 µL CD_2Cl_2 and phenol (3.3 mg, 35.0 µmol, 1.17 eq) was added. The solution was mixed constantly by a rotating machine for 26 hours. 4 µL Benzylacetate was added as internal standard and the ^{1}H NMR spectrum was recorded. Product **10** was formed with 54% yield.

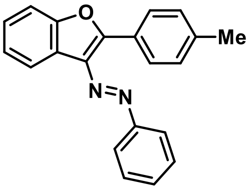

8$_{Me}$

Vinyl gold(I) complex **9** was dissolved in 500 µL CD_2Cl_2 and benzenediazonium tetrafluoroborate **2$_H$** was added. The solution was mixed constantly by a rotating machine for 24 hours. 4 µL Benzylacetate was added as internal standard and the ^{1}H NMR spectrum was recorded. Product **8$_{Me}$** was formed with an average yield of 46% (double determination).

A) **9** (20.0 mg, 30.0 µmol, 1.00 eq), **2$_H$** (6.4 mg, 33.5 µmol, 1.12 eq). Yield: 49%

B) **9** (20.0 mg, 30.0 µmol, 1.00 eq), **2$_H$** (6.3 mg, 33.0 µmol, 1.10 eq). Yield: 44%

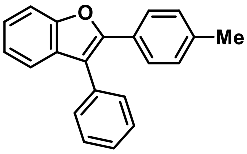

7$_{Me}$

Vinyl gold(I) complex **9** was dissolved in 500 µL acetonitrile, benzenediazonium tetrafluoroborate **2$_H$** and hexamethylbenzene (internal standard) were added. The mixture was irradiated with 450 nm blue LED at room temperature for two hours, analyzed *via* GC-MS and product **7$_{Me}$** was formed with an average yield of 65% (double determination).

A) **9** (20.0 mg, 30.0 µmol, 1.00 eq), **2$_H$** (6.3 mg, 33.0 µmol, 1.10 eq), HMB (4.7 mg, 29.0 µmol, 0.96 eq). Yield **7$_{Me}$**: 69%, yield **10**: 33%.

B) **9** (20.1 mg, 30.2 µmol, 1.01 eq), **2$_H$** (6.8 mg, 35.5 µmol, 1.20 eq), HMB (4.7 mg, 29.0 µmol, 0.96 eq). Yield **7$_{Me}$**: 62%, yield **10**: 8%.

1.7) Irradiation of Ph_3PAuCl/$Ph_3PAuNTf_2$ with *p*-Tolyldiazonium tetrafluoroborate

Ph_3PAuCl (12.4 mg, 25.1 µmol, 1.00 eq), $NaHCO_3$ (2.1 mg, 25.0 µmol, 1.00 eq) and *p*-tolyldiazonium tetrafluoroborate **2_{Me}** (5.2 mg, 26.8 µmol, 1.07 eq) were dissolved in 200 µL CD_3CN and 4 µL tetrachloroethane as internal standard were added. The solution was irradiated with a 405 nm LED light source for 144 min and the reaction was monitored every 36 s *via* ^1H NMR spectroscopy (499.86 MHz).

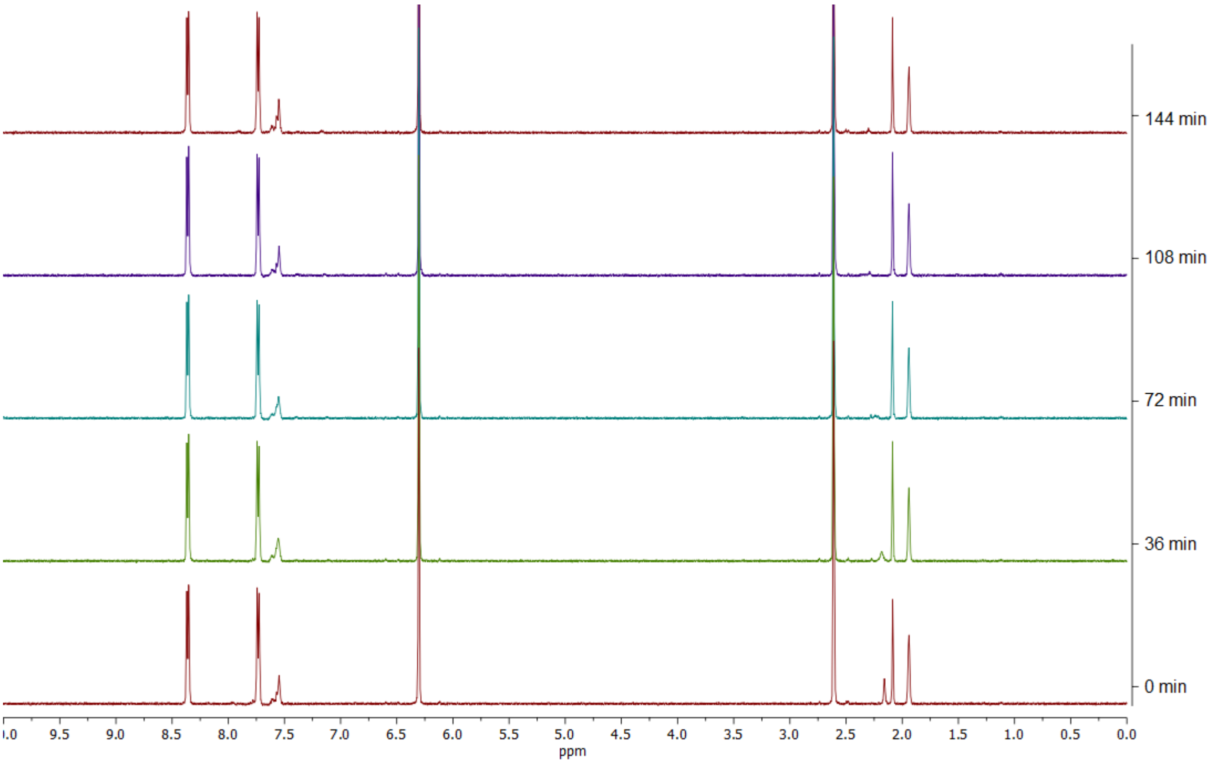

Figure S 3: ^1H NMR (499.86 MHz, CD_3CN) of Ph_3PAuCl with **2_{Me}** and $NaHCO_3$ at different times of irradiation, using tetrachloroethane as internal standard.

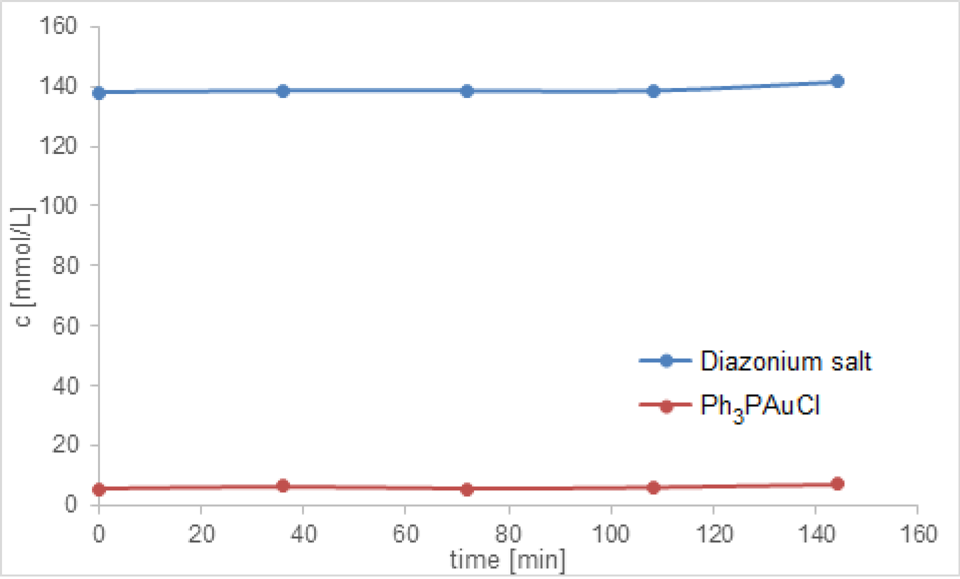

Figure S 4: Time-dependent change of concentration of the reaction of Ph_3PAuCl with $\mathbf{2_{Me}}$ and $NaHCO_3$ while being irradiated with a 405 nm blue LED lamp, determined by ^1H NMR (499.86 MHz, CD_3CN) using tetrachloroethane as internal standard.

As seen in **Figure S 4**, the concentration of Ph_3PAuCl in the sample is very low with, due to its poor solubility in CD_3CN. $Ph_3PAuNTf_2$ is fully soluble in CD_3CN (see **Figure S 5**), therefore we irradiated a similar sample using $Ph_3PAuNTf_2$, with and without $NaHCO_3$.

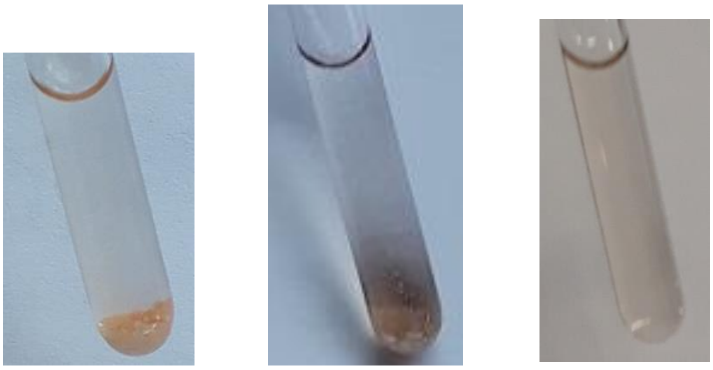

Figure S 5: Samples before irradiation. Left: Ph_3PAuCl (insoluble), *p*-tolyldiazonium tetrafluoroborate $\mathbf{2_{Me}}$ (soluble), $NaHCO_3$ in CD_3CN. Middle: $Ph_3PAuNTf_2$ (soluble), *p*-tolyldiazonium tetrafluoroborate $\mathbf{2_{Me}}$ (soluble), $NaHCO_3$ (insoluble) in CD_3CN. Right: $Ph_3PAuNTf_2$ (soluble), *p*-tolyldiazonium tetrafluoroborate $\mathbf{2_{Me}}$ (soluble) in CD_3CN.

$Ph_3PAuNTf_2$ (18.8 mg, 25.4 µmol, 1.02 eq), $NaHCO_3$ (2.1 mg, 25.0 µmol, 1.00 eq) and *p*-tolyldiazonium tetrafluoroborate $\mathbf{2_{Me}}$ (5.2 mg, 25.2 µmol, 1.01 eq) were dissolved in 200 µL CD_3CN and 4 µL tetrachloroethane as internal standard were added. The solution was irradiated with a 405 nm LED lamp for 144 min and the reaction was monitored every 36 s *via* ^1H NMR spectroscopy (499.86 MHz).

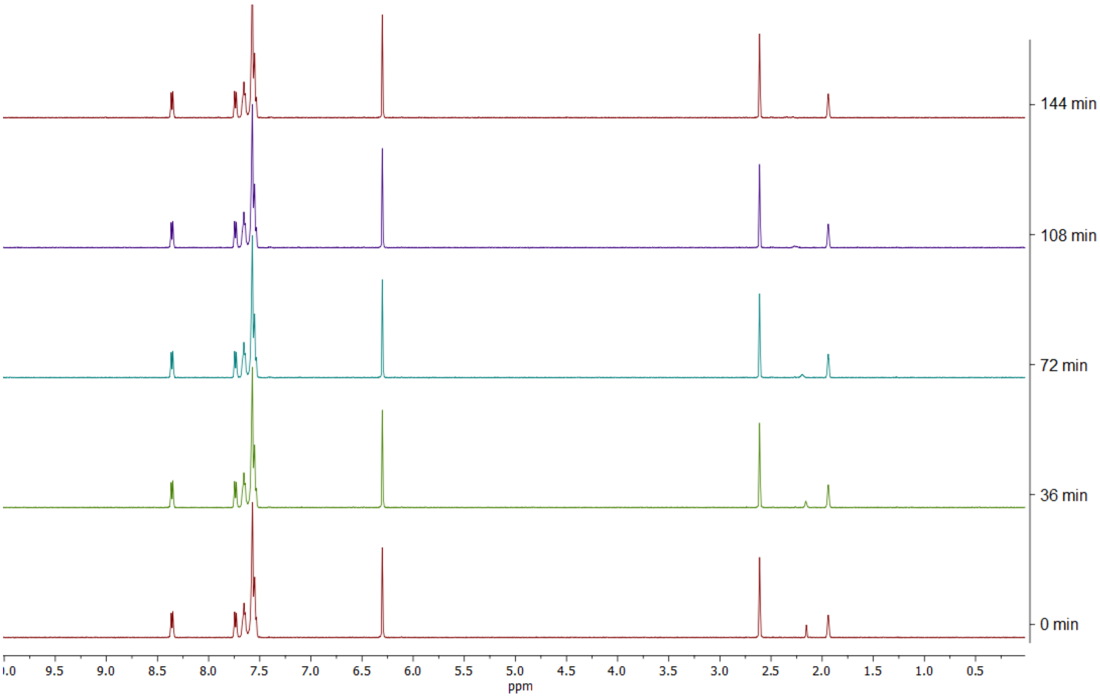

Figure S 6: ^{1}H NMR (499.86 MHz, CD_3CN) of $Ph_3PAuNTf_2$ with $\mathbf{2_{Me}}$ and $NaHCO_3$ at different times of irradiation, using tetrachloroethane as internal standard.

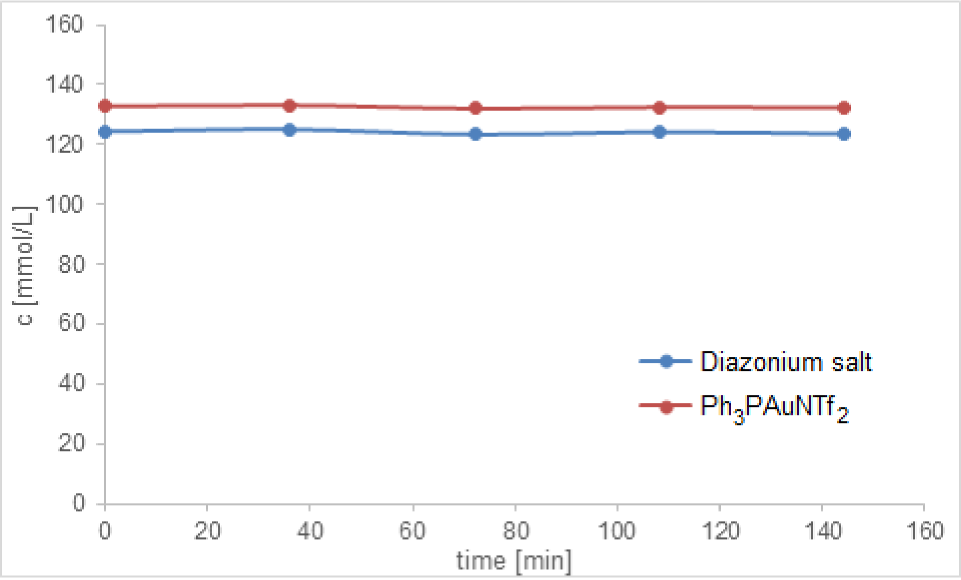

Figure S 7: Time-dependent concentration of the reaction of $Ph_3PAuNTf_2$ with $\mathbf{2_{Me}}$ and $NaHCO_3$ while being irradiated with a 405 nm blue LED lamp, determined by ^{1}H NMR (499.86 MHz, CD_3CN) using tetrachloroethane as internal standard.

$Ph_3PAuNTf_2$ (18.8 mg, 25.4 µmol, 1.02 eq) and *p*-tolyldiazonium tetrafluoroborate $\mathbf{2_{Me}}$ (5.2 mg, 25.2 µmol, 1.01 eq) were dissolved in 200 µL CD_3CN and 4 µL tetrachloroethane as internal standard were added. The solution was irradiated with a 405 nm LED lamp for 144 min and the reaction was monitored every 36 s *via* ^{1}H NMR spectroscopy (499.86 MHz).

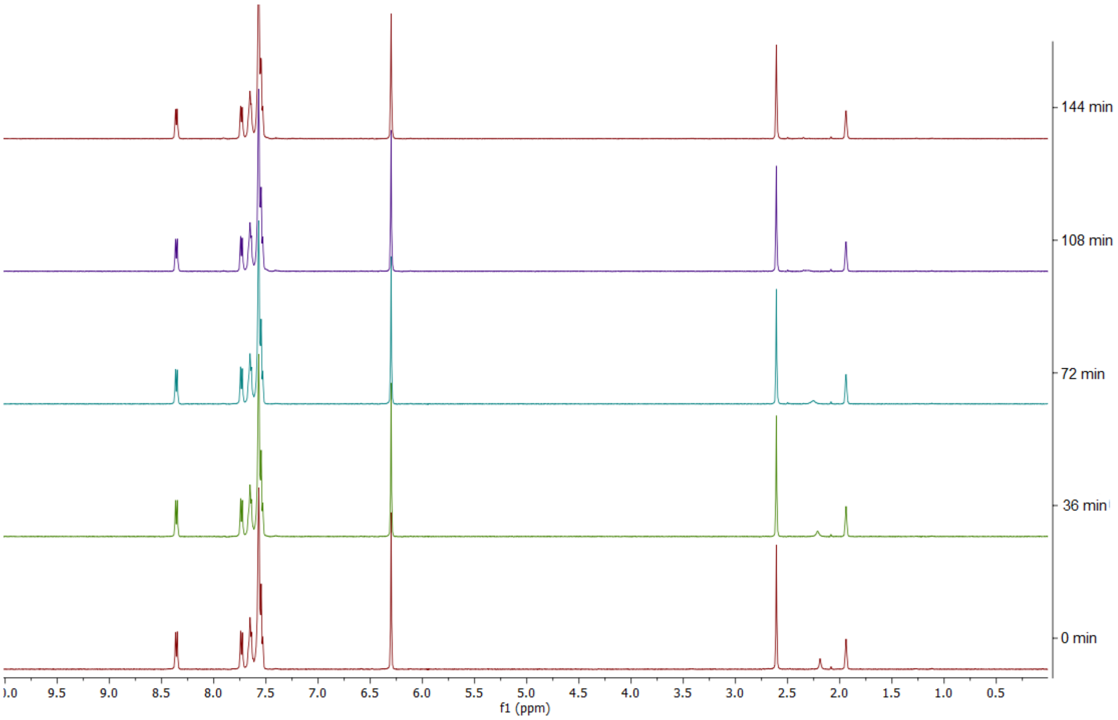

Figure S 8: ^{1}H NMR (499.86 MHz, CD_3CN) of $Ph_3PAuNTf_2$ with **2**$_{\mathbf{Me}}$ at different times of irradiation, using tetrachloroethane as internal standard.

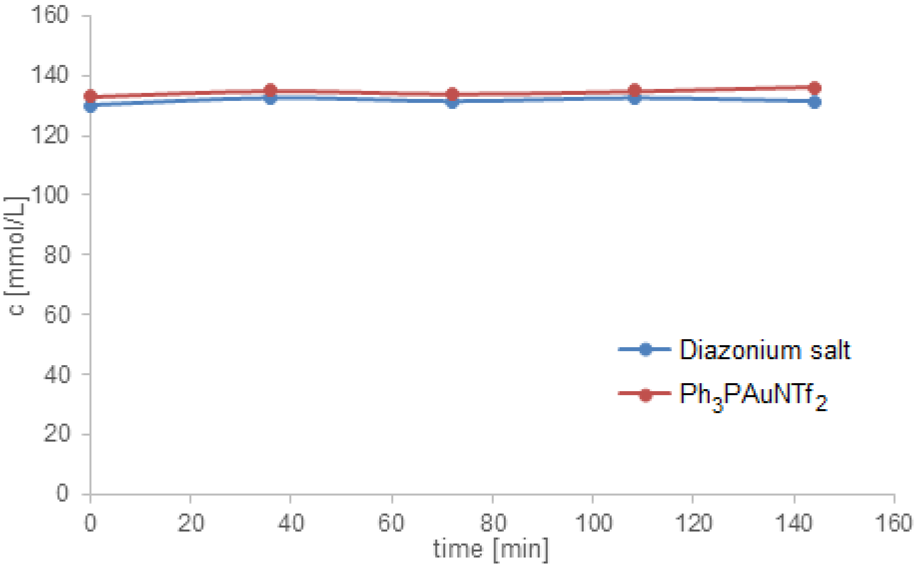

Figure S 9: Time-dependent concentration of the reaction of $Ph_3PAuNTf_2$ with **2**$_{\mathbf{Me}}$ while being irradiated with a 405 nm blue LED lamp, determined by ^{1}H NMR (499.86 MHz, CD_3CN) using tetrachloroethane as internal standard.

In all reactions, there was no change in concentration of diazonium salt **2**$_{\mathbf{Me}}$ or gold(I)catalyst observed (see **Figure S 4**, **Figure S 7** and **Figure S 9**).

1.8) Computational Details

DFT calculations were carried out using the electronic structure code Gaussian 16 revision B.01.[17] Geometries were optimized using the TPSS functional[18] in combination with Grimme's empirical dispersion correction D3 including Becke-Johnson damping.[19] The def2-SVP basis set[20] was used for all elements and calculations were accelerated using density fitting[21] in combination with Weigend's universal fitting basis set.[22] At these geometries electronic energies for ground and excited states (TD-DFT)[23] were computed using the CAM-B3LYP functional[24] ombined with the D3(BJ) dispersion correction. The def2-SVPD basis set was used including a small set of diffuse basis functions.[25] For all calculations, 60 inner electrons were replaced with an effective core potential (ECP) for Au,[26] an *ultrafine* integration grid was used and the PCM solvation model[27] mimicking MeCN solvation. The def2-SVP and def2-SVPD basis sets including the appropriate ECP were obtained from the *Basis Set Exchange* library.[28] Non-covalent complexes were optimized using Gaussian's *loose* convergence criteria. Structural depictions were made using Chemcraft.[29]

1.8.1) Geometry Donor-Acceptor Complex

In order to probe the conformational space of the donor-acceptor complex we employed Grimme's CREST algorithm (Version 2.7.1)[30] using the GFN2-xTB method[31] in combination with the generalized born model with solvent accessible surface area (GBSA) for MeCN. For all obtained structures single point calculations were carried out at the TPSS-D3(BJ)/def2-SVP/PCM(MeCN) level of theory. The lowest energy structure was subsequently fully optimized at this level of theory and used for further analysis. We do note here that several energetically similar structures were obtained and that our selection of the lowest energy structure only serves to provide a qualitative answer on the role of a donor-acceptor complex (**I**) for photochemical activation. From this structure (singlet ground state) we also fully optimized the triplet state for the donor-acceptor complex (**II**). Structural depictions are shown below in **Figure S 10**.

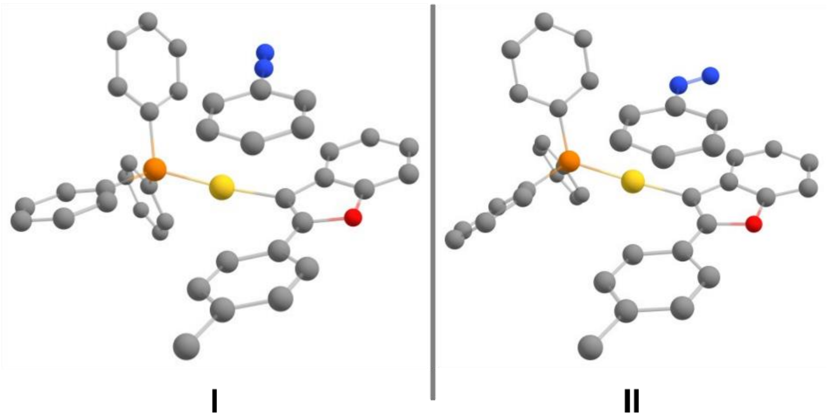

Figure S 10: Structural depictions of fully optimized geometries of a donor-acceptor complexes **I** and **II** at the TPSS-D3(BJ)/def2-SVP/PCM(MeCN) level of theory.

1.8.2) UV-Vis Spectrum Donor-Acceptor Complex

We computed UV-Vis spectra (nstates=50) for the donor-acceptor complex **I** at the TD-CAM-B3LYP-D3(BJ)/def2-SVPD/PCM(MeCN) level of theory. For comparison we also provide computed spectra of the isolated Au complex **9** and the diazonium salt PhN_2^+. For complex **I** a low-lying (low intensity) excited state can be found at 624 nm corresponding to charge-transfer from the HOMO located at the vinyl gold(I) complex portion of **I** to the LUMO which is located at the PhN_2^+ portion (*vide infra*). In contrast, **9** and PhN_2^+ have their lowest lying excited states at 319 nm and 293 nm, respectively. In addition, for **I** several additional excited states (429, 383, 377, 343 and 320 nm) can be found at lower energy than the lowest-lying excited states of **9** and PhN_2^+, supporting that the formation of a donor-acceptor complex leads to a red shift allowing for photochemistry to occur. We shall note here that TD-DFT is prone to over stabilize charge-transfer states,[32] even if long-range corrected functionals are employed, and hence the lowest lying excited state for **I** may in fact be closer to the wavelength used for irradiation (450 nm).

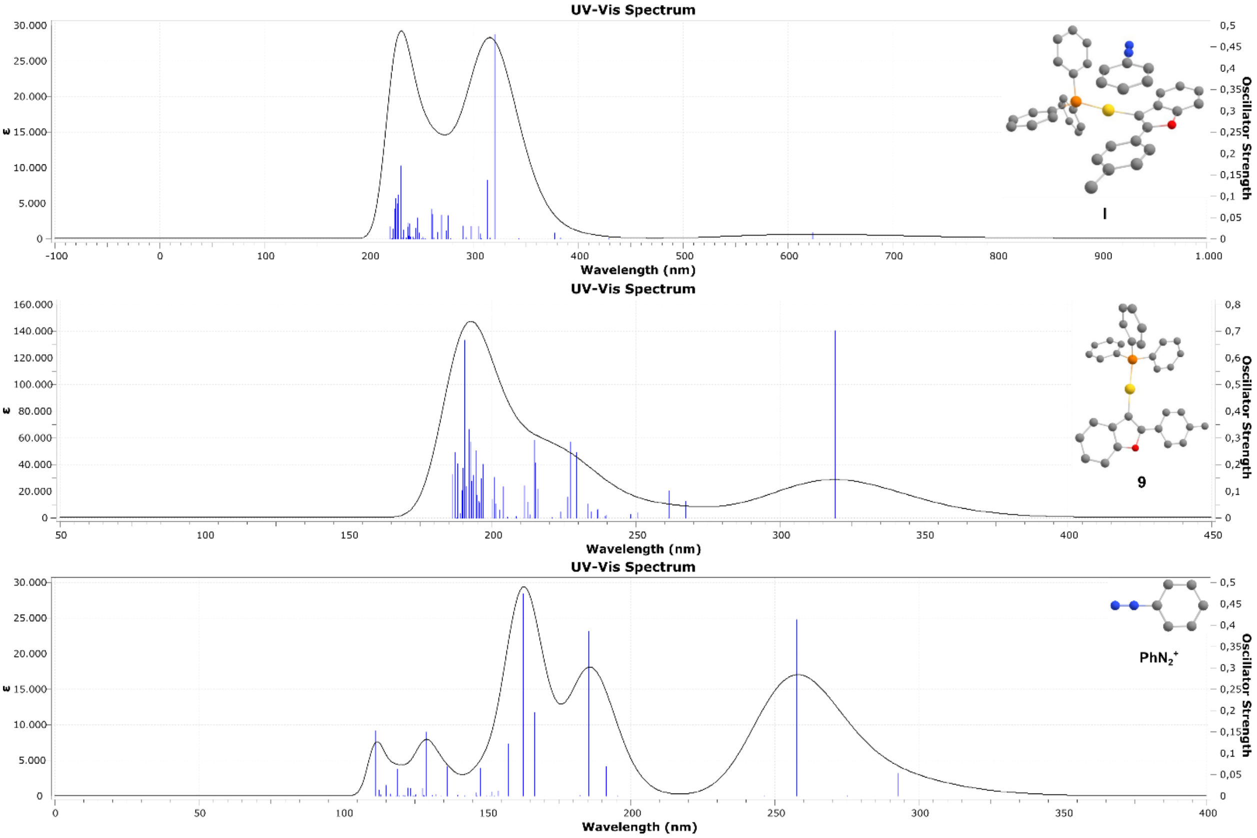

Figure S 11: Computed UV-Vis spectra for **I**, **9** and PhN_2^+ at the TD-CAM-B3LYP-D3(BJ)/def2-SVPD/PCM(MeCN)//TPSS-D3(BJ)/def2-SVP/PCM(MeCN) level of theory. Depicted spectra are generated from the computed line spectra fitting a Gaussian band shape with half-with at half-height of 0.333 eV.

1.8.3) Nature of the Excited State and Role for Reactivity

As indicated above, we can identify a low-lying excited state that corresponds to excitation from the HOMO to the LUMO (for depiction of orbitals see **Figure S 12**). In agreement with this attribution the natural transition orbitals (**Figure S 13**) are in excellent agreement with the frontier molecular orbital picture. The excited state lies 45.8 kcal mol^{-1} above the ground state for **I**. Notably, the triplet state is energetically favorable and lies 29.7 kcal mol^{-1} above the ground state for **I**, and the energy is further lowered to 13.2 kcal mol^{-1} with respect to **I** when computed at the fully relaxed triplet geometry **II**. In addition, inspection of the spin density for the triplet state is consistent with charge transfer from the vinyl gold(I) complex portion of **I** to the PhN_2^+ portion, which is also reflected by the spin population of the fragments (**Figure S 14**). We might therefore outline the following scenario for photochemical activation in the C-C bond forming reaction as follows: (i) initial excitation from the donor-acceptor complex leading to the lowest-lying excited singlet state, (ii) followed by intersystem crossing to the triplet surface and (iii) geometrical relaxation leading to **II** (**Figure S 15**). One notable geometrical feature that changes upon relaxation on the triplet surface is the C-N bond distance in the PhN_2^+ fragment, which elongates from 1.362 to 1.449 Å. We propose here that the subsequent C-C bond formation takes place on the triplet surface. We also note that we are not precluding that initial excitation may be to a higher-lying excited state, but envision that rapid internal conversion following Kasha's rule would lead to the lowest-lying excited singlet state from which the subsequent changes may occur. The details of these processes, including the role of the heavy element Au for intersystem crossing are subject of future studies.

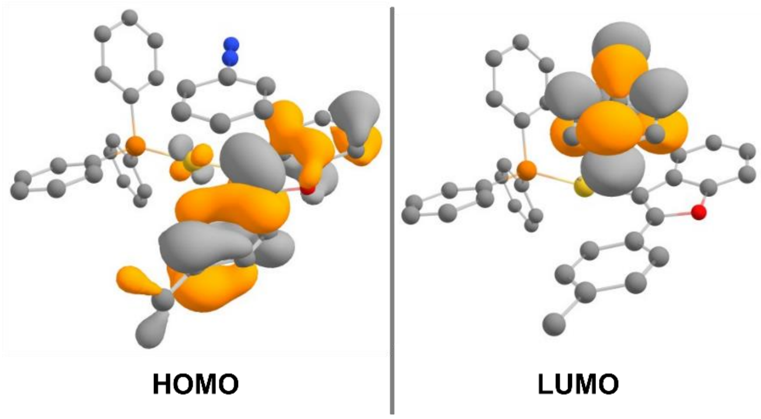

Figure S 12: HOMO and LUMO depictions of the donor-acceptor complex **I** at the CAM-B3LYP-D3(BJ)/def2-SVPD/PCM(MeCN)//TPSS-D3(BJ)/def2-SVP/PCM(MeCN) level of theory.

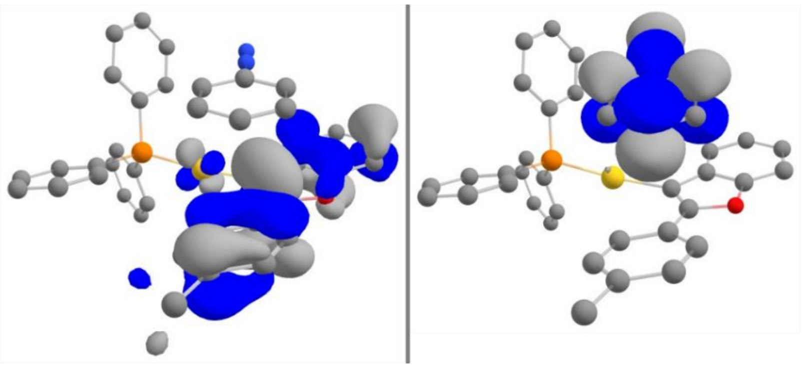

Figure S 13: Natural transition orbital depictions for the lowest lying singlet excited state of the donor-acceptor complex **I** at the TD-CAM-B3LYP-D3(BJ)/def2-SVPD/PCM(MeCN)//TPSS-D3(BJ)/def2-SVP/PCM(MeCN) level of theory.

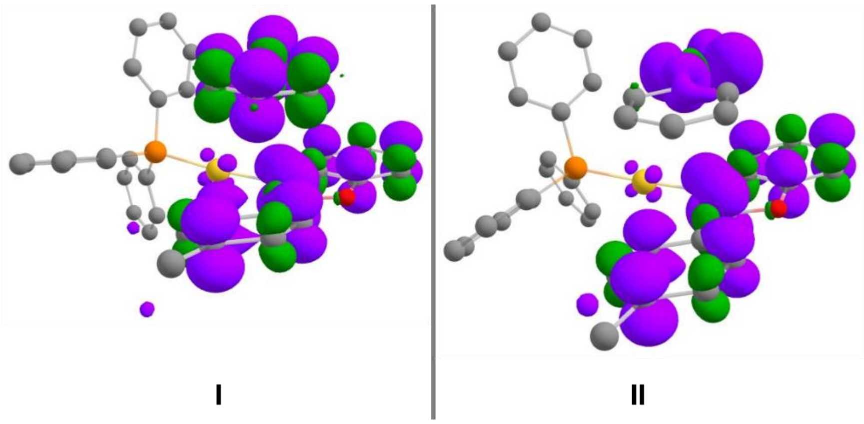

Figure S 14: Spin density plots for the triplet states of the donor-acceptor complexes **I** and **II** at the CAM-B3LYP-D3(BJ)/def2-SVPD/PCM(MeCN)//TPSS-D3(BJ)/def2-SVP/PCM(MeCN) level of theory (isosurface 0.003).

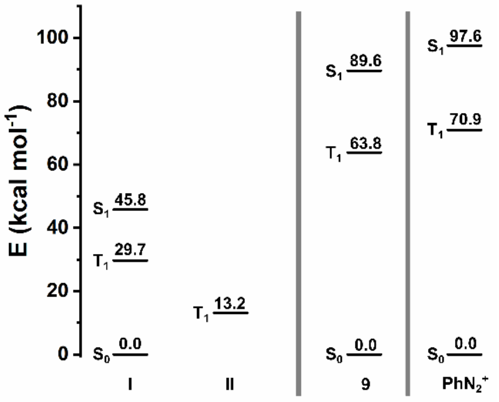

Figure S 15: Energy profile for relevant species for the photochemical activation *via* the donor-acceptor complex **I** at the (TD-)CAM-B3LYP-D3(BJ)/def2-SVPD/PCM(MeCN)//TPSS-D3(BJ)/def2-SVP/PCM(MeCN) level of theory.

2) Attachment

2.1) NMR Spectra

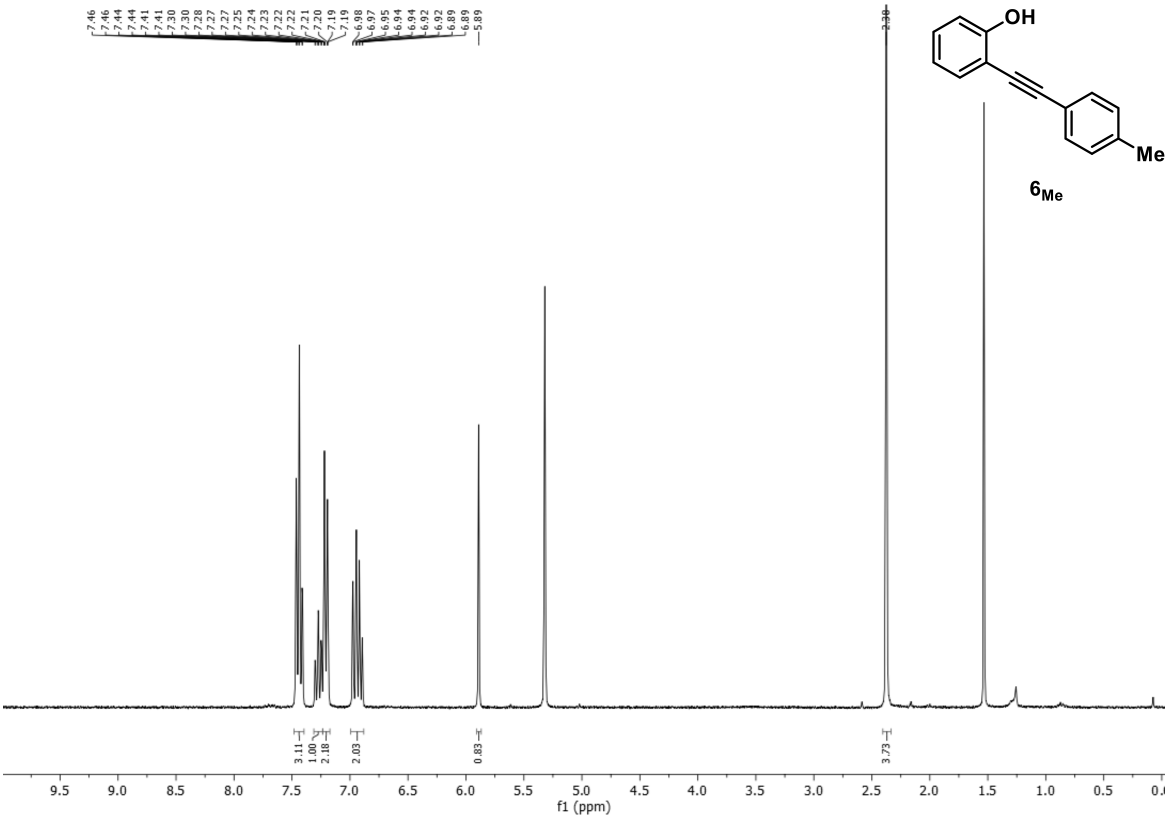

Figure S 16: ^{1}H NMR (299.95 MHz, $CDCl_3$) of **6$_{Me}$**.

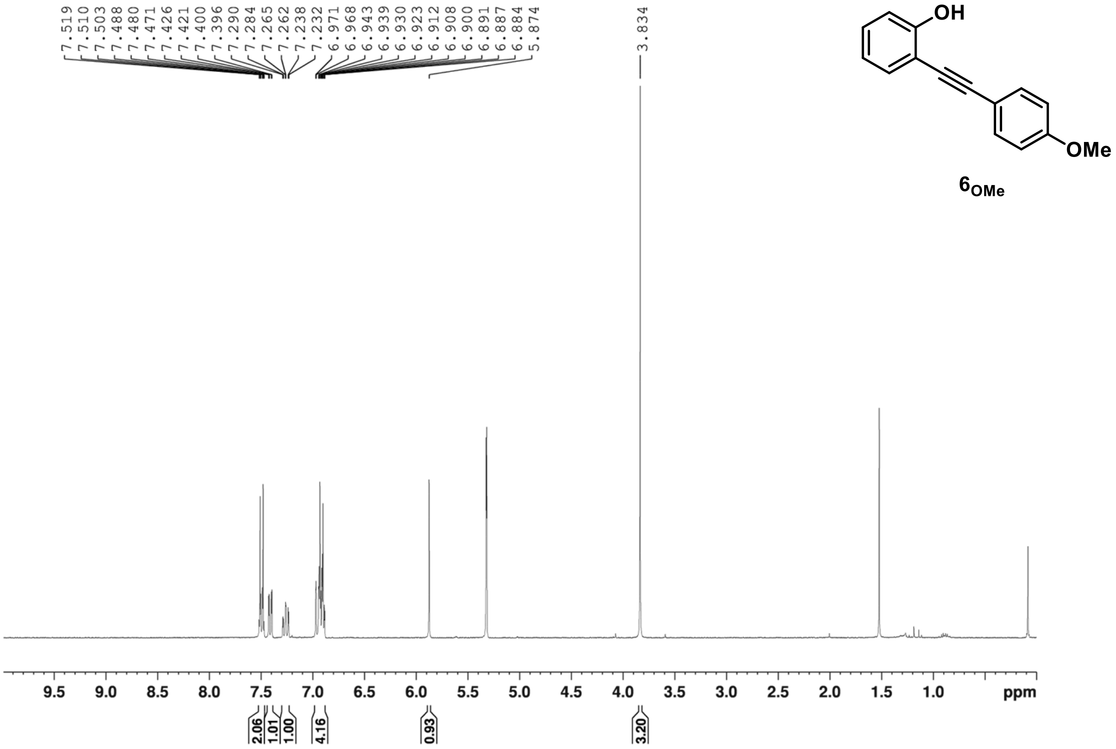

Figure S 17: ^{1}H NMR (300.51 MHz, CD_2Cl_2) of **6$_{OMe}$**.

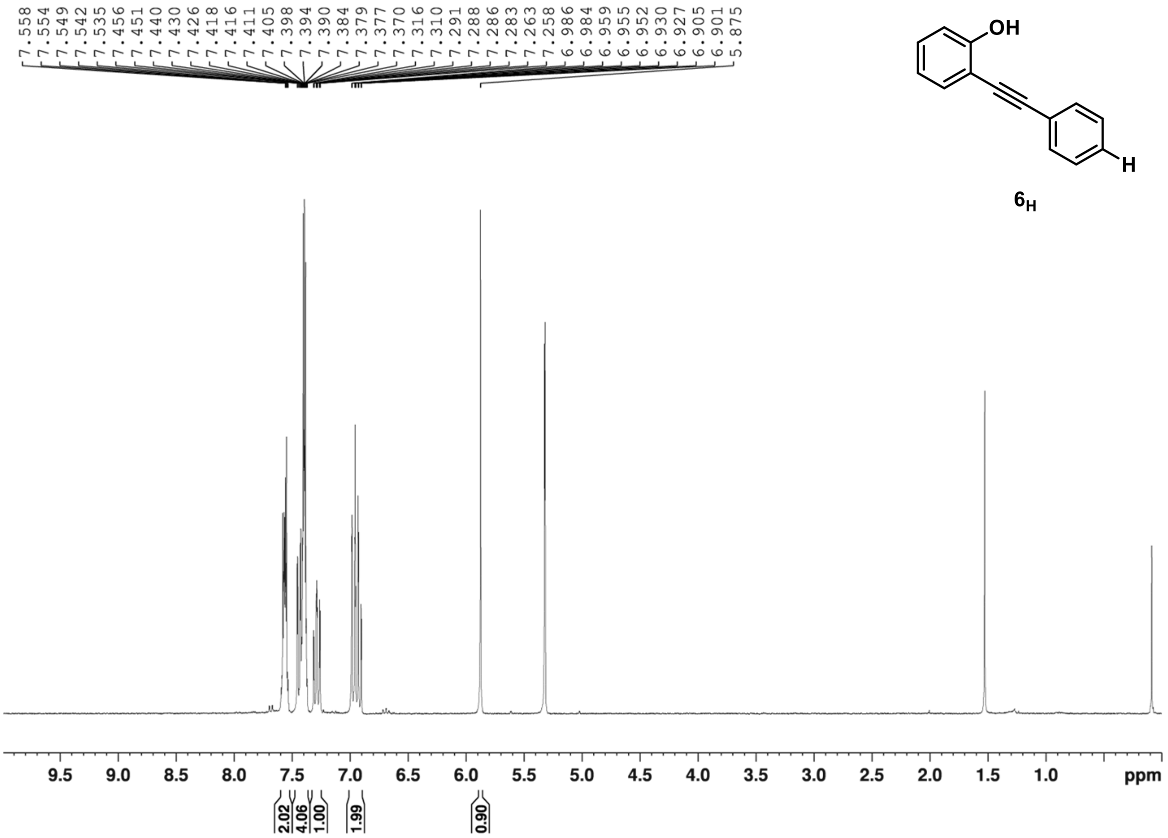

6_H

Figure S 18: ^{1}H NMR (300.51 MHz, CD_2Cl_2) of **6_H**.

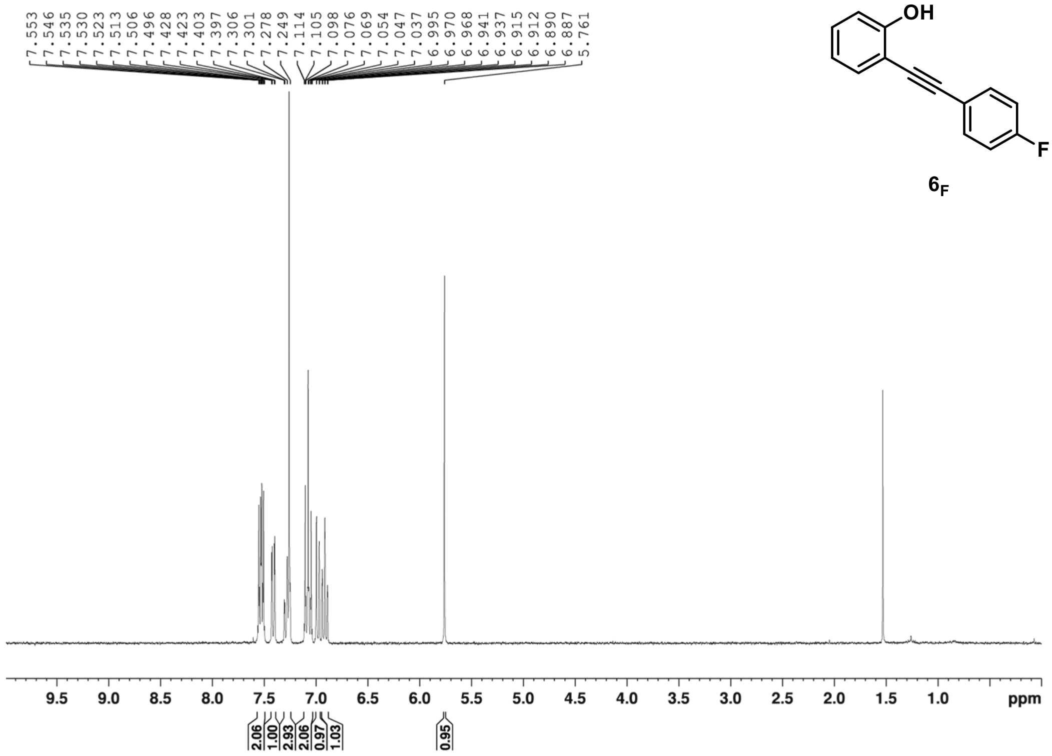

6_F

Figure S 19: ^{1}H NMR (300.51 MHz, $CDCl_3$) of **6_F**.

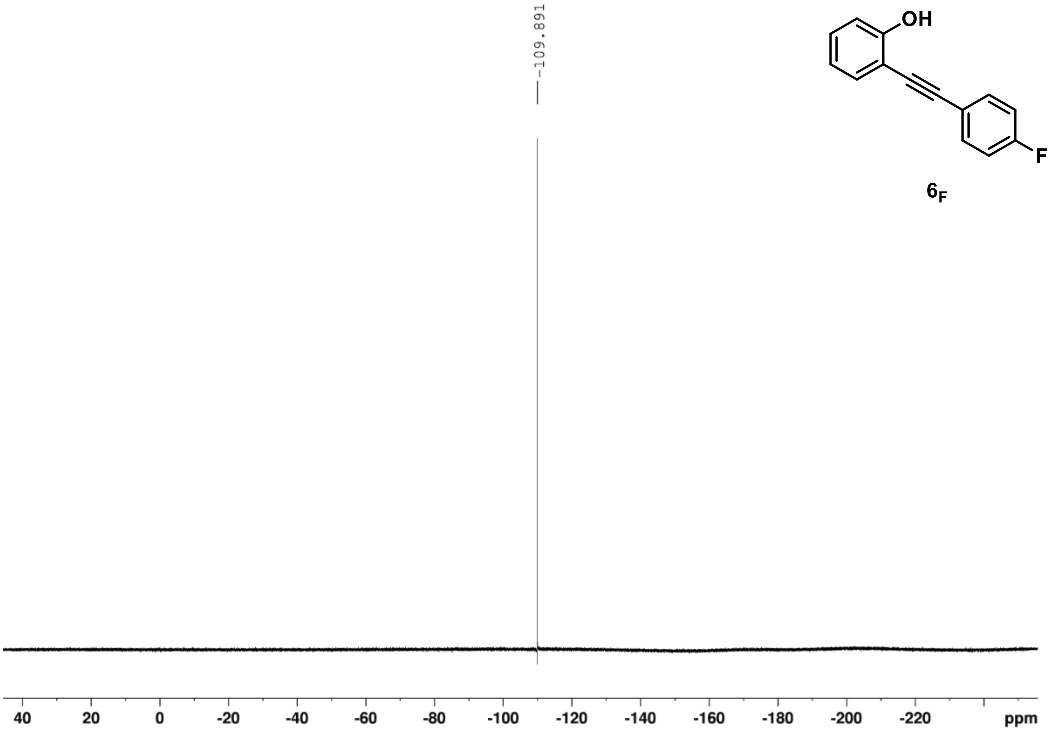

Figure S 20: ^{19}F NMR (282.76 MHz, $CDCl_3$) of **6_F**.

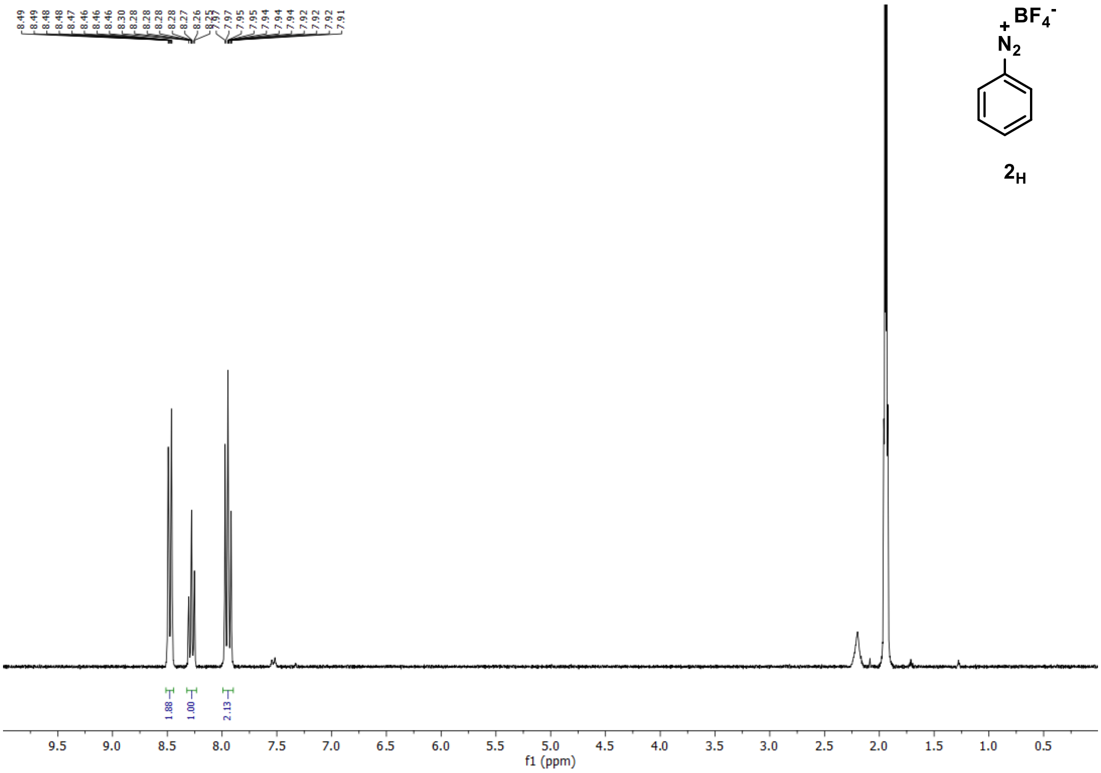

Figure S 21: ^{1}H NMR (299.95 MHz, CD_3CN) of **2_H**.

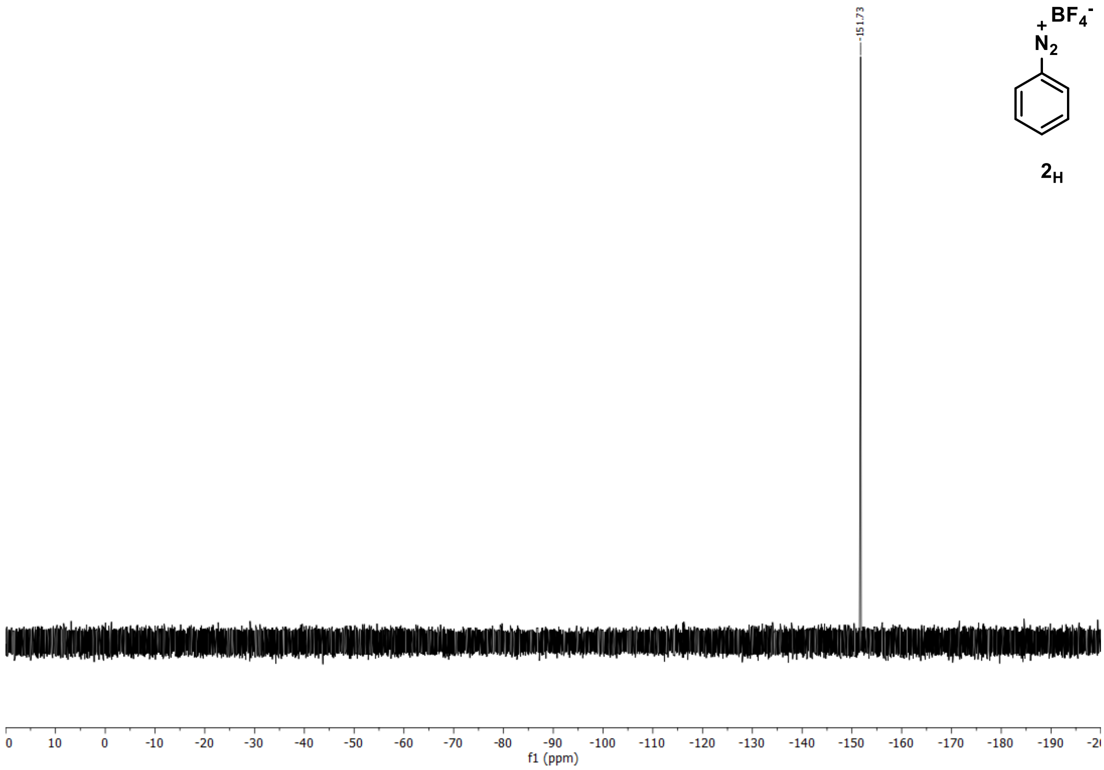

Figure S 22: ^{19}F NMR (282.21 MHz, CD_3CN) of $\mathbf{2_H}$.

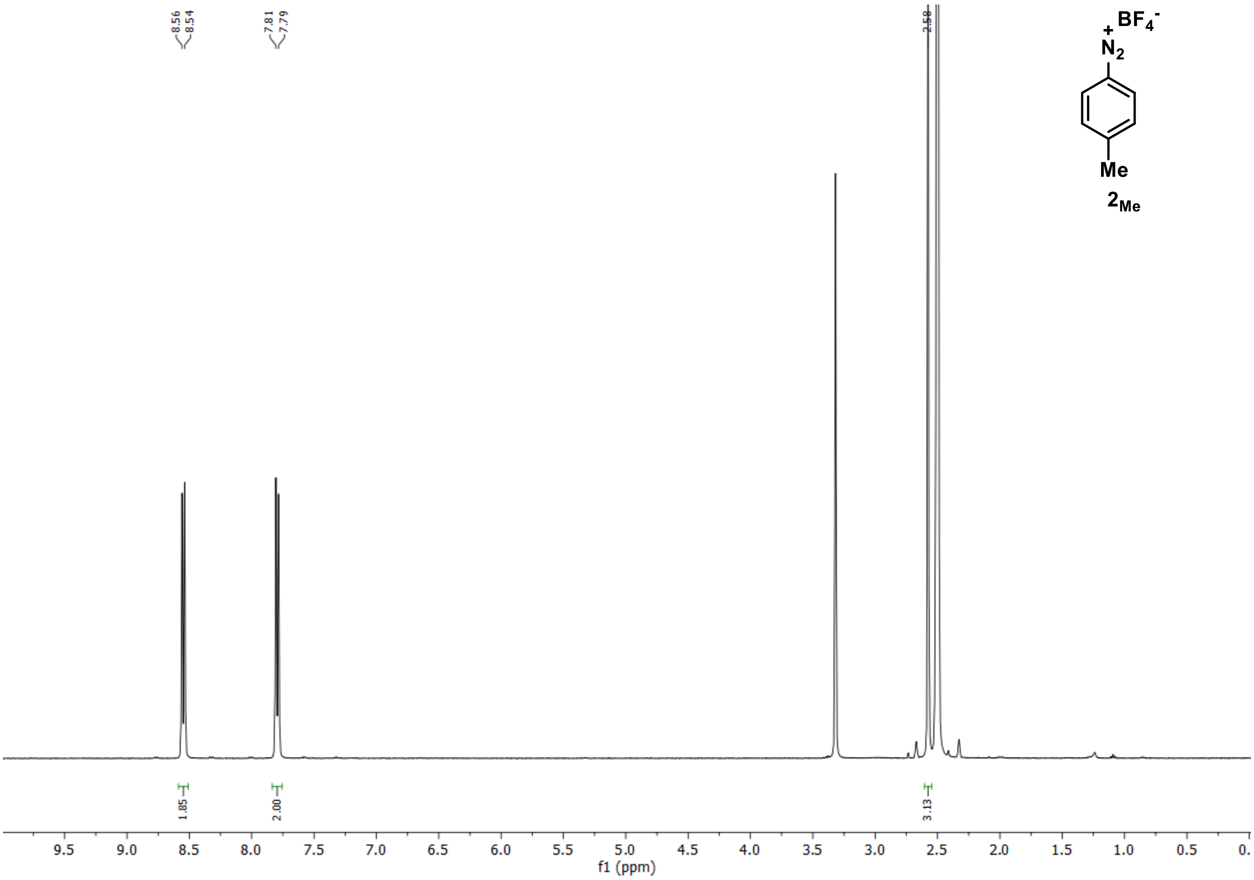

Figure S 23: ^{1}H NMR (399.82 MHz, DMSO-d^6) of $\mathbf{2_{Me}}$.

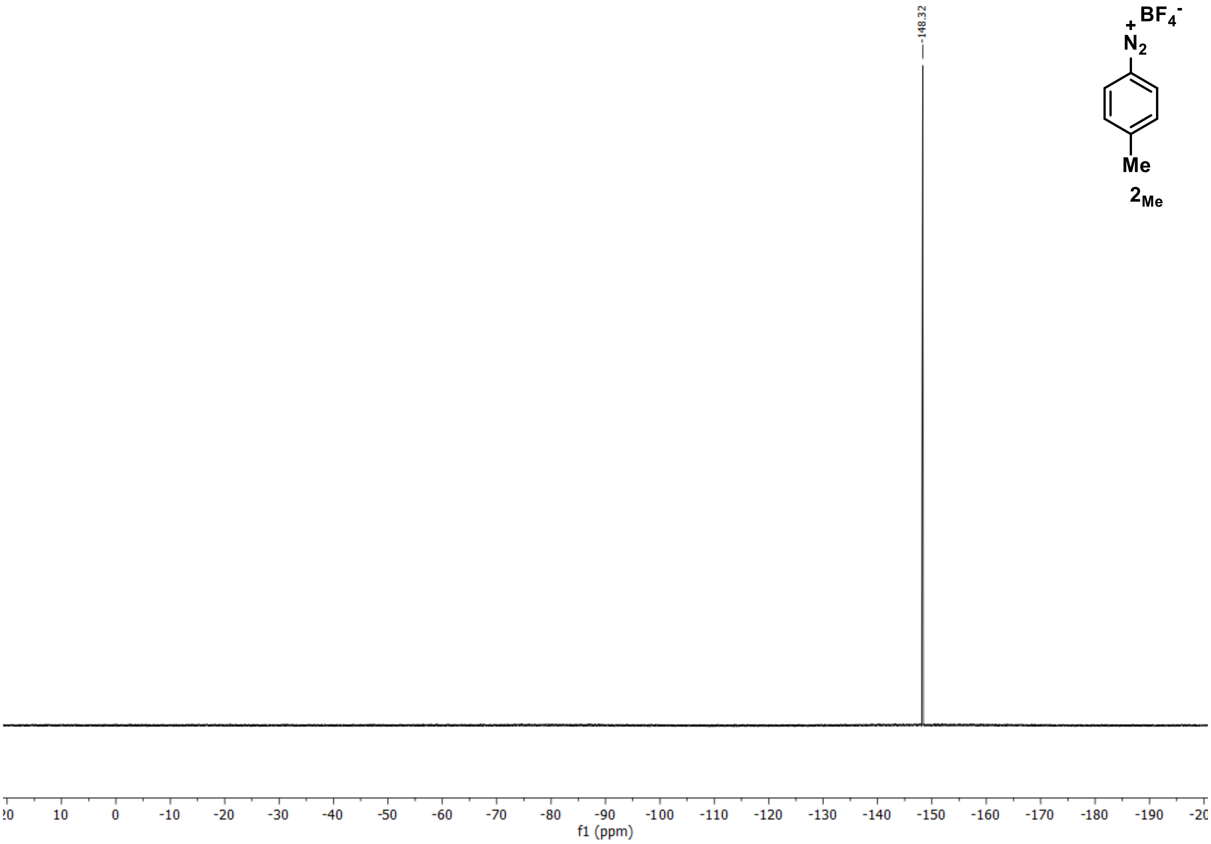

Figure S 24: ^{19}F NMR (376.17 MHz, DMSO-d^6) of **2$_{Me}$**.

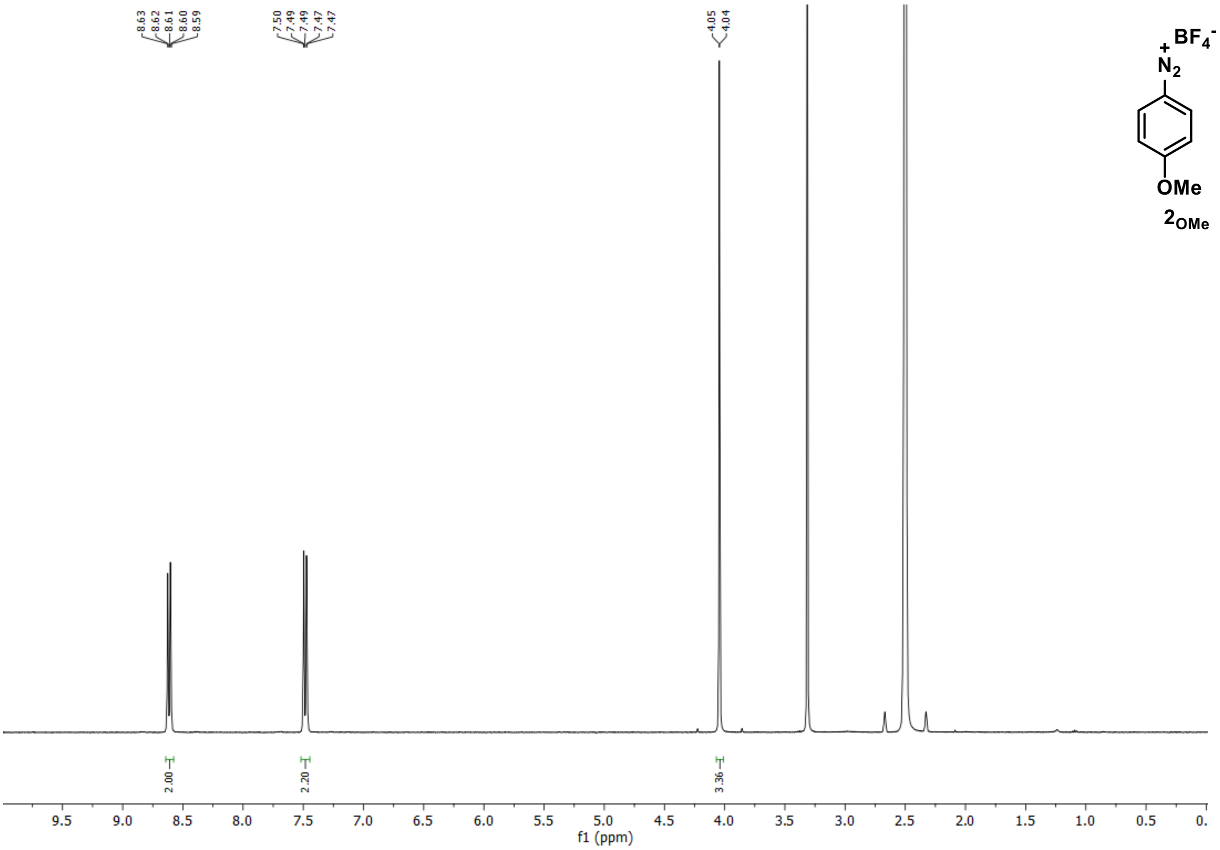

Figure S 25: ^{1}H NMR (399.82 MHz, DMSO-d^6) of **2$_{OMe}$**.

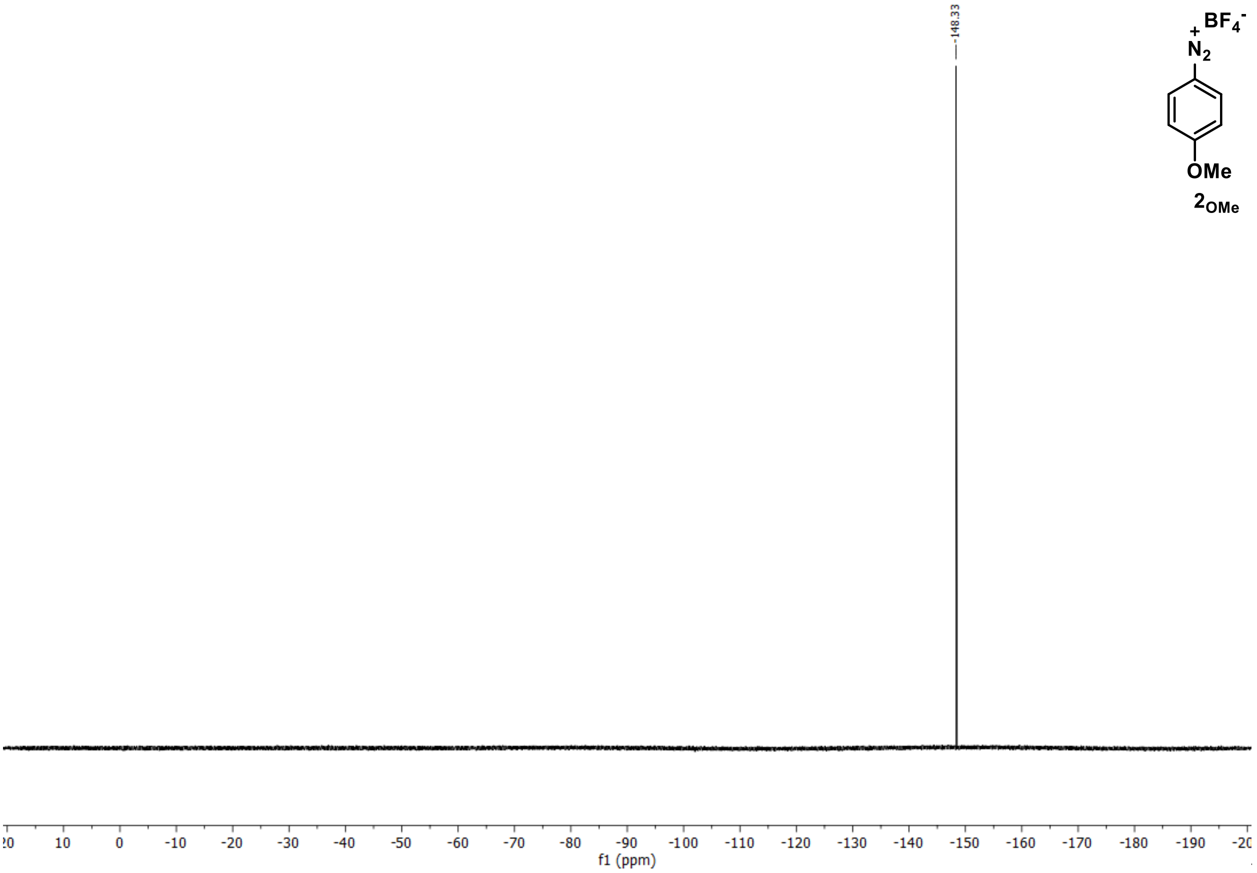

Figure S 26: ^{19}F NMR (376.17 MHz, DMSO-d^6) of **2$_{\mathrm{OMe}}$**.

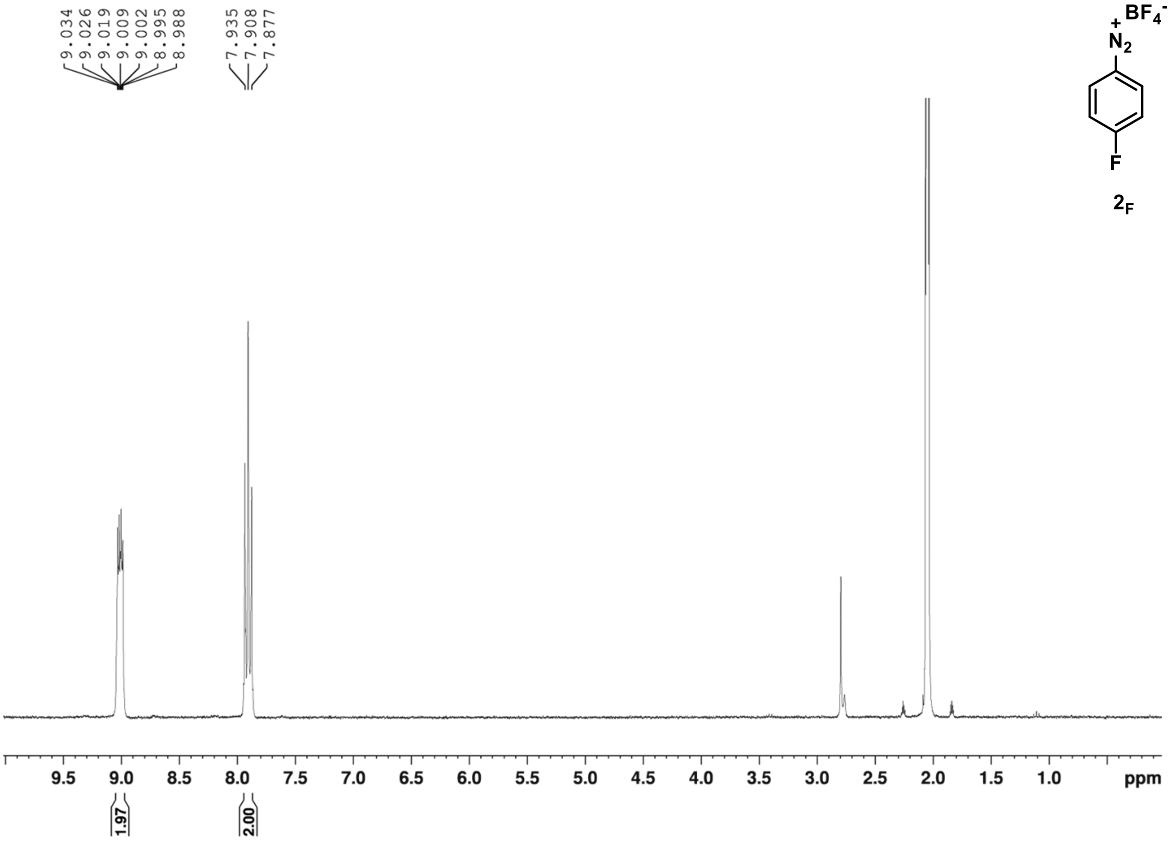

Figure S 27: ^{1}H NMR (300.51 MHz, $(CD_3)_2CO$) of **2$_{\mathrm{F}}$**.

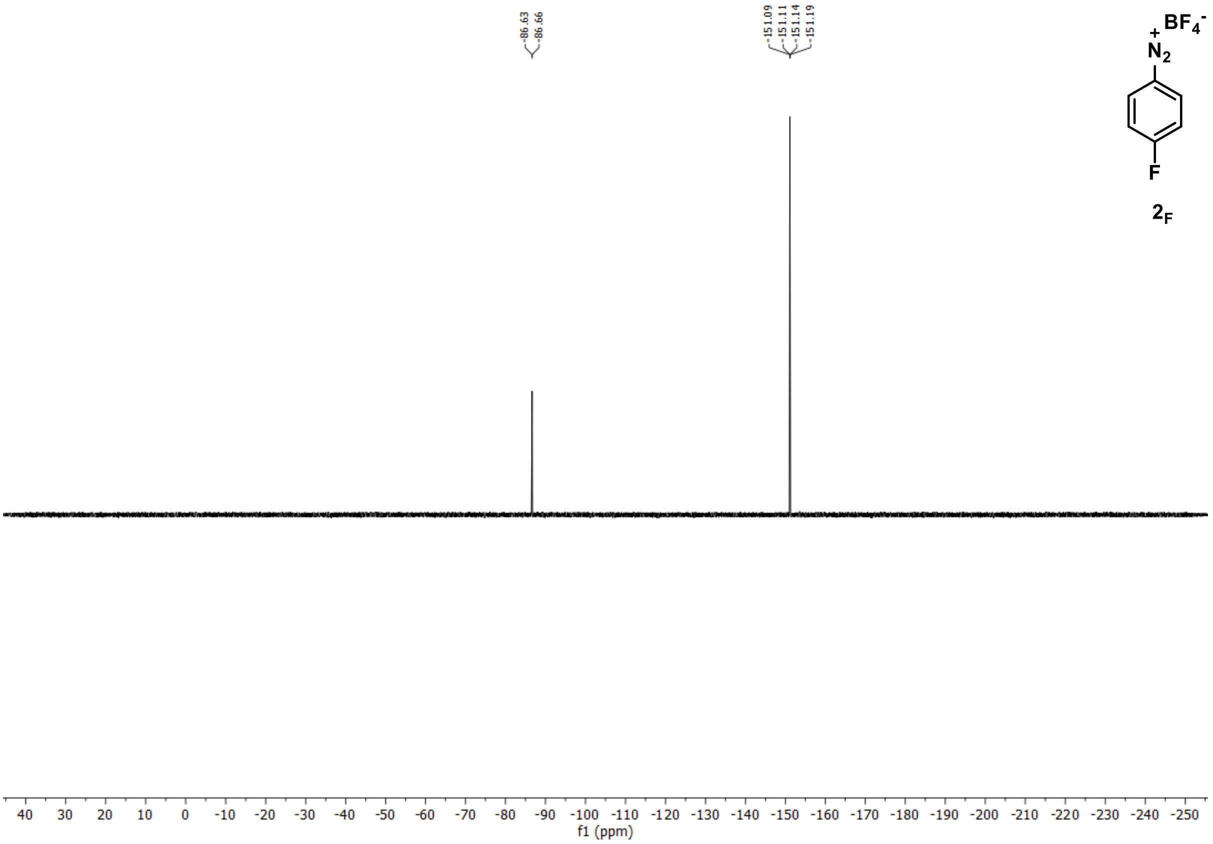

Figure S 28: ^{19}F NMR (282.76 MHz, $(CD_3)_2CO$) of $\mathbf{2_F}$.

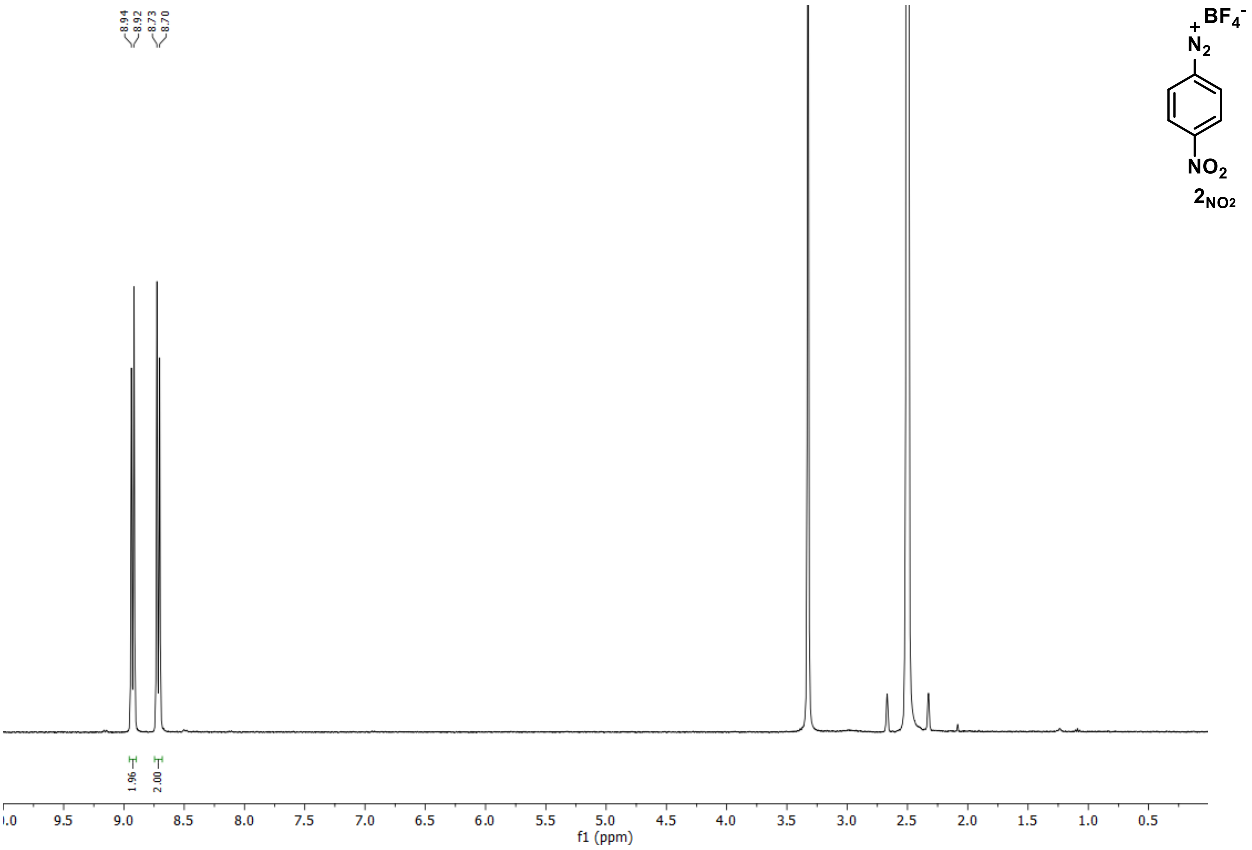

Figure S 29: ^{1}H NMR (399.82 MHz, DMSO-d^6) of $\mathbf{2_{NO2}}$.

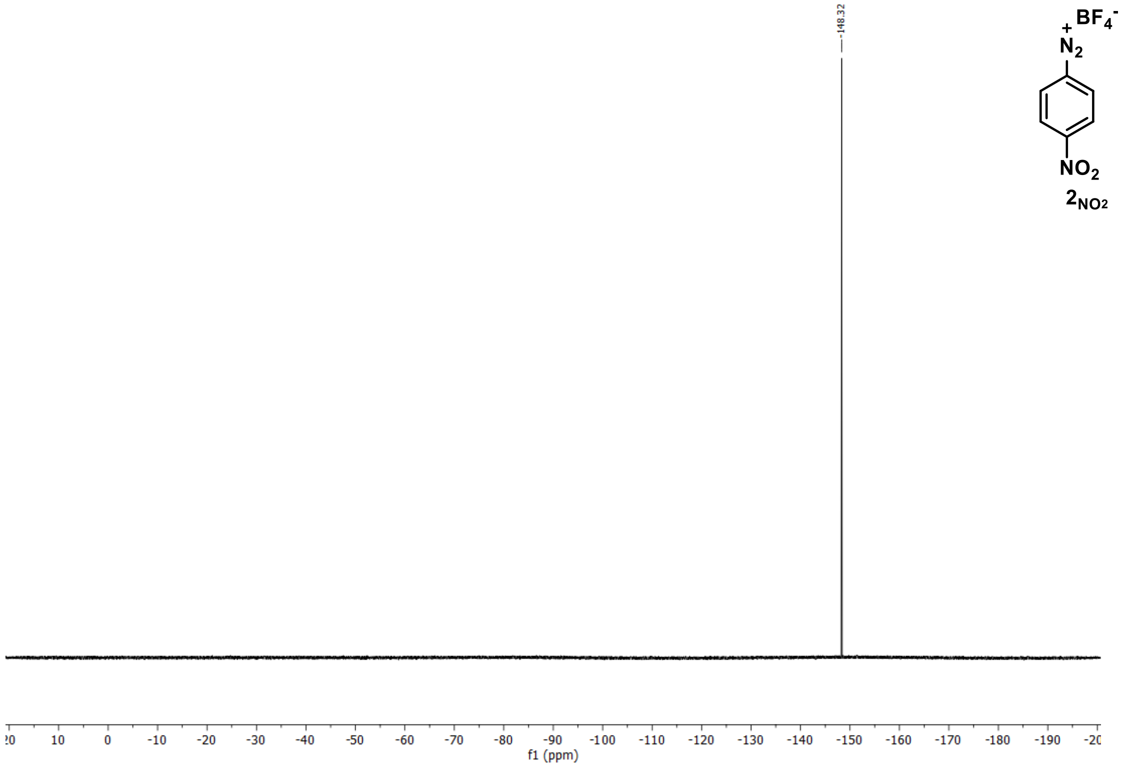

Figure S 30: ^{19}F NMR (376.17 MHz, DMSO-d^6) of **2_{NO2}**.

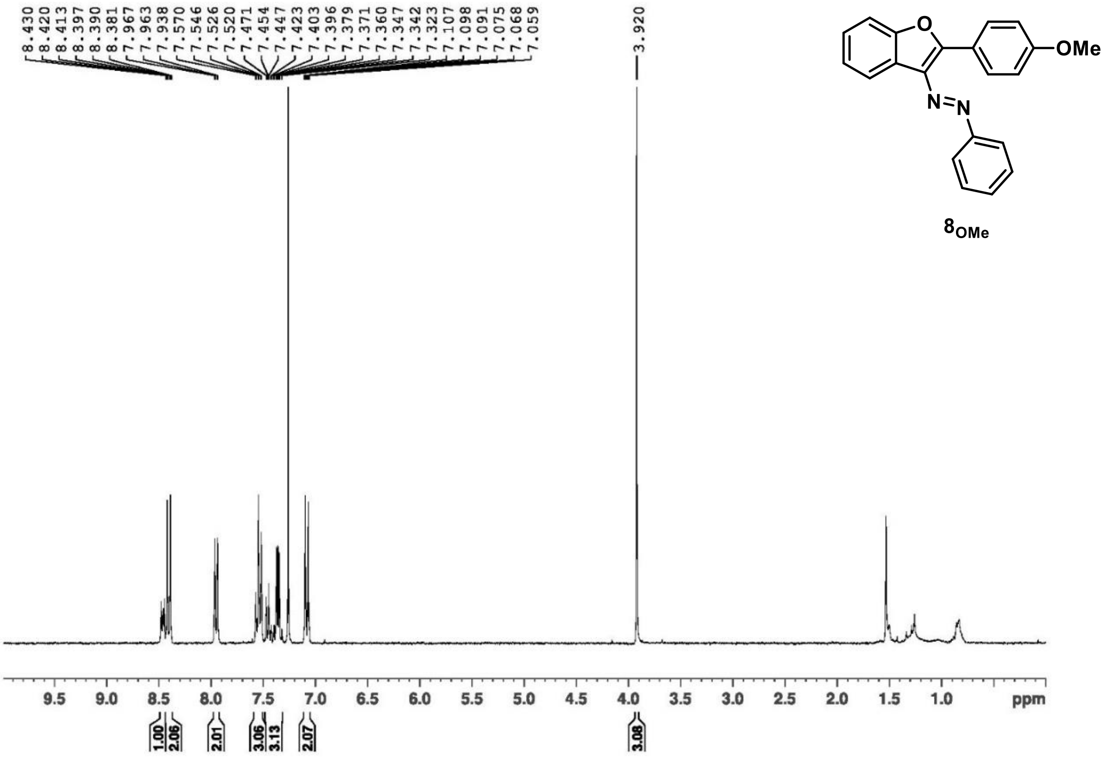

Figure S 31: ^{1}H NMR (300.51 MHz, CDCl$_3$) of **8_{OMe}**.

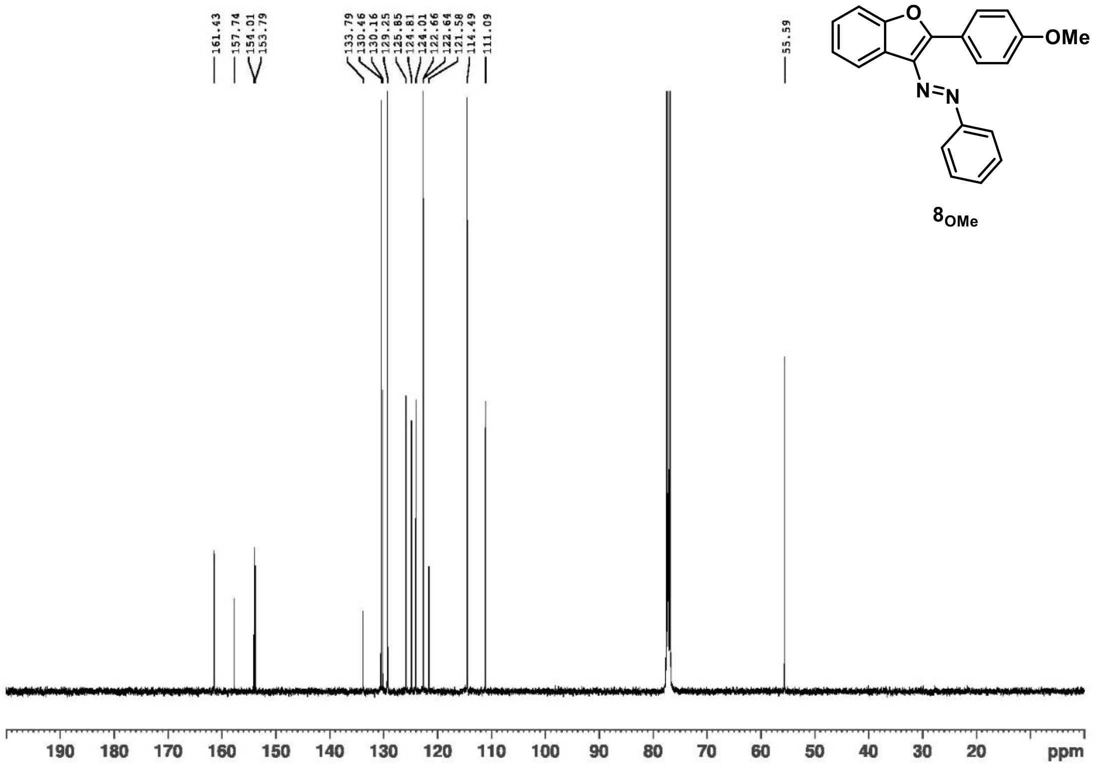

Figure S 32: ^{13}C NMR (100.66 MHz, $CDCl_3$) of **8_{OMe}**.

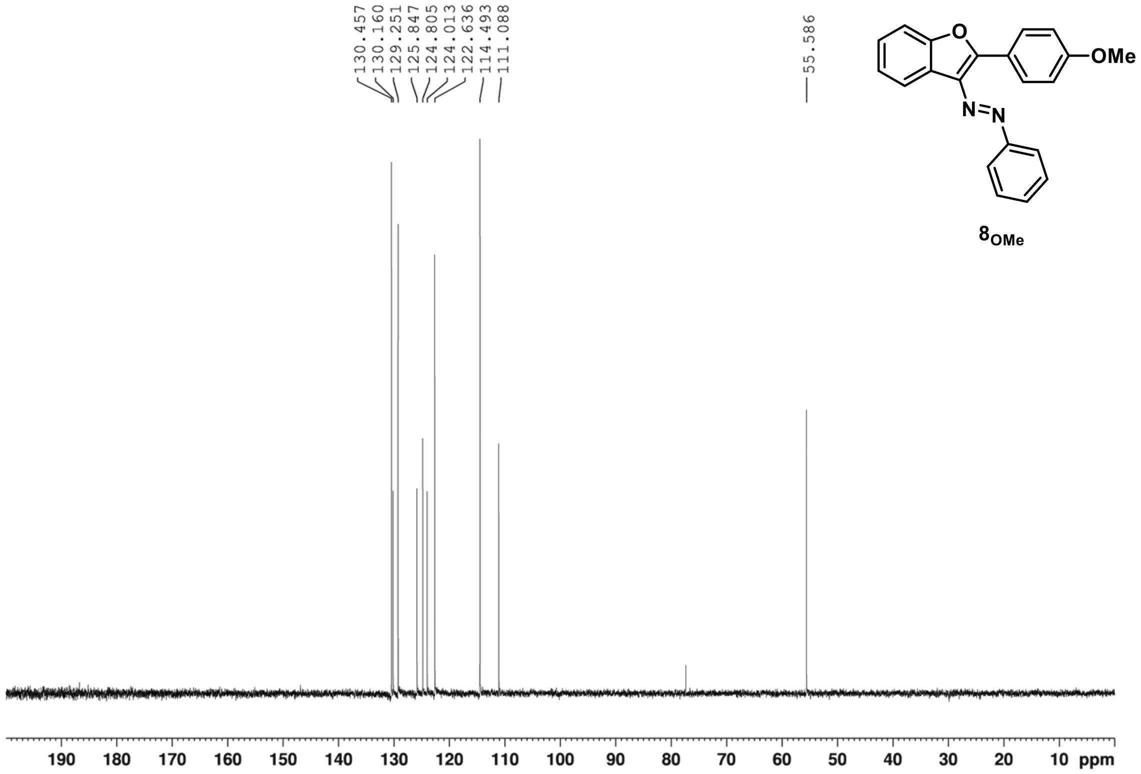

Figure S 33: DEPT135 NMR (100.66 MHz, $CDCl_3$) of **8_{OMe}**.

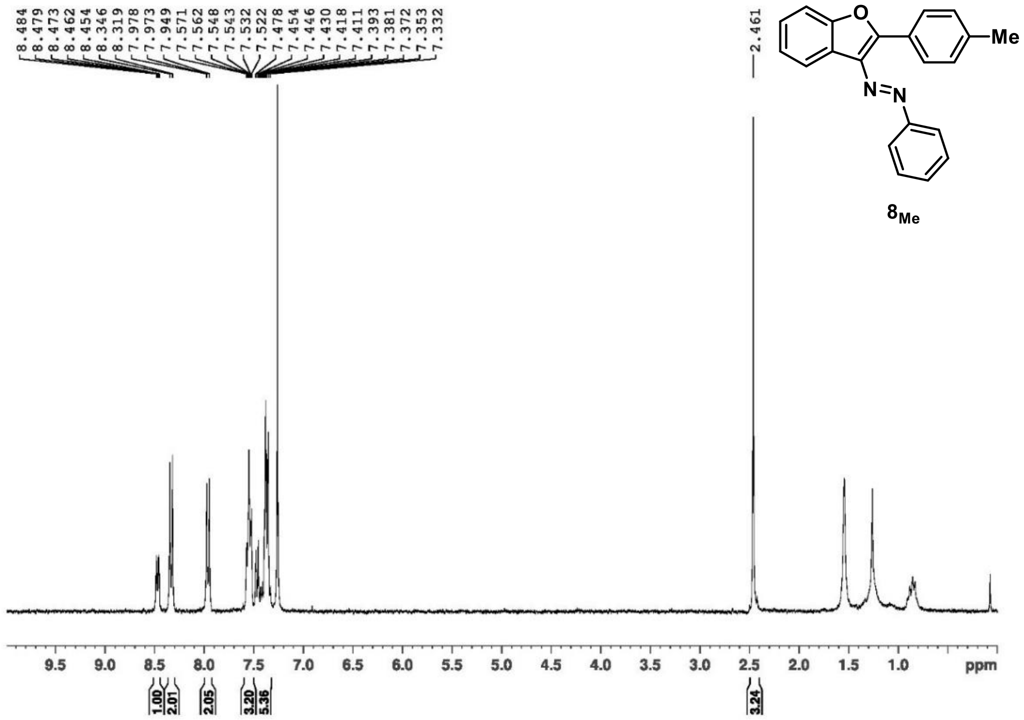

Figure S 34: ^{1}H NMR (300.51 MHz, CDCl$_3$) of **8$_{Me}$.**

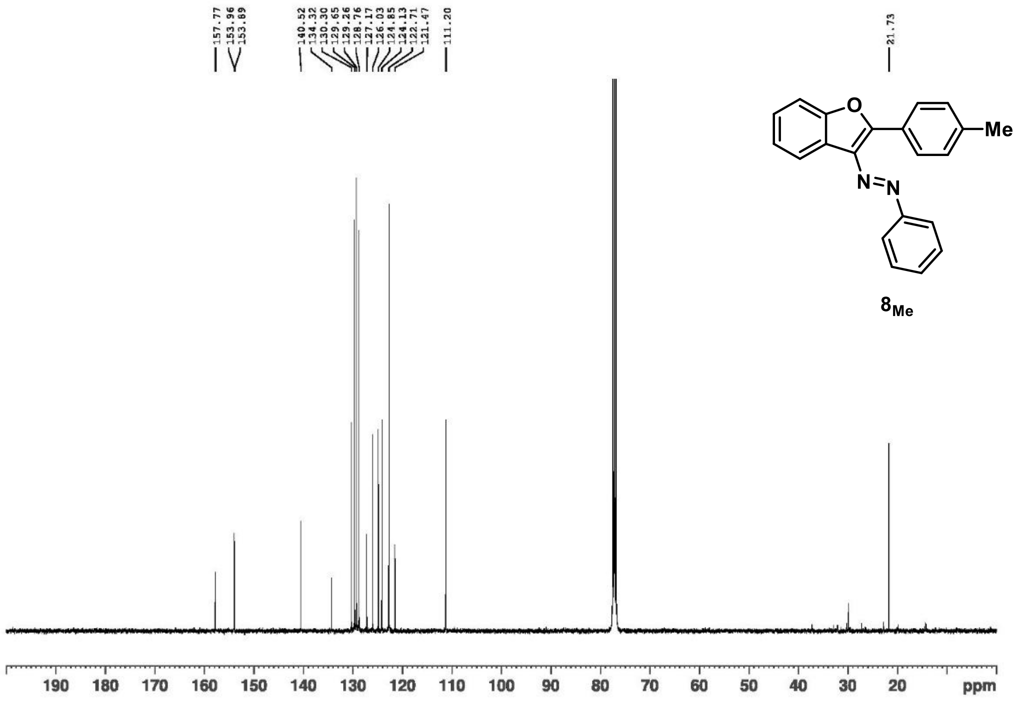

Figure S 35: ^{13}C NMR (100.66 MHz, CDCl$_3$) of **8$_{Me}$.**

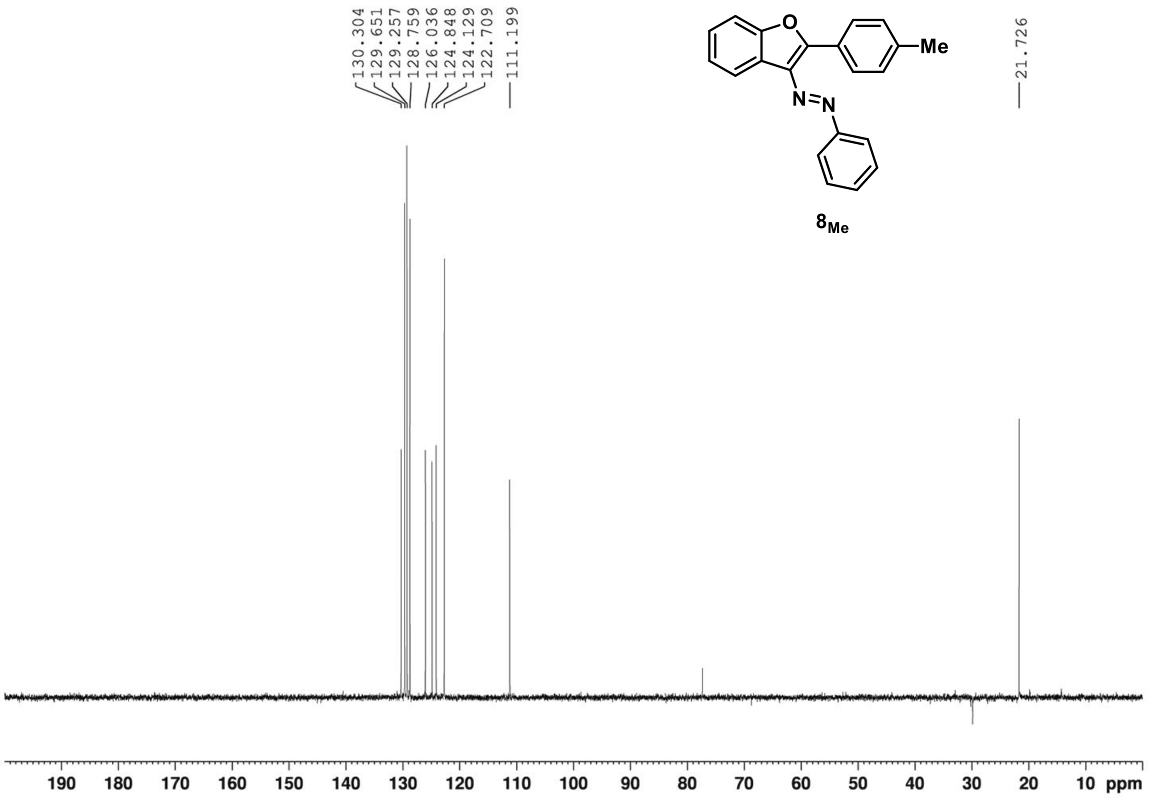

Figure S 36: DEPT135 NMR (100.66 MHz, $CDCl_3$) of **8_{Me}**.

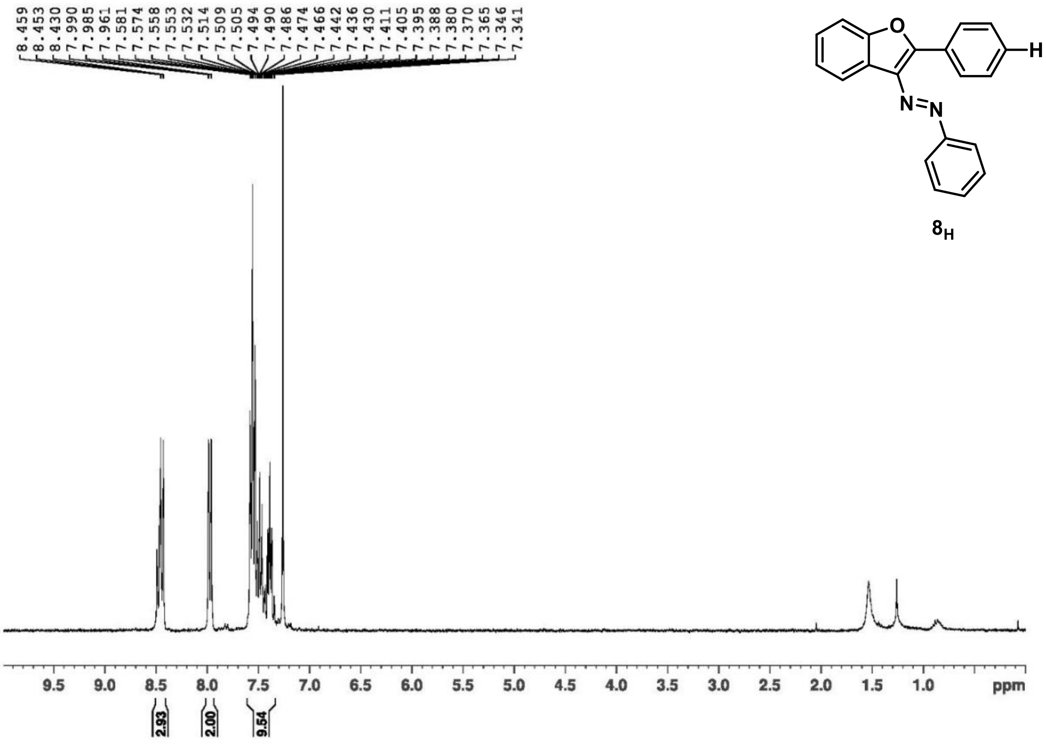

Figure S 37: ^1H NMR (300.51 MHz, $CDCl_3$) of **8_H**.

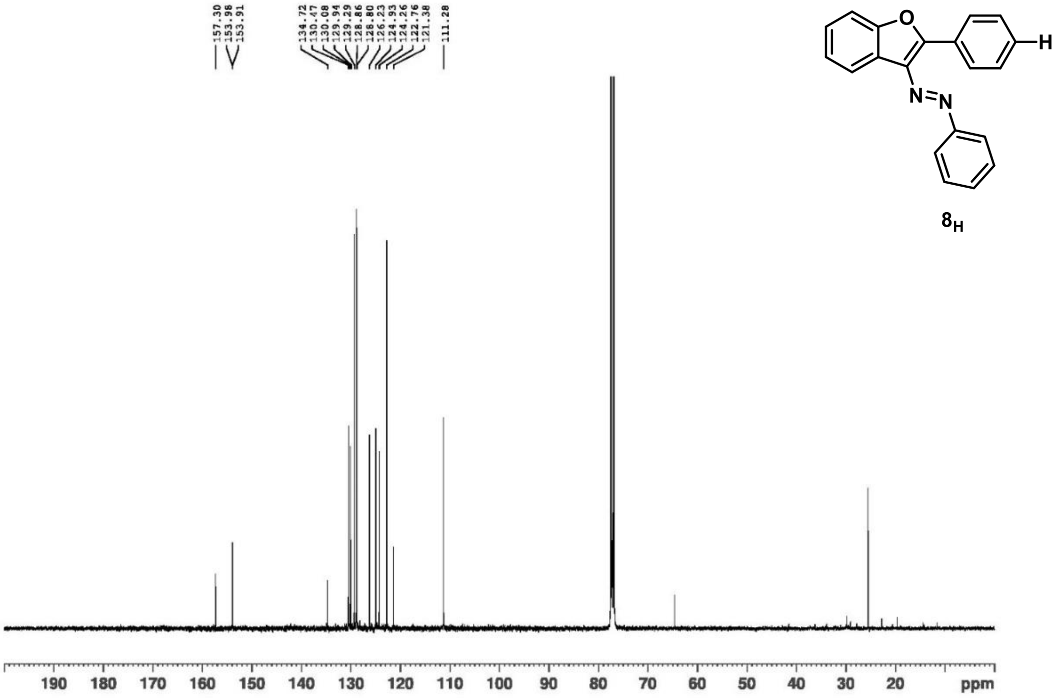

Figure S 38: ^{13}C NMR (100.66 MHz, $CDCl_3$) of **8_H**.

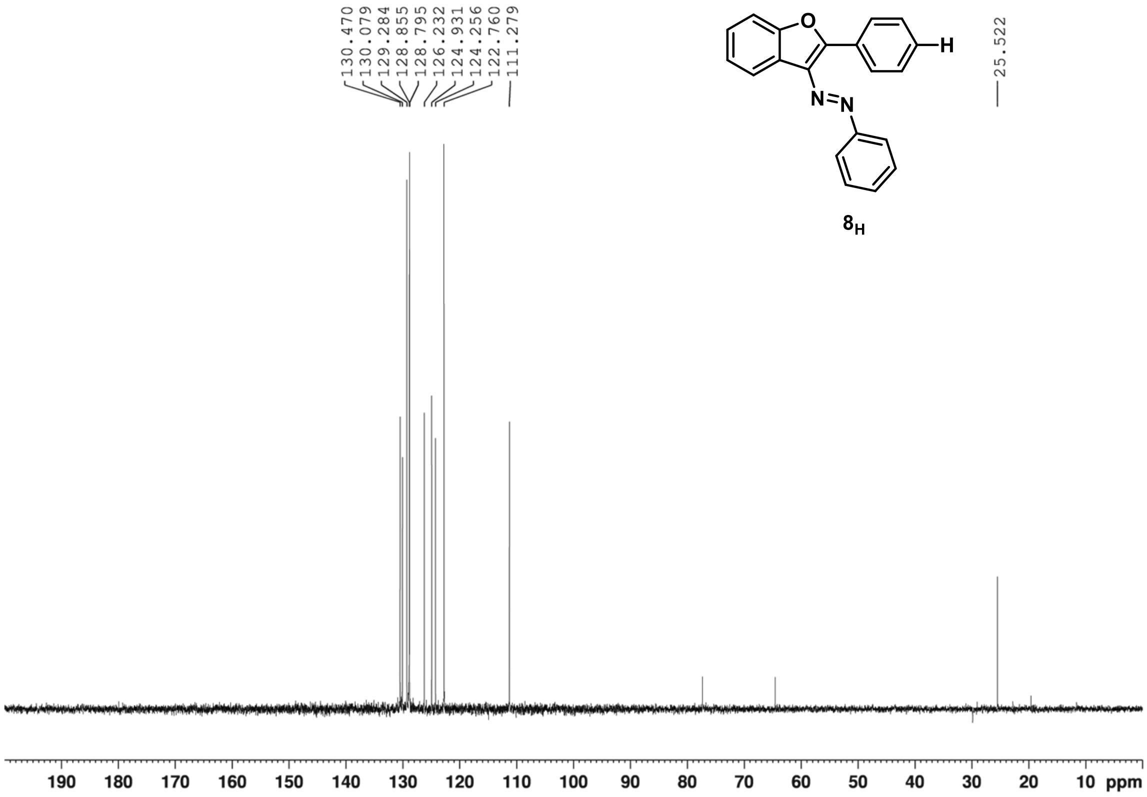

Figure S 39: DEPT135 NMR (100.66 MHz, $CDCl_3$) of **8_H**.

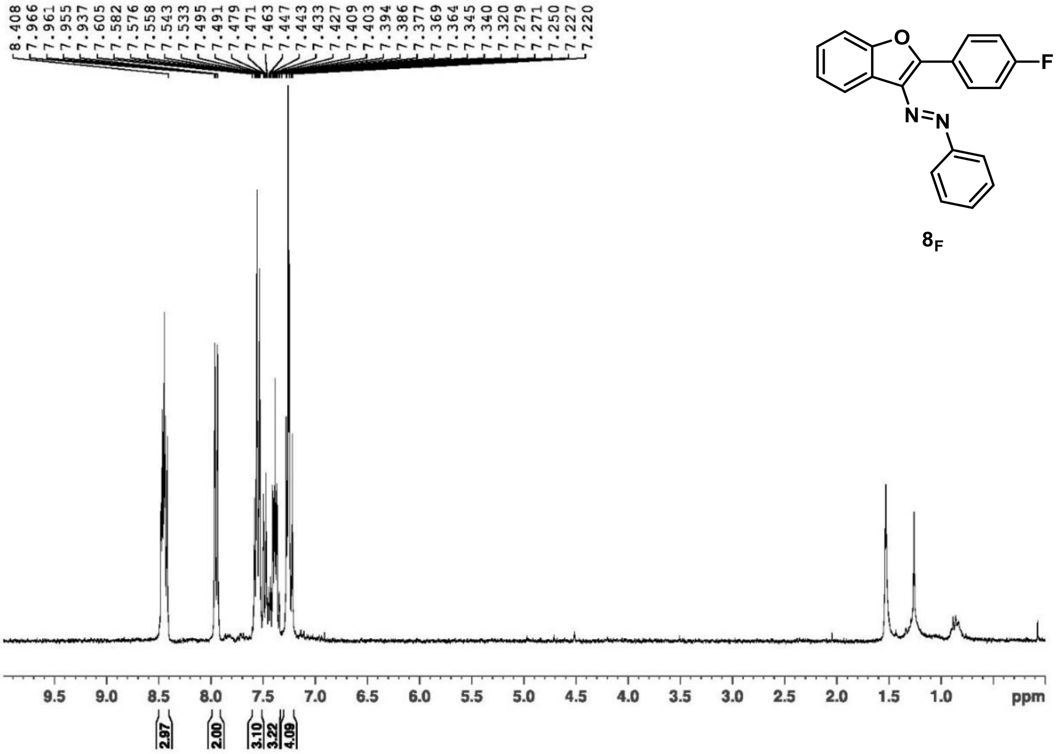

Figure S 40: ^{1}H NMR (300.51 MHz, CDCl$_3$) of $\mathbf{8_F}$.

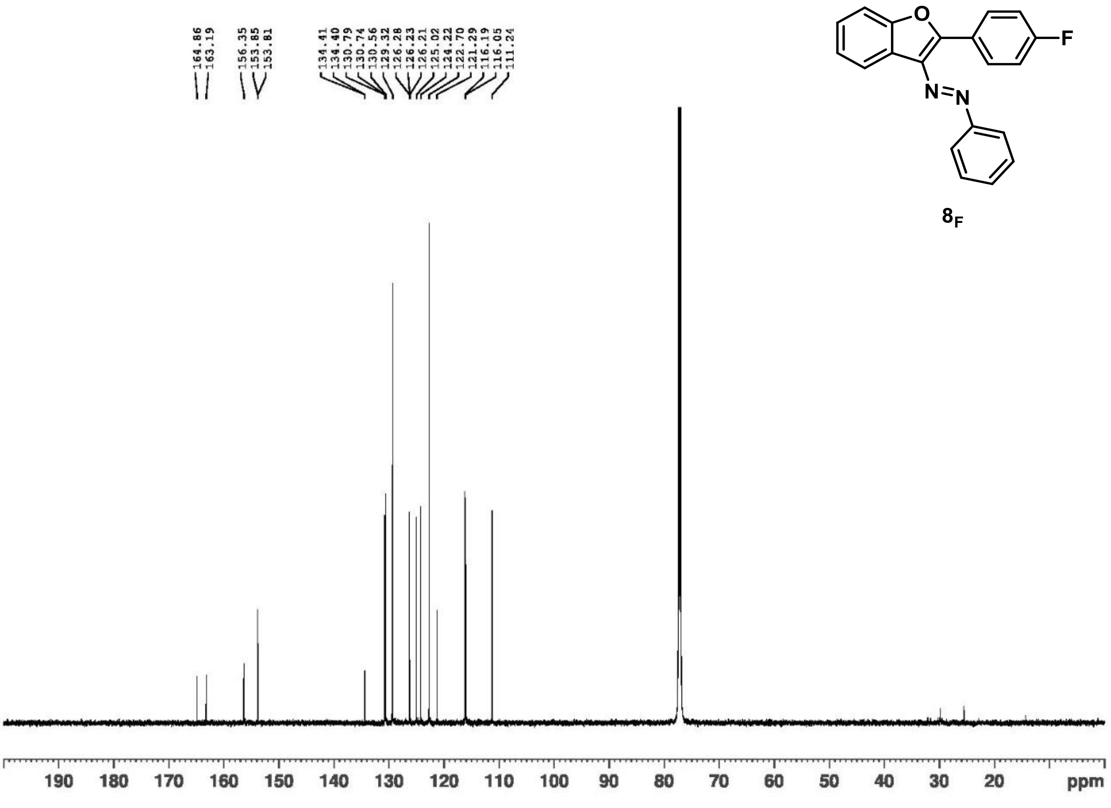

Figure S 41: ^{13}C NMR (150.93 MHz, CDCl$_3$) of $\mathbf{8_F}$.

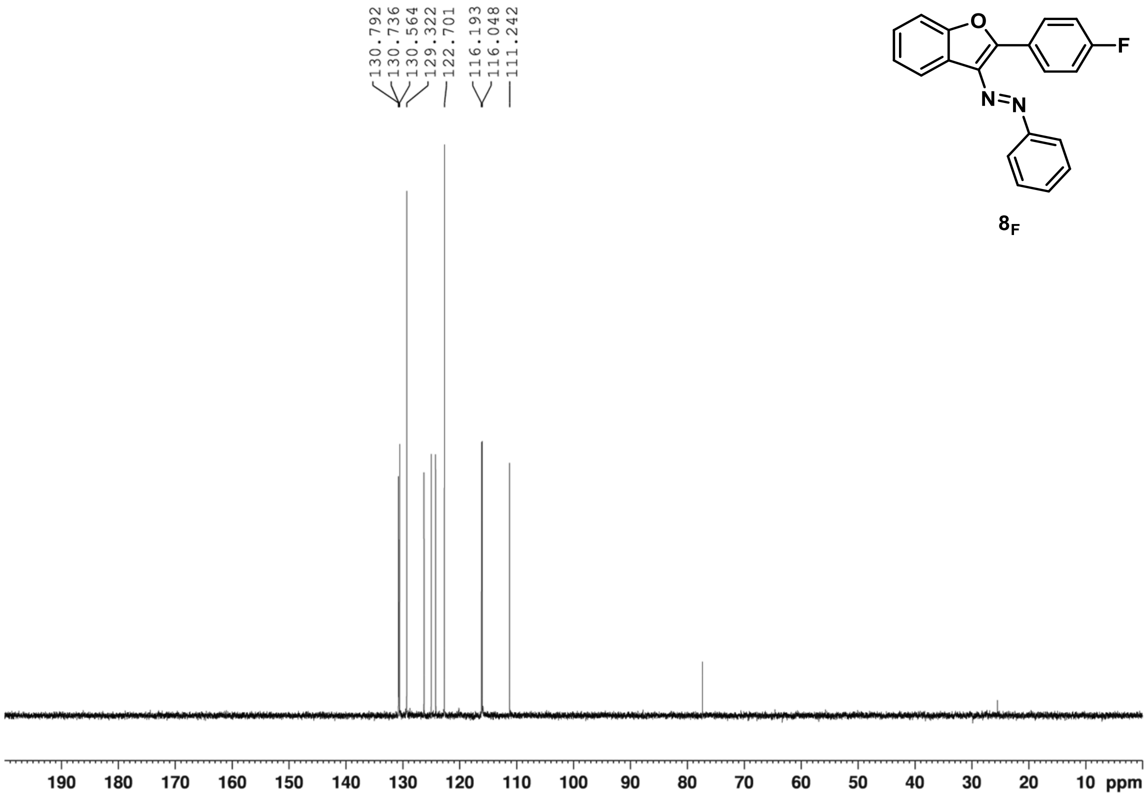

Figure S 42: DEPT135 NMR (150.93 MHz, CDCl$_3$) of **8$_F$**.

Figure S 43: ^{19}F NMR (282.76 MHz, CDCl$_3$) of **8$_F$**.

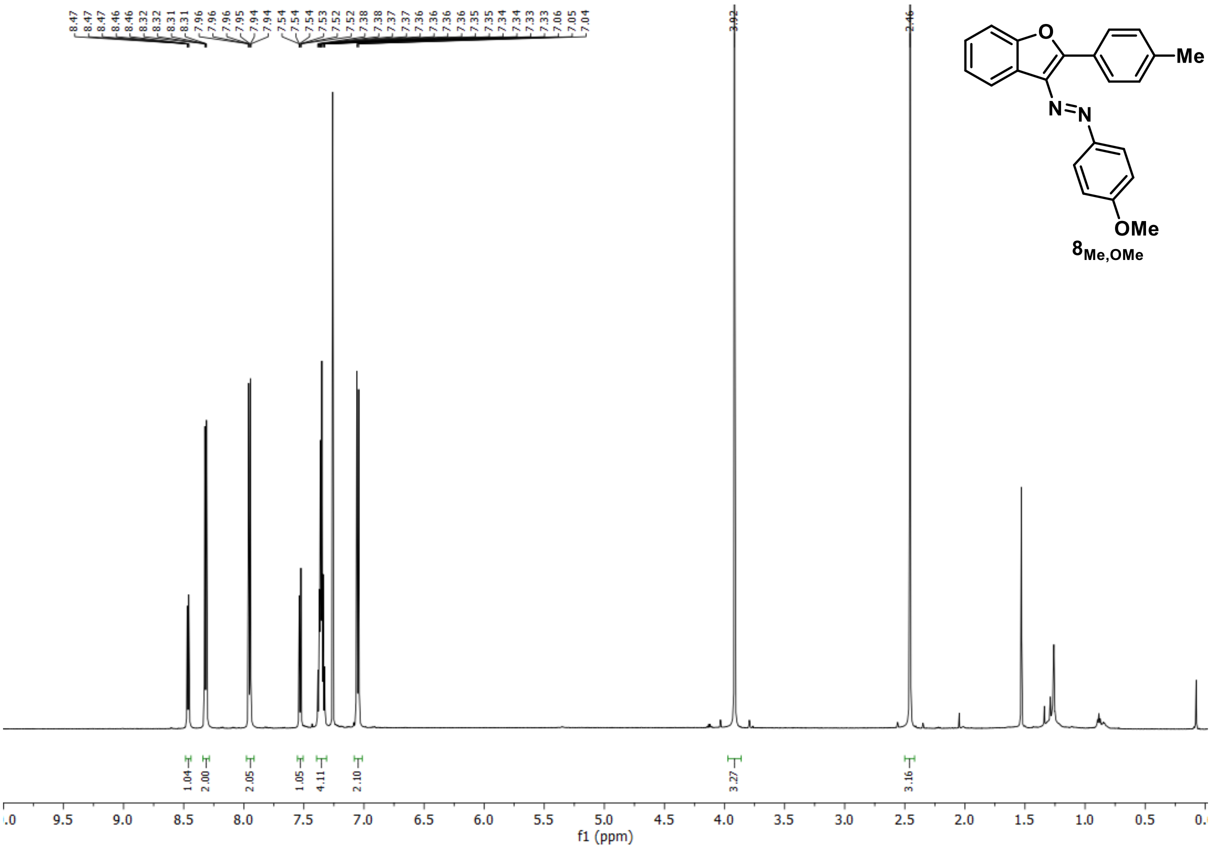

Figure S 44: ^{1}H NMR (600.13 MHz, CDCl$_3$) of $\mathbf{8_{Me,OMe}}$.

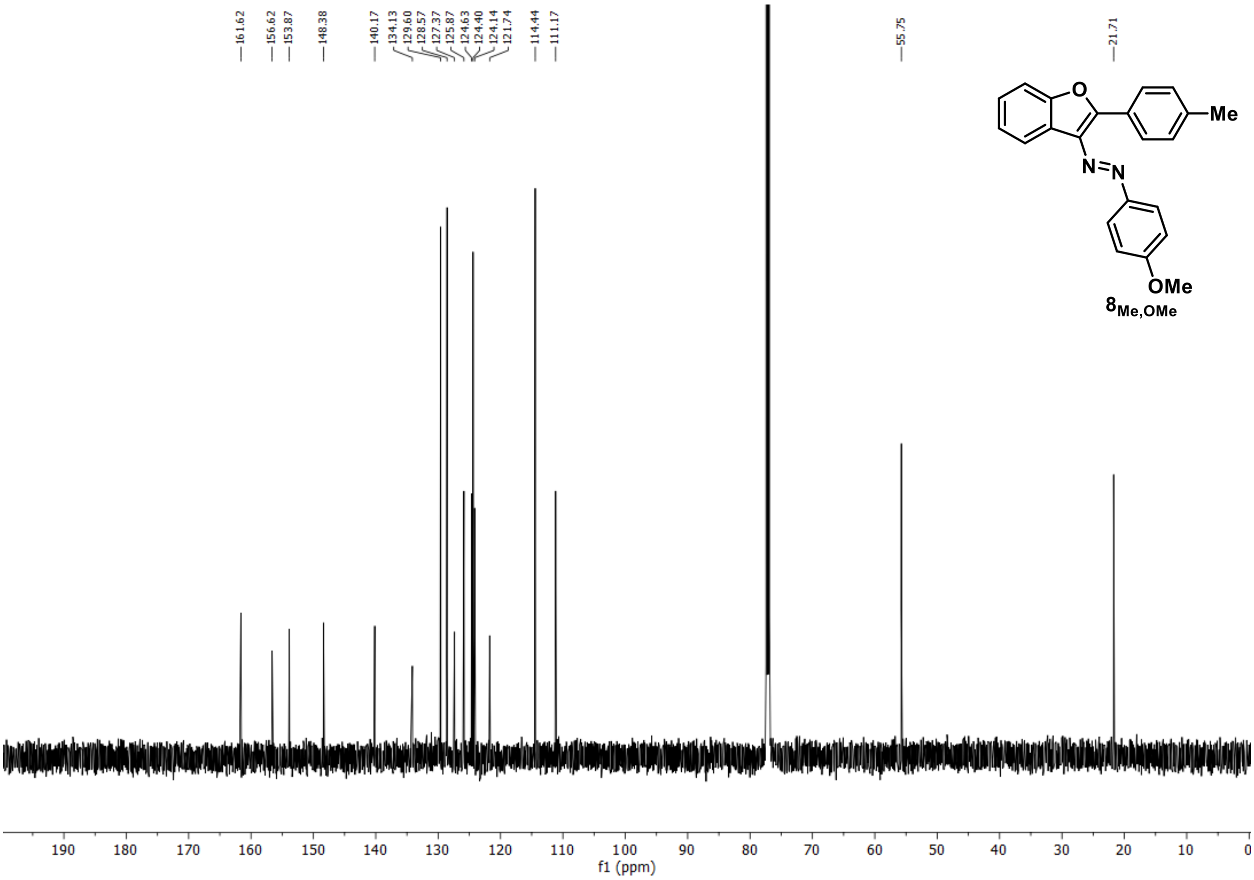

Figure S 45: ^{13}C NMR (150.91 MHz, CDCl$_3$) of $\mathbf{8_{Me,OMe}}$.

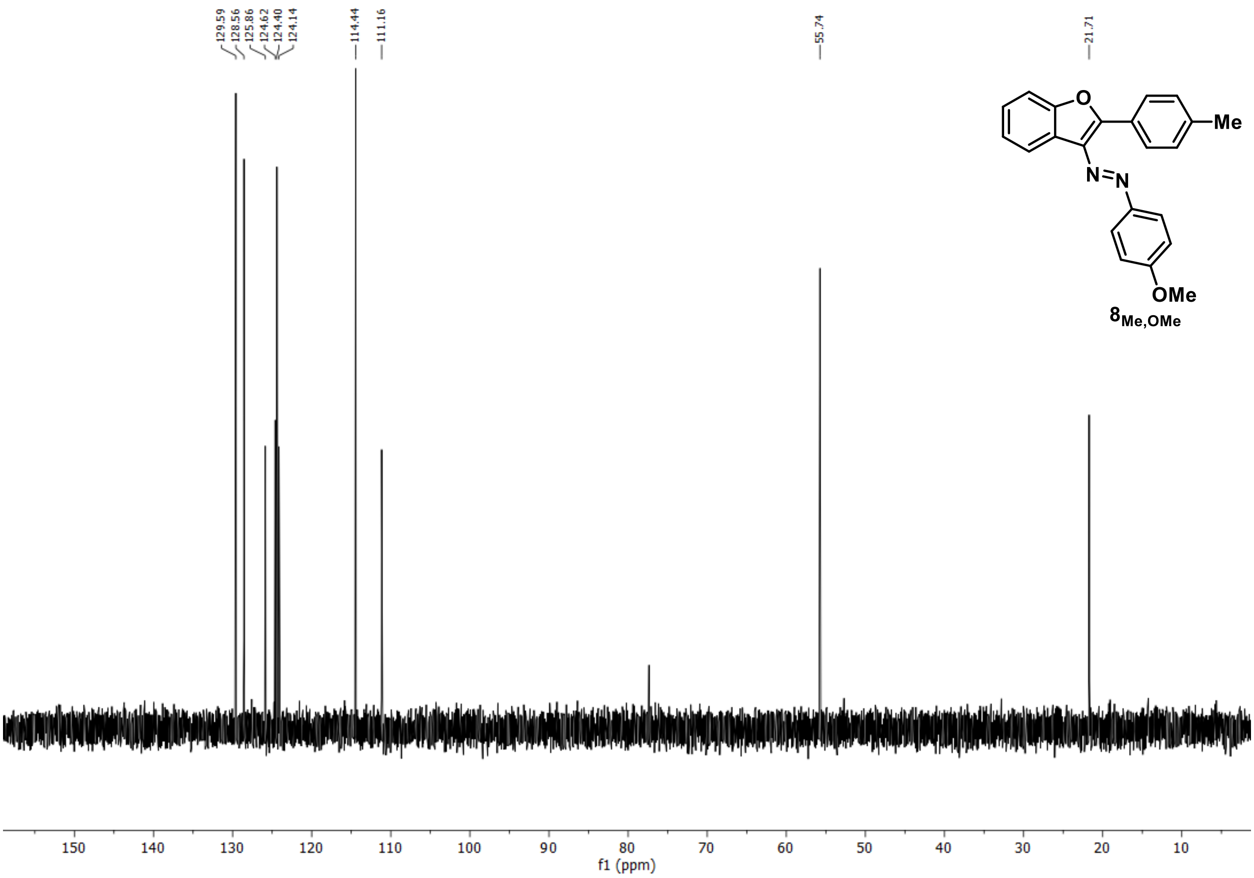

Figure S 46: DEPT135 NMR (150.92 MHz, $CDCl_3$) of $\mathbf{8}_{\mathbf{Me,OMe}}$.

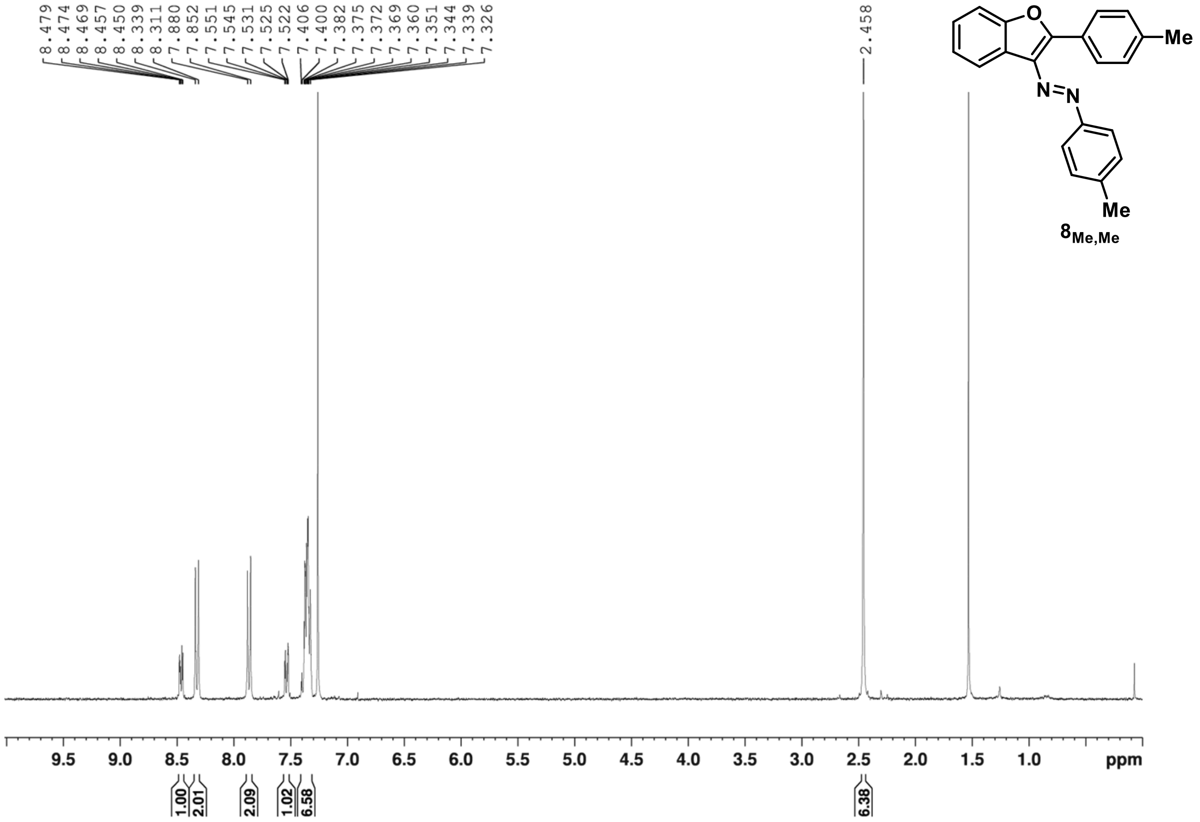

Figure S 47: ^1H NMR (300.51 MHz, $CDCl_3$) of $\mathbf{8}_{\mathbf{Me,Me}}$.

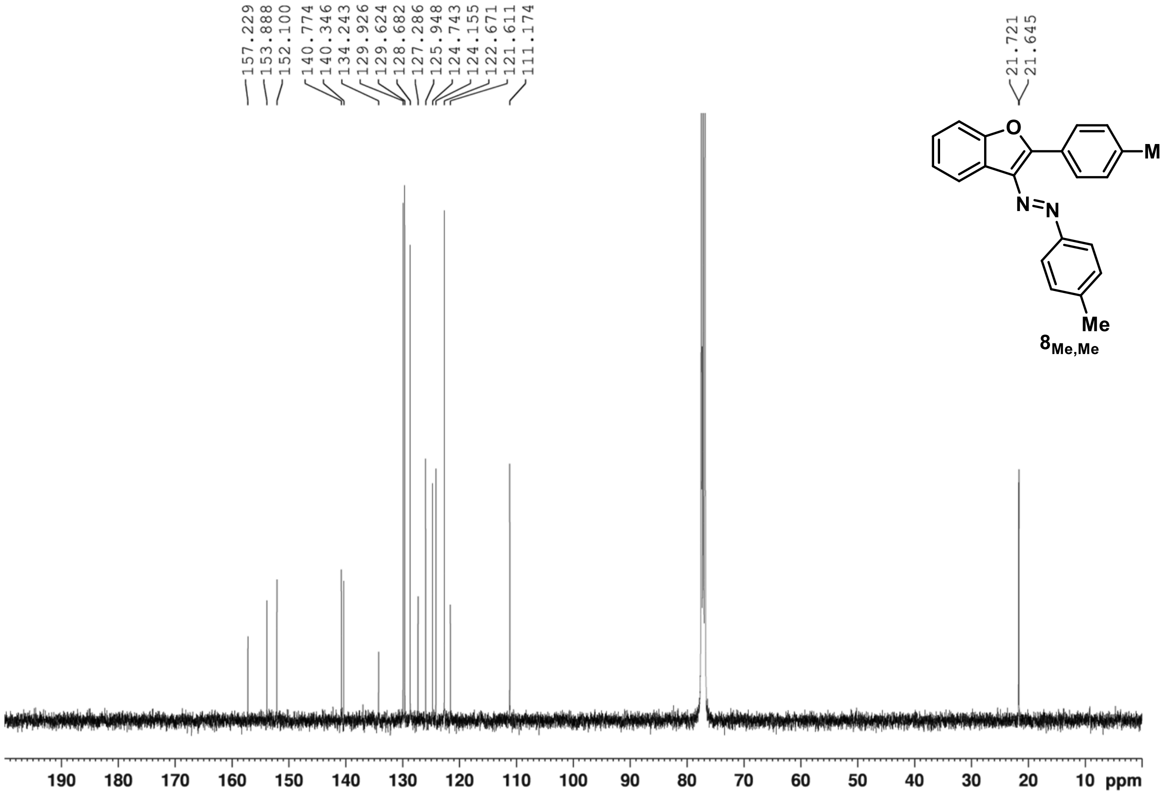

Figure S 48: ^{13}C NMR (100.66 MHz, $CDCl_3$) of **$8_{Me,Me}$**.

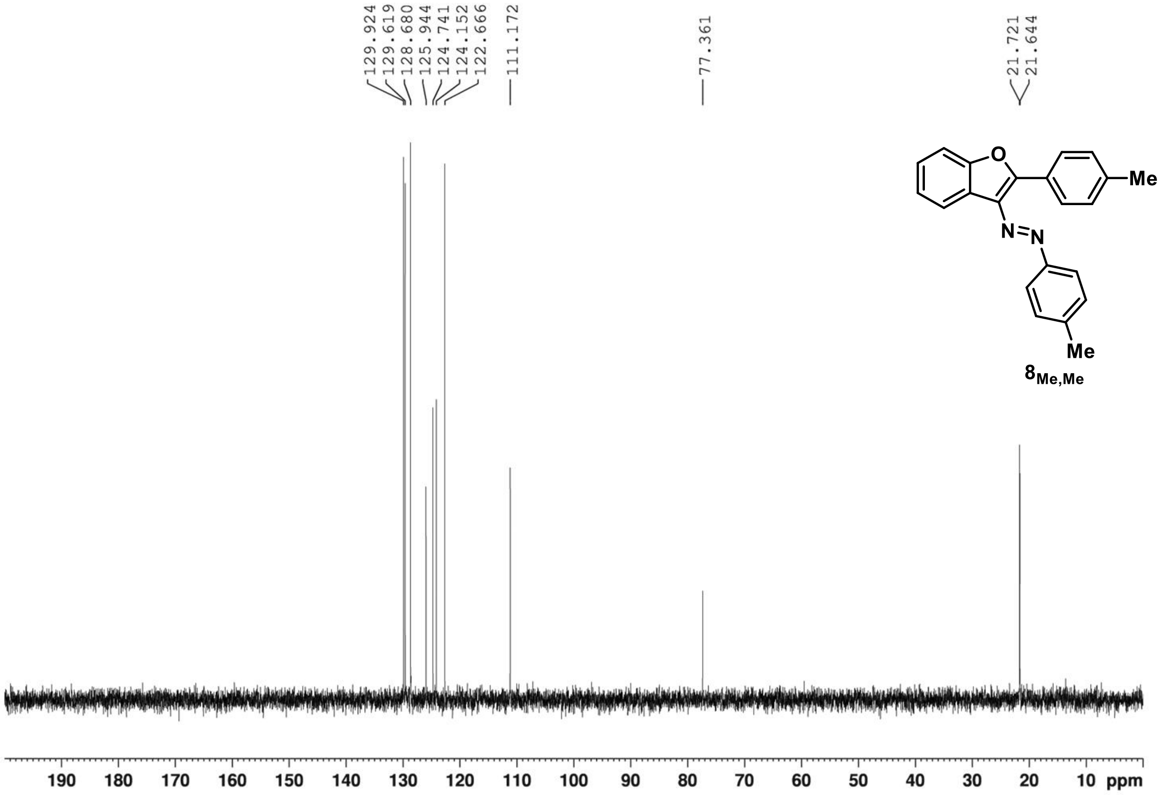

Figure S 49: DEPT135 NMR (100.66 MHz, $CDCl_3$) of **$8_{Me,Me}$**.

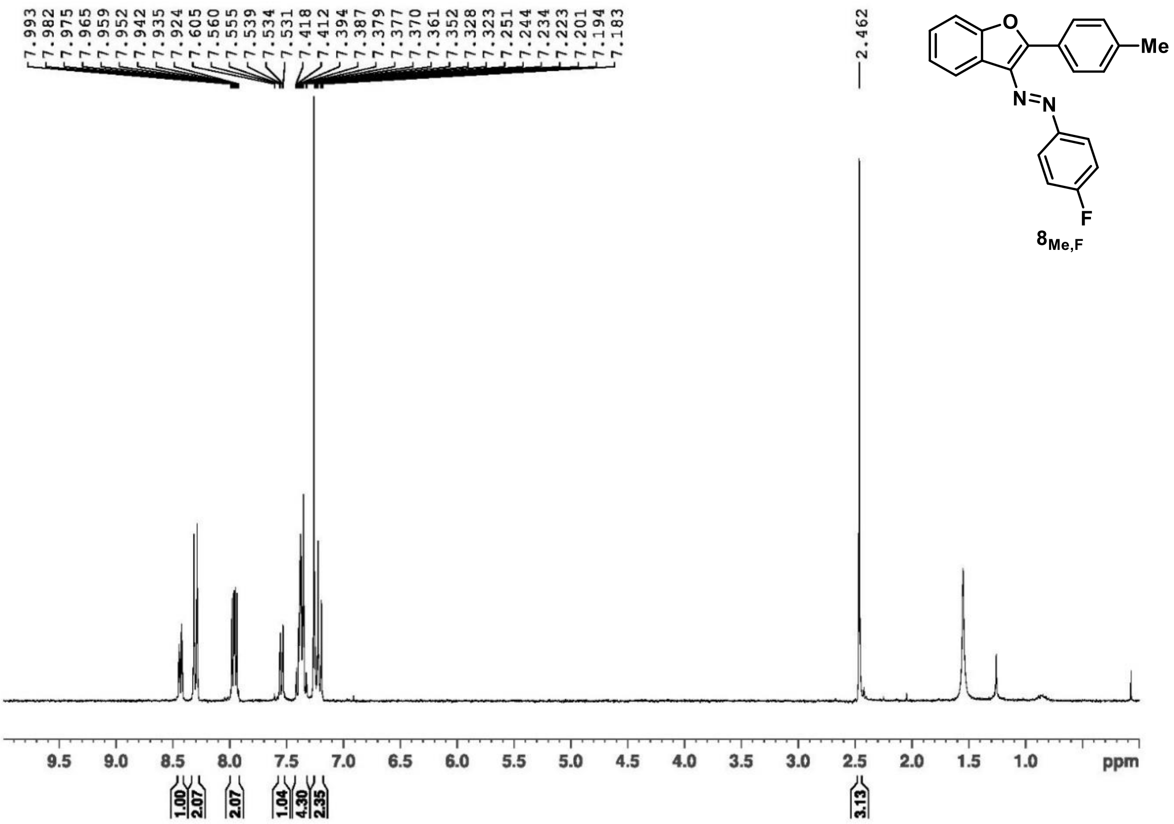

Figure S 50: ^{1}H NMR (300.51 MHz, $CDCl_3$) of **$8_{Me,F}$**.

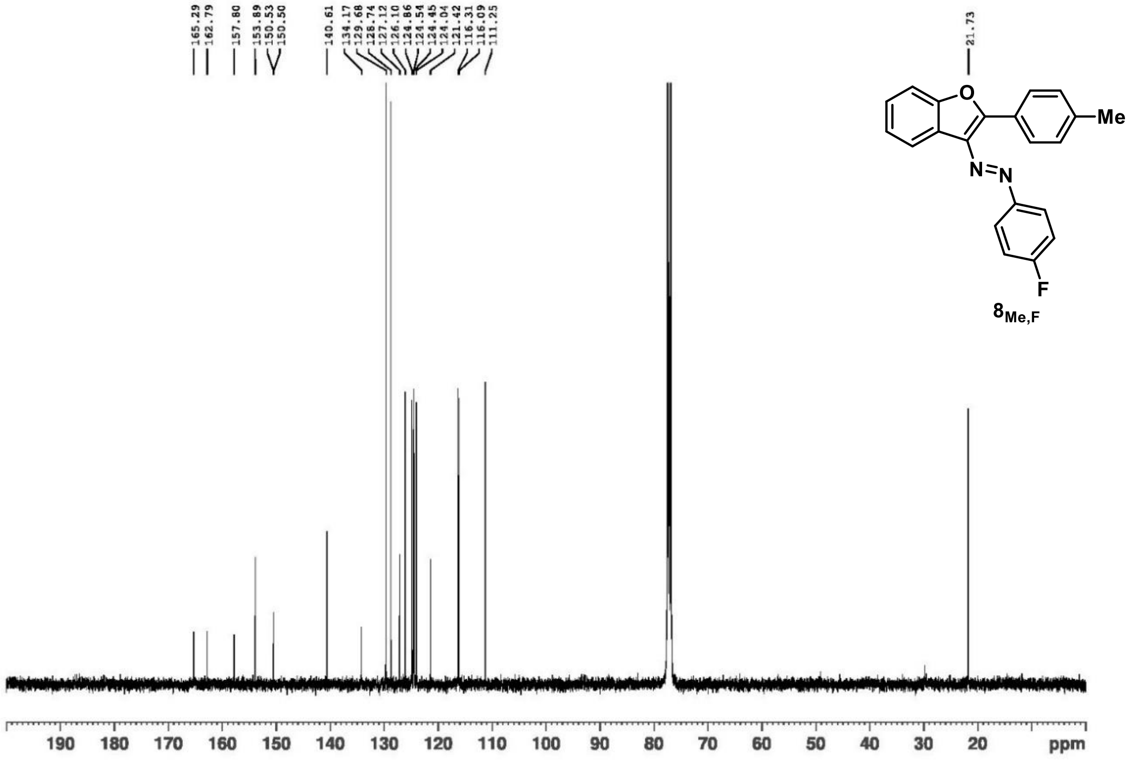

Figure S 51: ^{13}C NMR (100.66 MHz, $CDCl_3$) of **$8_{Me,F}$**.

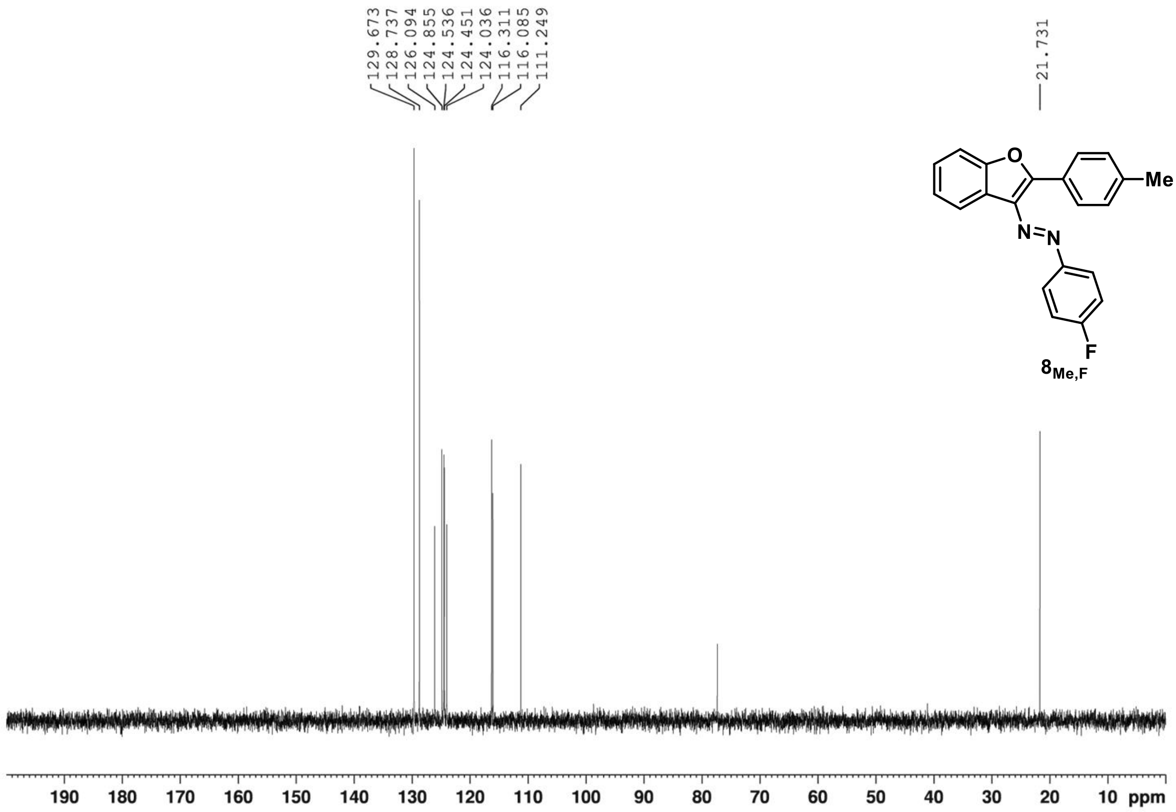

Figure S 52: DEPT135 (100.66 MHz, $CDCl_3$) of $\mathbf{8_{Me,F}}$.

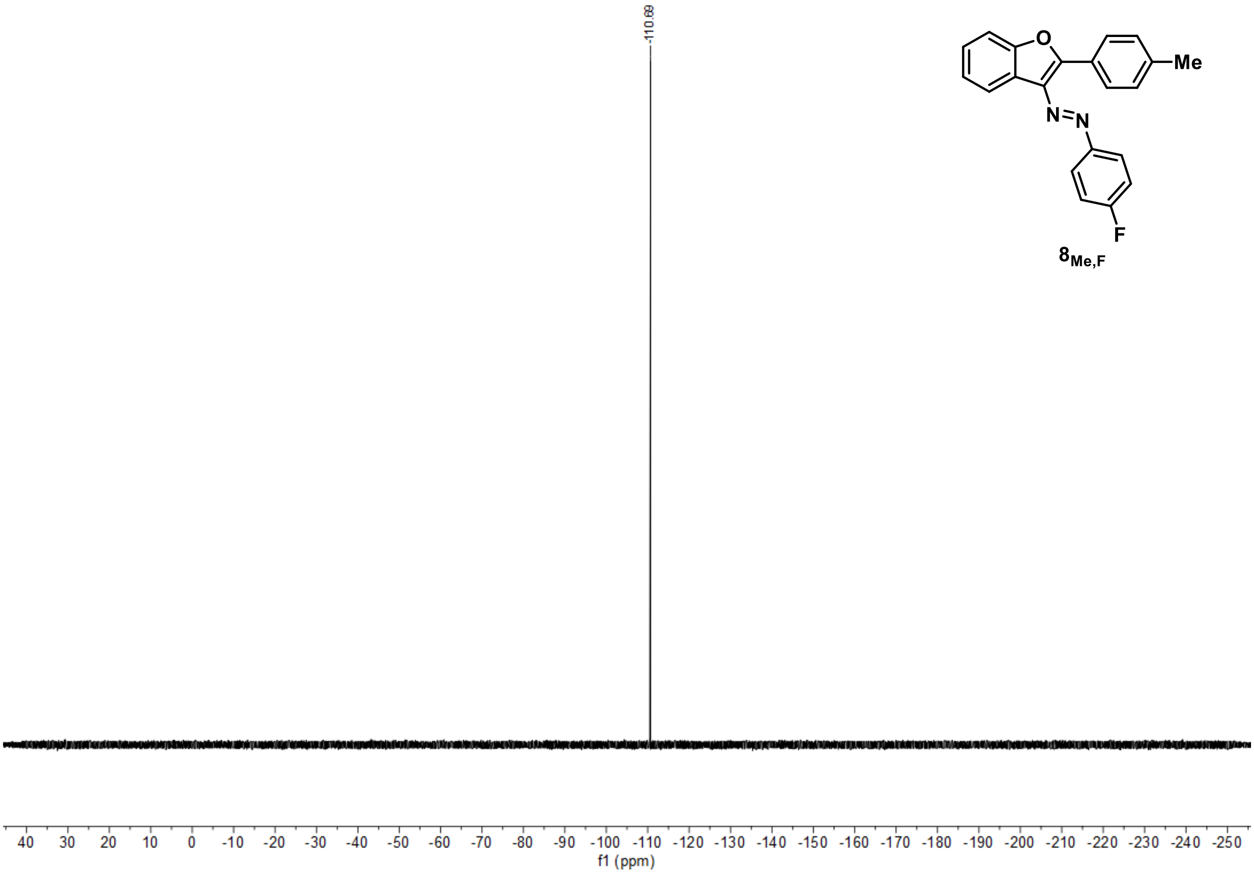

Figure S 53: ^{19}F NMR (282.76 MHz, $CDCl_3$) of $\mathbf{8_{Me,F}}$.

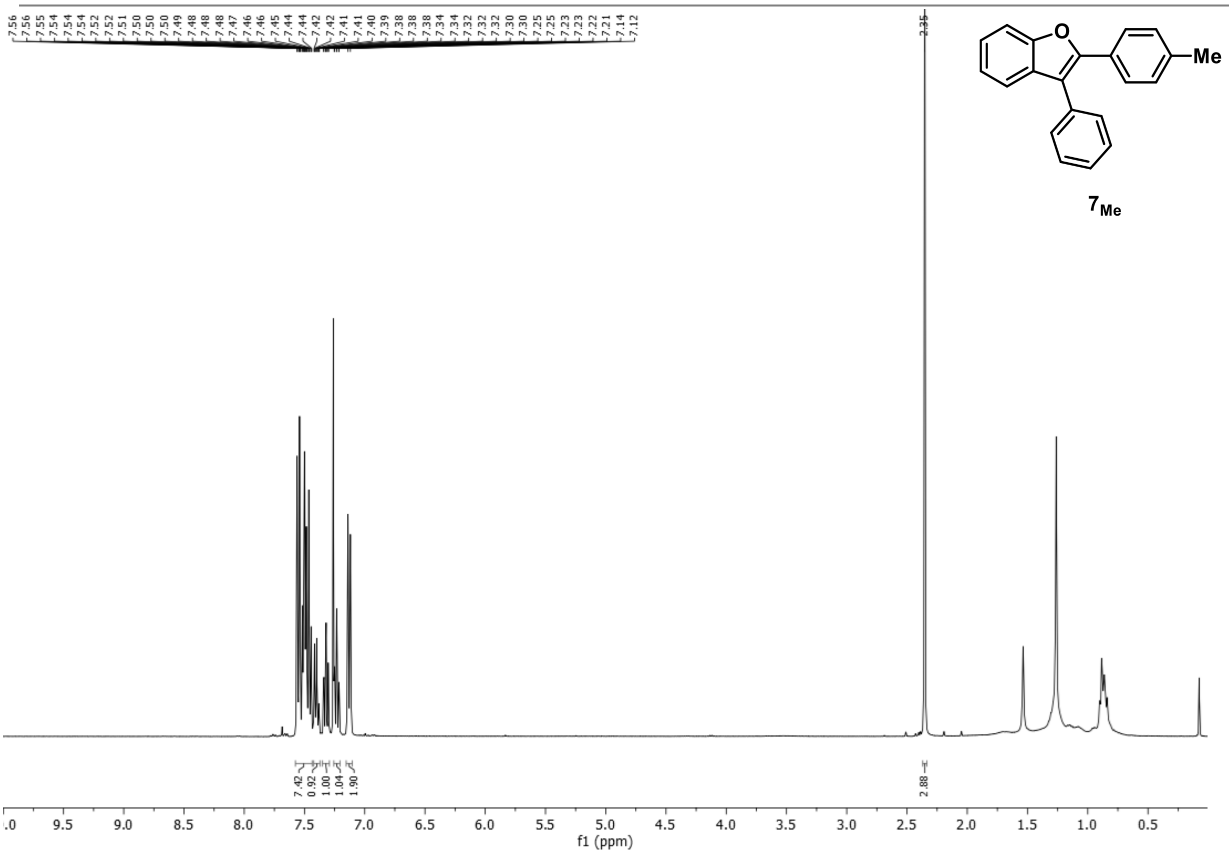

Figure S 54: ^{1}H NMR (399.82 MHz, CDCl$_3$) of **$7_{Me(10\ mol\%)}$**.

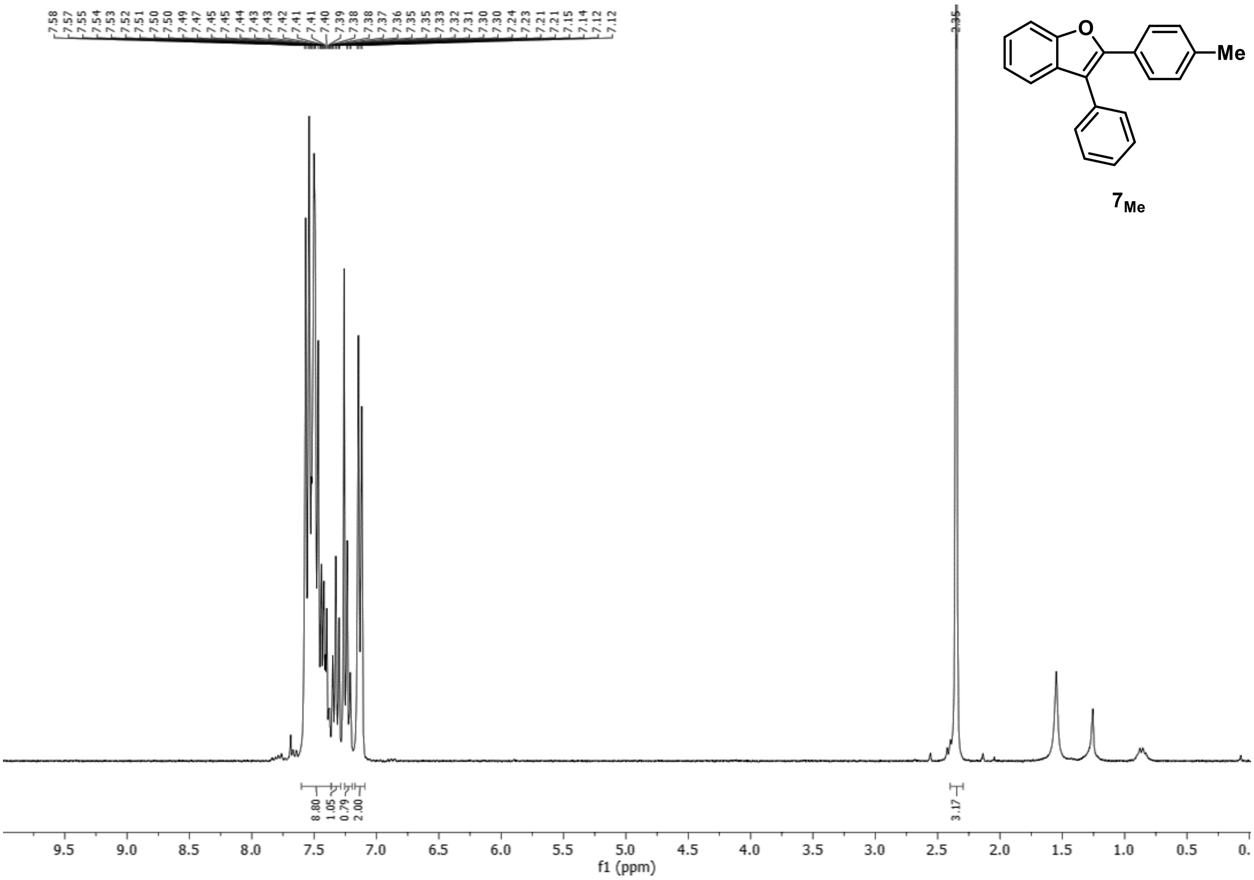

Figure S 55: ^{1}H NMR (299.95 MHz, CDCl$_3$) of **$7_{Me(5\ mol\%)}$**.

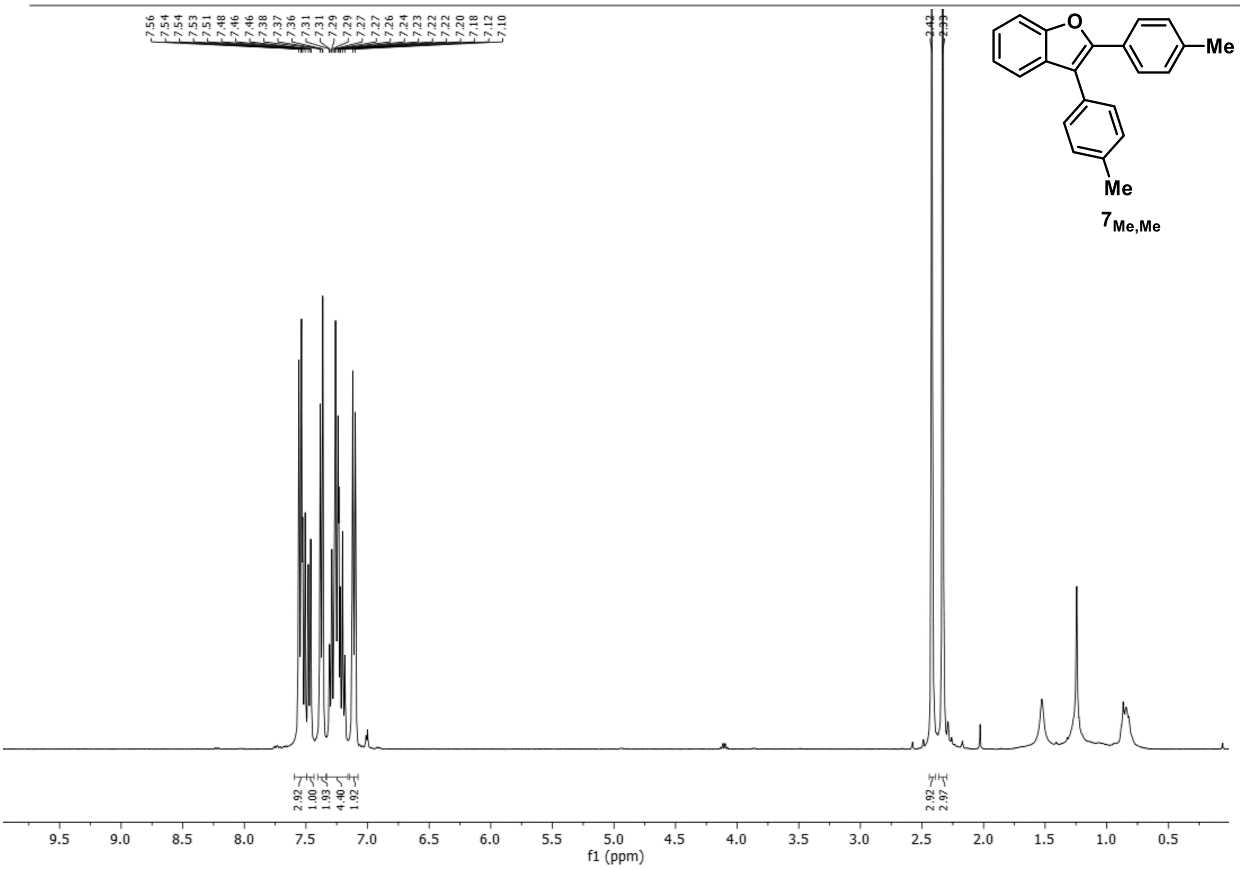

Figure S 56: ^{1}H NMR (399.82 MHz, $CDCl_3$) of **$7_{Me,Me}$**.

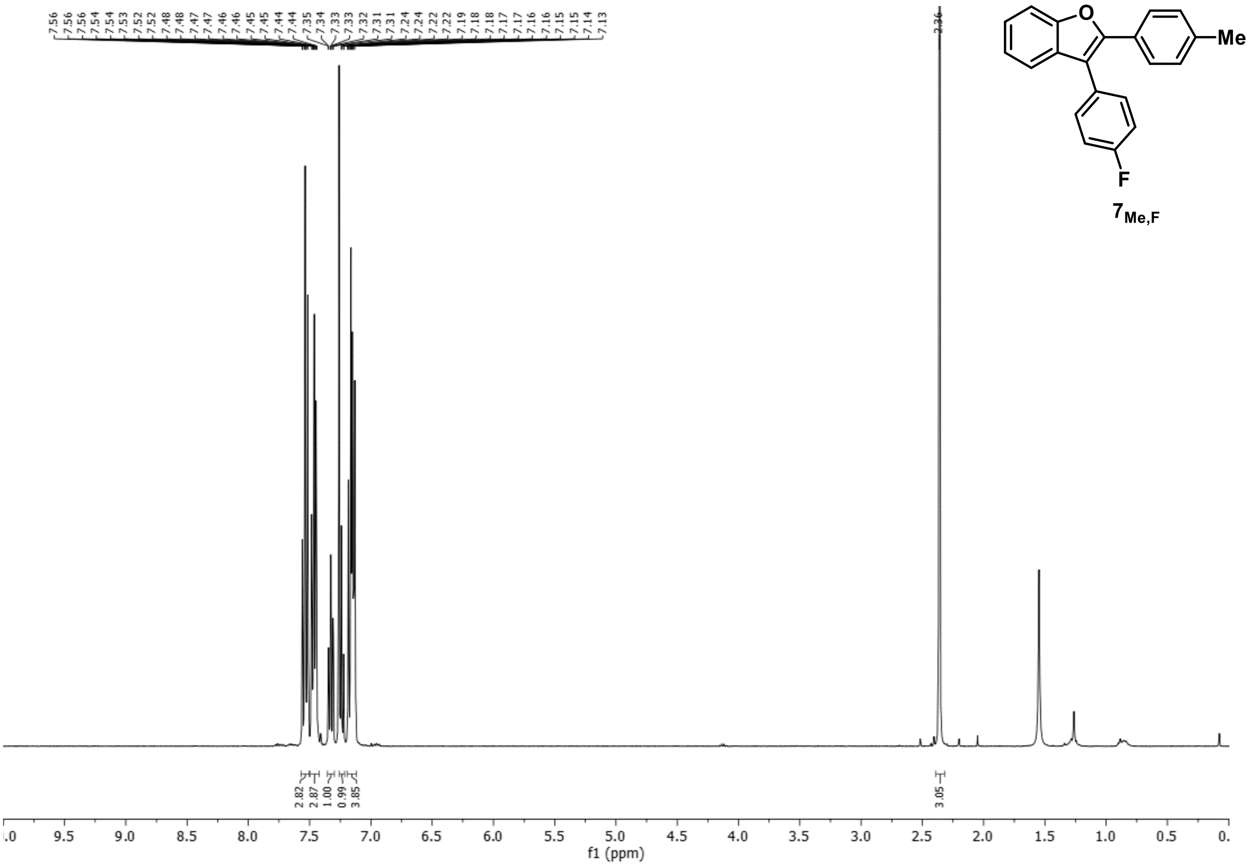

Figure S 57: ^{1}H NMR (399.82 MHz, $CDCl_3$) of **$7_{Me,F}$**.

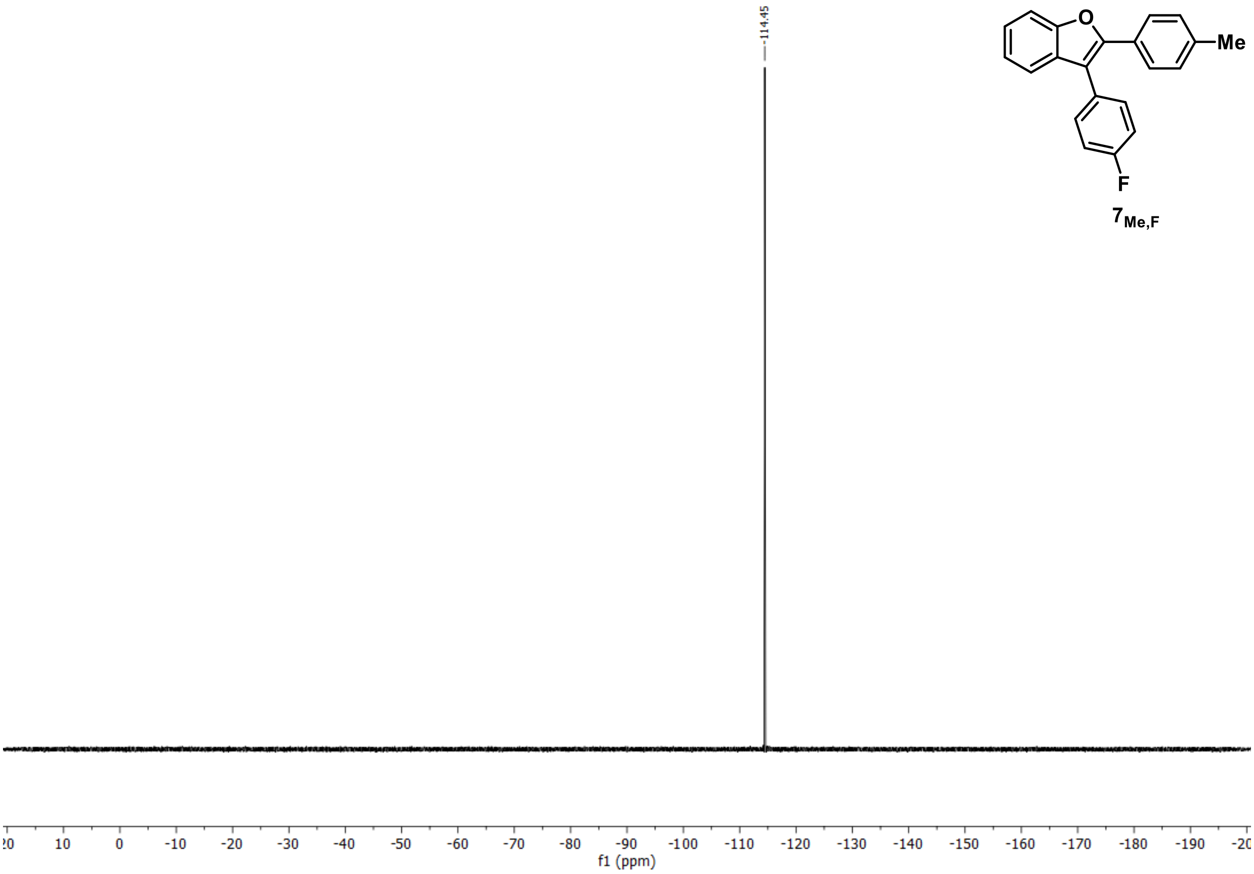

$7_{Me,F}$

Figure S 58: ^{19}F NMR (376.17 MHz, CDCl$_3$) of **$7_{Me,F}$**.

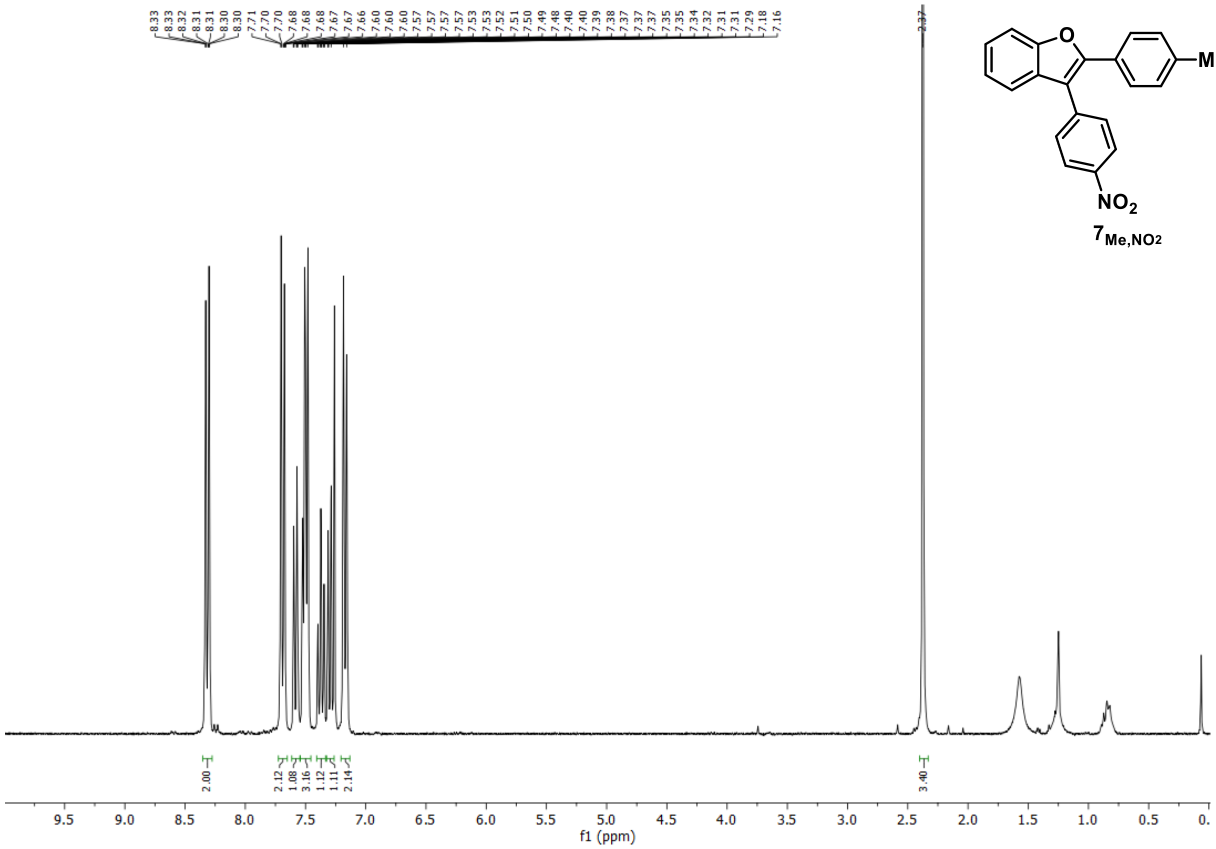

$7_{Me,NO_2}$

Figure S 59: ^{1}H NMR (299.95 MHz, CDCl$_3$) of **$7_{Me,NO_2\ 2h}$**.

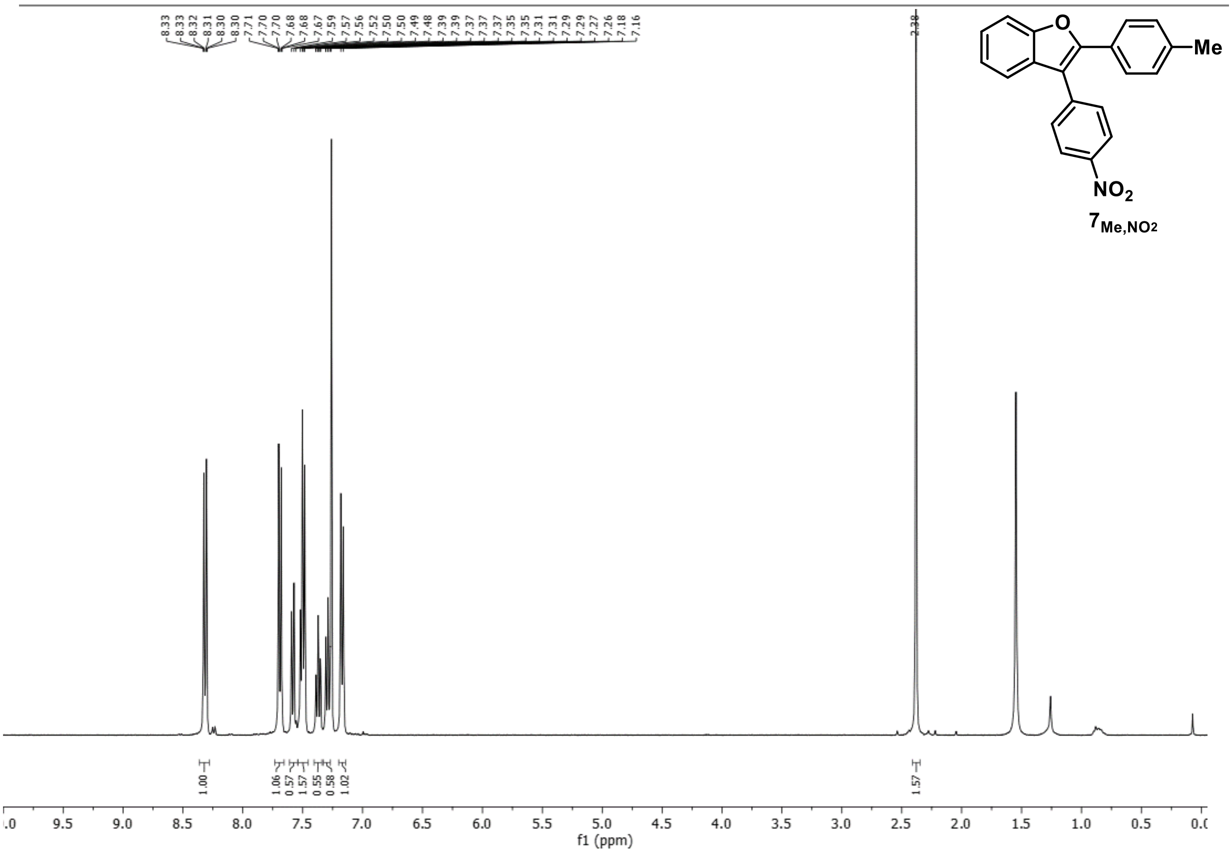

Figure S 60: ^{1}H NMR (399.82 MHz, CDCl$_3$) of **$7_{Me,NO2\ 30min}$**.

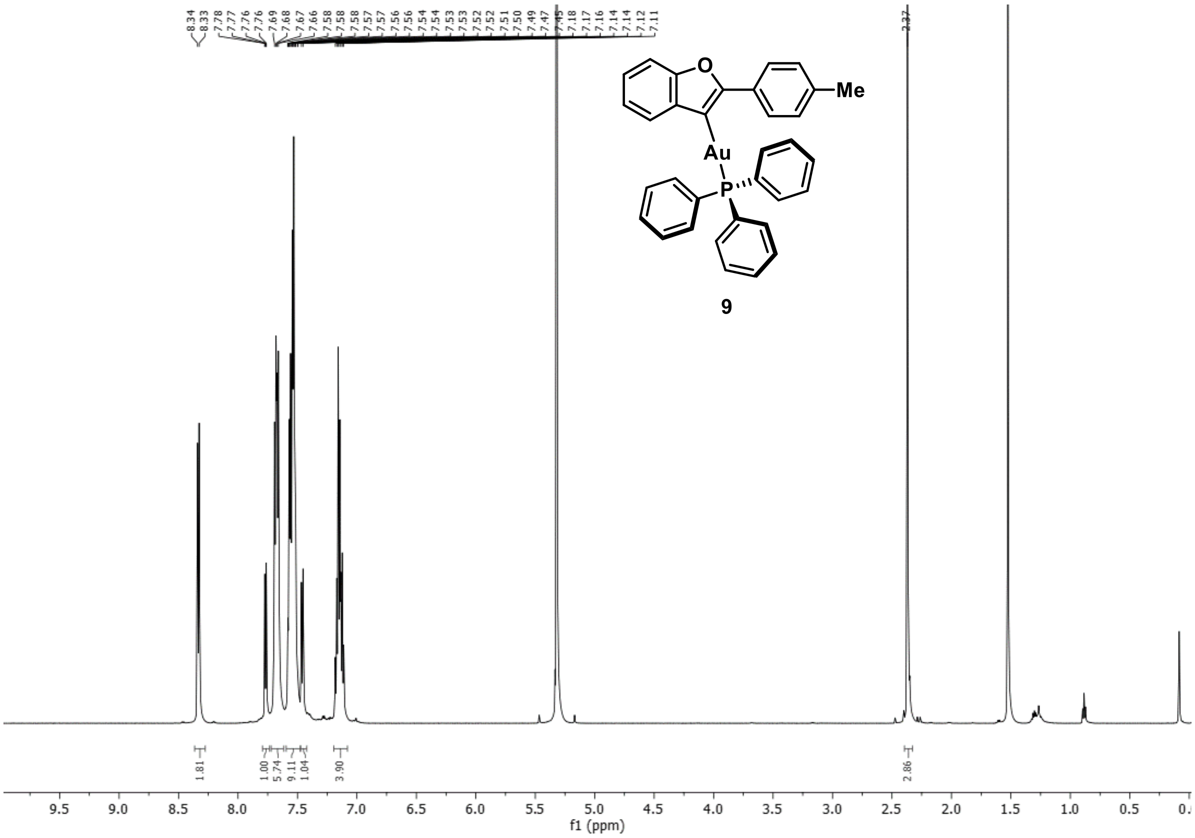

Figure S 61: ^{1}H NMR (600.13 MHz, CD$_2$Cl$_2$) of **9**.

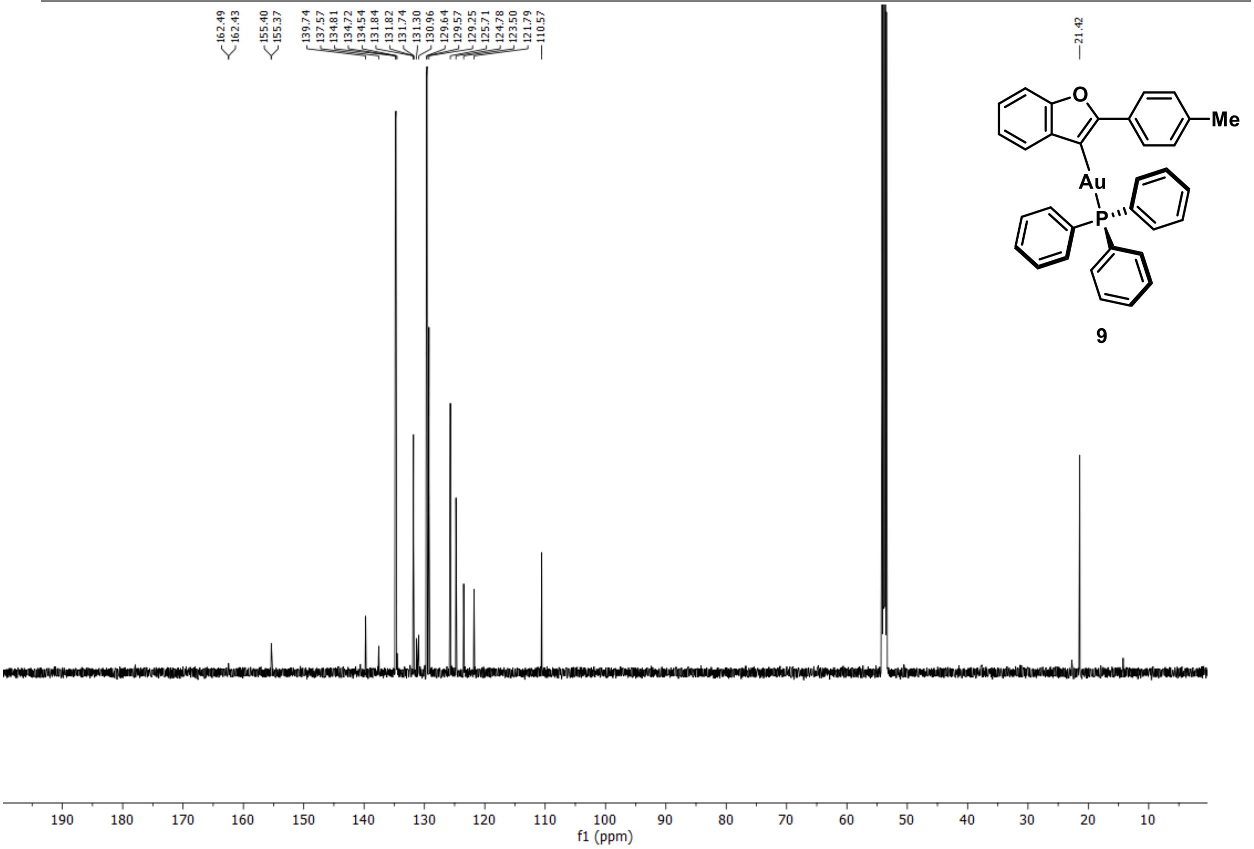

Figure S 62: ^{13}C NMR (150.92 MHz, CD_2Cl_2) of **9**.

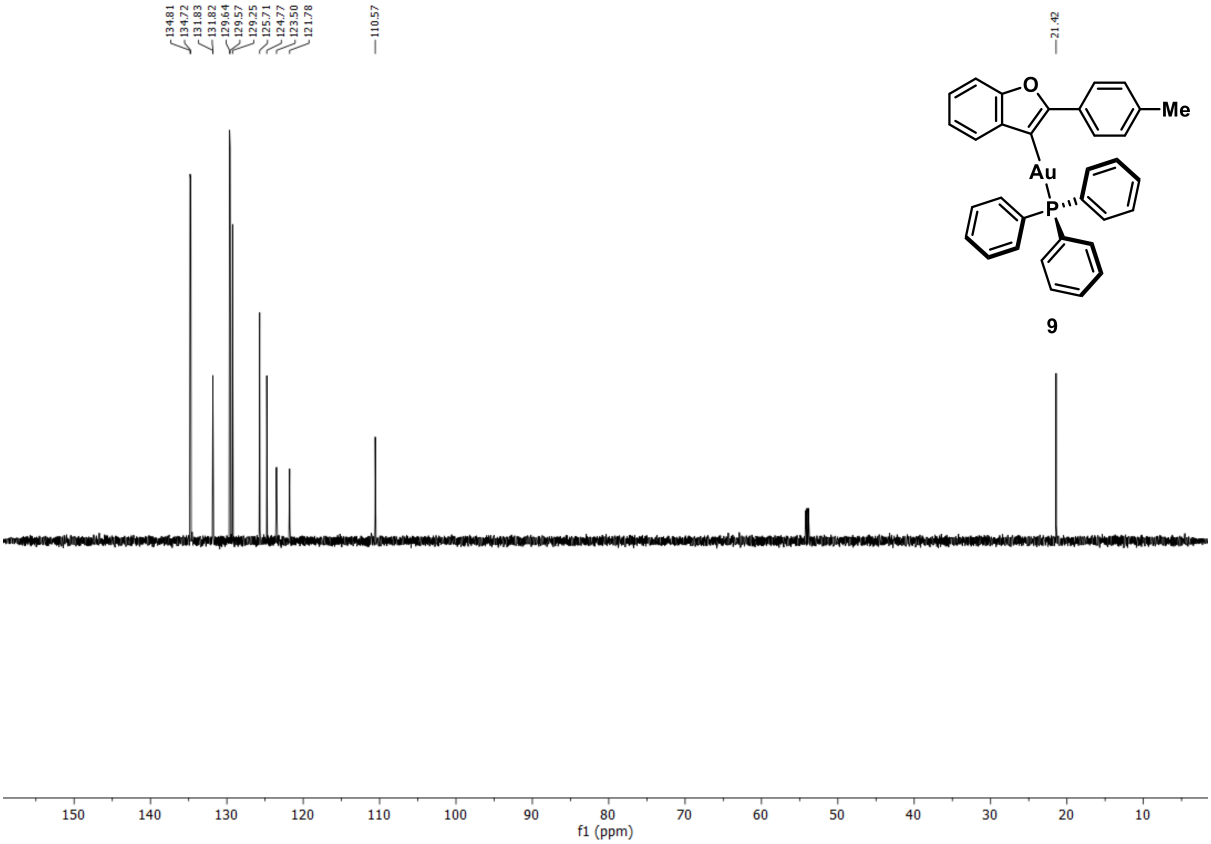

Figure S 63: DEPT135 NMR (150.91 MHz, CD_2Cl_2) of **9**.

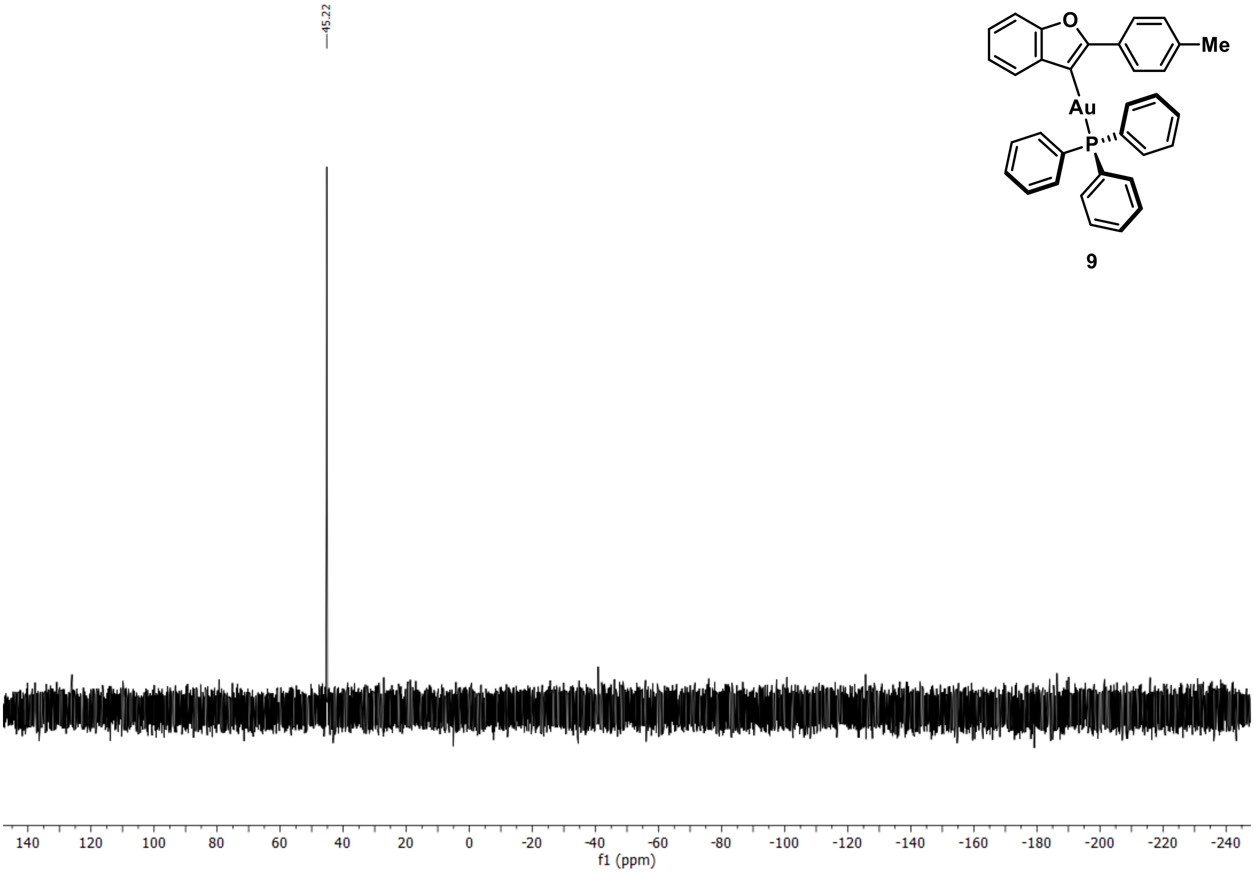

Figure S 64: ^{31}P NMR (242.92 MHz, CD_2Cl_2) of **9**.

2.2) Crytallographic Data

2.2.1.1) (*E*)-1-Phenyl-2-(2-(*p*-tolyl)benzofuran-3-yl)diazene

Table S 3: Crystal data and structure refinement for $\mathbf{8}_{\mathbf{Me}}$.

Identification code	$\mathbf{8}_{\mathbf{Me}}$	
Empirical formula	$C_{21}H_{16}N_2O$	
Formula weight	312.36	
Temperature	200(2) K	
Wavelength	0.71073 Å	
Crystal system	monoclinic	
Space group	$P2_1$	
Z	2	
Unit cell dimensions	a = 10.013(2) Å	α = 90 deg.
	b =4.9243(11) Å	β = 106.720(6) deg.
	c = 16.842(4) Å	γ = 90 deg.
Volume	795.3(3) $Å^3$	
Density (calculated)	1.30 g/cm^3	
Absorption coefficient	0.08 mm^{-1}	
Crystal shape	needle	
Crystal size	0.172 x 0.072 x 0.046 mm^3	
Crystal color	yellow	
Theta range for data collection	2.1 to 21.0 deg.	
Index ranges	$-10 \leq h \leq 9$, $-4 \leq k \leq 4$, $-17 \leq l \leq 17$	
Reflections collected	5423	
Independent reflections	1695 (R(int) = 0.0779)	
Observed reflections	1086 ($I > 2\sigma(I)$)	
Absorption correction	Semi-empirical from equivalents	
Max. and min. transmission	0.96 and 0.83	
Refinement method	Full-matrix least-squares on F^2	
Data/restraints/parameters	1695 / 193 / 218	
Goodness-of-fit on F^2	1.03	
Final R indices (I>2sigma(I))	R1 = 0.071, wR2 = 0.149	
Absolute structure parameter	-6.1(10)	
Largest diff. peak and hole	0.24 and -0.21 $eÅ^{-3}$	

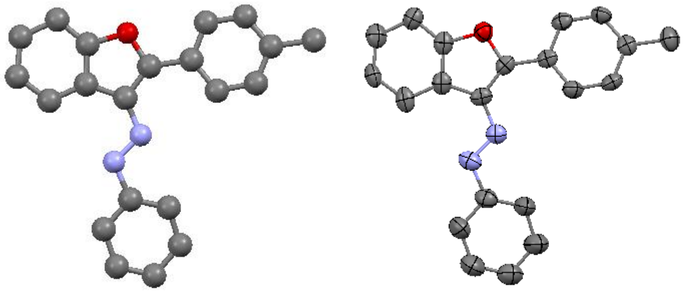

Table S 4: Atomic coordinates and equivalent isotropic displacement parameters (Å2) for **8**$_{\mathbf{Me}}$**.** Ueq is defined as one third of the trace of the orthogonalized Uij tensor.

Atom	x	y	z	U_{eq}
O1	0.5737(7)	0.3671(16)	0.8859(4)	0.050(2)
C2	0.4718(11)	0.424(2)	0.8130(7)	0.040(3)
C3	0.4884(11)	0.258(2)	0.7510(6)	0.041(3)
N4	0.3914(9)	0.2614(19)	0.6727(5)	0.048(2)
N5	0.4193(9)	0.086(2)	0.6219(6)	0.055(3)
C11	0.6593(11)	0.153(2)	0.8689(8)	0.047(3)
C12	0.7689(11)	0.039(2)	0.9253(7)	0.050(3)
H12	0.7982	0.0961	0.9815	0.060
C13	0.8369(12)	-0.171(2)	0.8957(8)	0.057(3)
H13	0.9138	-0.2623	0.9323	0.068
C14	0.7915(10)	-0.245(2)	0.8131(7)	0.050(3)
H14	0.8392	-0.3849	0.7937	0.060
C15	0.6778(11)	-0.119(2)	0.7574(7)	0.052(3)
H15	0.6490	-0.1727	0.7009	0.062
C16	0.6069(11)	0.085(3)	0.7858(7)	0.046(3)
C21	0.3720(10)	0.636(2)	0.8204(7)	0.038(3)
C22	0.2675(11)	0.723(2)	0.7507(6)	0.048(3)
H22	0.2598	0.6486	0.6975	0.058
C23	0.1759(11)	0.919(2)	0.7610(6)	0.045(3)
H23	0.1031	0.9758	0.7140	0.054
C24	0.1853(11)	1.038(2)	0.8367(7)	0.043(3)
C25	0.2903(11)	0.952(2)	0.9041(7)	0.048(3)
H25	0.2989	1.0306	0.9569	0.057
C26	0.3827(10)	0.756(2)	0.8965(7)	0.046(3)
H26	0.4552	0.7020	0.9439	0.055
C28	0.0806(11)	1.248(3)	0.8439(7)	0.061(3)
H28A	0.0540	1.2170	0.8948	0.092
H28B	-0.0022	1.2359	0.7959	0.092
H28C	0.1219	1.4296	0.8458	0.092
C31	0.3135(13)	0.079(3)	0.5448(7)	0.055(3)
C32	0.1919(12)	0.225(3)	0.5257(7)	0.069(4)
H32	0.1741	0.3492	0.5646	0.082
C33	0.0969(14)	0.191(3)	0.4501(8)	0.081(4)
H33	0.0112	0.2872	0.4378	0.097
C34	0.1214(14)	0.019(3)	0.3906(8)	0.072(4)
H34	0.0553	-0.0012	0.3377	0.086
C35	0.2423(14)	-0.118(3)	0.4108(8)	0.078(4)
H35	0.2621	-0.2336	0.3705	0.093
C36	0.3388(13)	-0.098(3)	0.4873(7)	0.070(4)
H36	0.4214	-0.2048	0.5003	0.084

Table S 5: Hydrogen coordinates and isotropic displacement parameters (Å^{2}) for **8**$_{\mathbf{Me}}$**.**

Atom	x	y	z	U_{eq}
H12	0.7982	0.0961	0.9815	0.060
H13	0.9138	-0.2623	0.9323	0.068
H14	0.8392	-0.3849	0.7937	0.060
H15	0.6490	-0.1727	0.7009	0.062
H22	0.2598	0.6486	0.6975	0.058
H23	0.1031	0.9758	0.7140	0.054
H25	0.2989	1.0306	0.9569	0.057
H26	0.4552	0.7020	0.9439	0.055
H28A	0.0540	1.2170	0.8948	0.092

H28B	-0.0022	1.2359	0.7959	0.092
H28C	0.1219	1.4296	0.8458	0.092
H32	0.1741	0.3492	0.5646	0.082
H33	0.0112	0.2872	0.4378	0.097
H34	0.0553	-0.0012	0.3377	0.086
H35	0.2621	-0.2336	0.3705	0.093
H36	0.4214	-0.2048	0.5003	0.084

Table S 6: Anisotropic displacement parameters (Å^2) for **8$_{Me}$**. The anisotropic displacement factor exponent takes the form: -2 pi^2 (h^2 a^{*2} U$_{11}$ + ... + 2 h k a* b* U$_{12}$)

Atom	U$_{11}$	U$_{22}$	U$_{33}$	U$_{23}$	U$_{13}$	U$_{12}$
O1	0.047(5)	0.053(5)	0.050(4)	0.001(4)	0.015(4)	0.001(4)
C2	0.035(6)	0.042(7)	0.044(6)	0.011(5)	0.012(5)	-0.008(5)
C3	0.046(7)	0.042(7)	0.037(5)	0.008(5)	0.013(5)	-0.014(5)
N4	0.049(6)	0.051(6)	0.047(5)	0.002(5)	0.017(4)	-0.005(5)
N5	0.060(6)	0.060(7)	0.050(5)	-0.011(5)	0.023(5)	-0.011(6)
C11	0.043(7)	0.036(8)	0.067(7)	0.010(6)	0.024(5)	-0.007(5)
C12	0.042(7)	0.050(8)	0.059(7)	0.011(6)	0.017(6)	-0.003(6)
C13	0.056(8)	0.042(8)	0.075(7)	0.004(6)	0.023(6)	-0.006(6)
C14	0.045(7)	0.039(7)	0.073(7)	-0.003(7)	0.030(6)	0.003(6)
C15	0.047(7)	0.040(7)	0.078(8)	0.005(7)	0.035(6)	-0.006(6)
C16	0.044(7)	0.041(7)	0.059(6)	0.010(6)	0.027(5)	-0.005(5)
C21	0.033(6)	0.043(7)	0.041(6)	0.005(5)	0.014(5)	-0.014(5)
C22	0.058(7)	0.047(8)	0.038(6)	-0.001(6)	0.012(5)	-0.003(6)
C23	0.043(7)	0.050(8)	0.038(6)	0.007(6)	0.002(5)	-0.008(5)
C24	0.042(7)	0.035(7)	0.055(6)	0.000(6)	0.019(5)	-0.012(5)
C25	0.052(8)	0.057(9)	0.037(6)	-0.004(6)	0.017(5)	-0.003(5)
C26	0.039(7)	0.055(8)	0.042(6)	0.001(6)	0.009(5)	-0.009(5)
C28	0.064(8)	0.045(8)	0.079(9)	0.000(7)	0.026(7)	0.003(6)
C31	0.058(7)	0.057(8)	0.053(7)	-0.008(6)	0.018(5)	-0.012(6)
C32	0.064(8)	0.082(10)	0.053(7)	-0.018(8)	0.007(6)	0.012(7)
C33	0.074(9)	0.103(13)	0.059(8)	-0.016(8)	0.009(6)	0.004(8)
C34	0.082(9)	0.074(11)	0.056(8)	-0.002(7)	0.015(7)	-0.007(7)
C35	0.088(10)	0.073(11)	0.069(8)	-0.021(8)	0.018(7)	0.001(8)
C36	0.070(9)	0.079(10)	0.064(8)	-0.015(8)	0.023(6)	0.010(8)

Table S 7: Bond lengths (Å) and angles (deg) for **8$_{Me}$**.

O1-C2	1.380(11)
O1-C11	1.436(12)
C2-C3	1.374(13)
C2-C21	1.476(13)
C3-N4	1.395(11)
C3-C16	1.440(15)
N4-N5	1.300(11)
N5-C31	1.421(12)
C11-C12	1.352(13)
C11-C16	1.387(13)
C12-C13	1.406(15)
C12-H12	0.9500
C13-C14	1.380(13)
C13-H13	0.9500
C14-C15	1.394(14)
C14-H14	0.9500
C15-C16	1.393(15)
C15-H15	0.9500
C21-C26	1.388(12)
C21-C22	1.396(12)
C22-C23	1.378(14)
C22-H22	0.9500
C23-C24	1.380(13)
C23-H23	0.9500
C24-C25	1.373(13)
C24-C28	1.504(15)
C25-C26	1.368(14)
C25-H25	0.9500
C26-H26	0.9500
C28-H28A	0.9800
C28-H28B	0.9800
C28-H28C	0.9800
C31-C32	1.370(16)
C31-C36	1.381(15)
C32-C33	1.363(13)
C32-H32	0.9500

C33-C34	1.386(16)
C33-H33	0.9500
C34-C35	1.341(16)
C34-H34	0.9500
C35-C36	1.372(14)
C35-H35	0.9500
C36-H36	0.9500
C2-O1-C11	107.6(8)
C3-C2-O1	109.5(9)
C3-C2-C21	135.9(10)
O1-C2-C21	114.5(9)
C2-C3-N4	120.5(10)
C2-C3-C16	107.9(10)
N4-C3-C16	131.3(11)
N5-N4-C3	113.0(9)
N4-N5-C31	112.0(9)
C12-C11-C16	127.1(11)
C12-C11-O1	125.2(11)
C16-C11-O1	107.7(10)
C11-C12-C13	115.8(11)
C11-C12-H12	122.1
C13-C12-H12	122.1
C14-C13-C12	119.9(11)
C14-C13-H13	120.1
C12-C13-H13	120.1
C13-C14-C15	122.0(11)
C13-C14-H14	119.0
C15-C14-H14	119.0
C16-C15-C14	119.2(12)
C16-C15-H15	120.4
C14-C15-H15	120.4
C11-C16-C15	116.0(11)
C11-C16-C3	107.2(11)
C15-C16-C3	136.8(12)
C26-C21-C22	119.1(10)
C26-C21-C2	120.3(10)
C22-C21-C2	120.5(10)
C23-C22-C21	118.3(10)
C23-C22-H22	120.8
C21-C22-H22	120.8
C22-C23-C24	122.8(10)
C22-C23-H23	118.6
C24-C23-H23	118.6
C25-C24-C23	117.9(11)
C25-C24-C28	122.0(11)
C23-C24-C28	120.1(10)
C26-C25-C24	121.1(11)
C26-C25-H25	119.4
C24-C25-H25	119.4
C25-C26-C21	120.8(10)
C25-C26-H26	119.6
C21-C26-H26	119.6
C24-C28-H28A	109.5
C24-C28-H28B	109.5
H28A-C28-H28B	109.5
C24-C28-H28C	109.5
H28A-C28-H28C	109.5
H28B-C28-H28C	109.5
C32-C31-C36	119.8(12)
C32-C31-N5	125.4(11)
C36-C31-N5	114.8(11)
C33-C32-C31	119.2(13)
C33-C32-H32	120.4
C31-C32-H32	120.4
C32-C33-C34	122.0(14)
C32-C33-H33	119.0
C34-C33-H33	119.0
C35-C34-C33	117.2(13)
C35-C34-H34	121.4
C33-C34-H34	121.4
C34-C35-C36	123.0(14)
C34-C35-H35	118.5
C36-C35-H35	118.5
C35-C36-C31	118.7(13)
C35-C36-H36	120.6
C31-C36-H36	120.6

Short experimental description:

yellow crystal (needle), dimensions 0.172 x 0.072 x 0.046 mm^3, crystal system monoclinic, space group $P2_1$, Z=2, a=10.013(2) Å, b=4.9243(11) Å, c=16.842(4) Å, alpha=90 deg, beta=106.720(6) deg, gamma=90 deg, V=795.3(3) Å^3, rho=1.304 g/cm^3, T=200(2) K, Theta$_{max}$= 21.031 deg, radiation Mo Kalpha, lambda=0.71073 Å, 0.5 deg omega-scans with CCD area detector, covering the asymmetric unit in reciprocal space with a mean redundancy of 5.55 and a completeness of 99.9% to a resolution of 0.95 Å,[33] 5423 reflections measured, 1695 unique (R(int)=0.0779), 1086 observed ($I > 2\sigma(I)$), intensities were corrected for Lorentz and polarization effects, an empirical scaling and absorption correction was applied using SADABS[34] based on the Laue symmetry of the reciprocal space, T$_{min}$=0.83, T$_{max}$=0.96, structure solved with SHELXT-2014 (Sheldrick 2014)[35] and refined against F^2 with a Full-matrix least-squares algorithm using the SHELXL-2016/6 (Sheldrick, 2016) software,[36] 218 parameters refined, hydrogen atoms were treated using appropriate riding models, Flack absolute structure parameter -6.1(10), goodness of fit 1.03 for observed reflections, final residual values R1(F)=0.071, wR(F^2)=0.149 for observed reflections, residual electron density -0.21 to 0.24 eÅ^{-3}.

CCDC 1915768 contains the supplementary crystallographic data for this paper. These data can be obtained free of charge from The Cambridge Crystallographic Data Centre *via* https://www.ccdc.cam.ac.uk/structures/.

2.2.1.2) (*E*)-1-(2-(4-Methoxyphenyl)benzofuran-3-yl)-2-phenyldiazene

Table S 8: Crystal data and structure refinement for **8**$_{\mathrm{OMe}}$.

Identification code	**8**$_{\mathrm{OMe}}$	
Empirical formula	$C_{21}H_{16}N_2O_2$	
Formula weight	328.36	
Temperature	200(2) K	
Wavelength	0.71073 Å	
Crystal system	monoclinic	
Space group	$P2_1/c$	
Z	4	
Unit cell dimensions	a = 18.331(5) Å	α = 90 deg.
	b =4.6232(14) Å	β = 107.210(8) deg.
	c = 19.854(6) Å	γ = 90 deg.
Volume	1607.3(8) Å^3	
Density (calculated)	1.36 g/cm^3	
Absorption coefficient	0.09 mm^{-1}	
Crystal shape	plank	
Crystal size	0.142 x 0.050 x 0.047 mm^3	
Crystal color	orange	
Theta range for data collection	1.2 to 19.8 deg.	
Index ranges	$-17 \le h \le 17$, $-4 \le k \le 4$, $-18 \le l \le 18$	
Reflections collected	5655	
Independent reflections	1458 (R(int) = 0.1032)	
Observed reflections	861 ($I > 2\sigma(I)$)	
Absorption correction	Semi-empirical from equivalents	
Max. and min. transmission	0.96 and 0.84	
Refinement method	Full-matrix least-squares on F^2	
Data/restraints/parameters	1458 / 198 / 227	
Goodness-of-fit on F^2	0.98	
Final R indices (I>2sigma(I))	R1 = 0.058, wR2 = 0.124	
Largest diff. peak and hole	0.20 and -0.24 eÅ^{-3}	

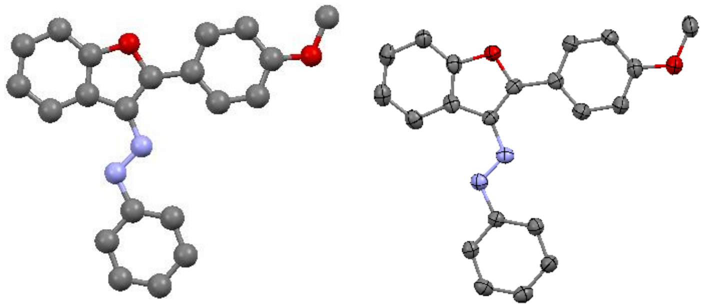

Table S 9: Atomic coordinates and equivalent isotropic displacement parameters (Å^2) for **8**$_{\mathrm{OMe}}$. U_{eq} is defined as one third of the trace of the orthogonalized U_{ij} tensor.

Atom	x	y	z	U_{eq}
O1	0.6723(2)	1.1478(8)	0.6698(2)	0.0369(11)
C2	0.6995(3)	0.9722(13)	0.7284(3)	0.0321(15)
C3	0.7610(3)	0.8174(13)	0.7226(3)	0.0315(15)
N4	0.7967(3)	0.6108(11)	0.7735(2)	0.0350(14)
N5	0.8544(3)	0.4861(11)	0.7620(2)	0.0369(14)
C11	0.7195(3)	1.1008(14)	0.6272(3)	0.0377(17)
C12	0.7112(3)	1.2370(14)	0.5636(3)	0.0437(18)
H12	0.6709	1.3702	0.5445	0.052

C13	0.7637(4)	1.1709(14)	0.5294(3)	0.0484(19)
H13	0.7601	1.2586	0.4853	0.058
C14	0.8228(4)	0.9745(14)	0.5590(3)	0.0470(18)
H14	0.8592	0.9329	0.5348	0.056
C15	0.8291(4)	0.8398(13)	0.6229(3)	0.0430(18)
H15	0.8694	0.7075	0.6425	0.052
C16	0.7752(3)	0.9016(13)	0.6579(3)	0.0338(16)
C21	0.6587(3)	0.9958(13)	0.7807(3)	0.0332(16)
C22	0.6787(3)	0.8356(14)	0.8428(3)	0.0423(18)
H22	0.7208	0.7065	0.8520	0.051
C23	0.6385(4)	0.8609(14)	0.8910(3)	0.0454(18)
H23	0.6532	0.7514	0.9334	0.054
C24	0.5769(3)	1.0447(14)	0.8778(3)	0.0391(17)
C25	0.5563(3)	1.2069(14)	0.8174(3)	0.0434(18)
H25	0.5143	1.3362	0.8088	0.052
C26	0.5969(3)	1.1821(14)	0.7689(3)	0.0397(18)
H26	0.5822	1.2943	0.7269	0.048
O28	0.5399(2)	1.0513(9)	0.9288(2)	0.0505(13)
C28	0.4754(3)	1.2436(15)	0.9173(3)	0.055(2)
H28A	0.4537	1.2270	0.9567	0.083
H28B	0.4366	1.1911	0.8733	0.083
H28C	0.4920	1.4432	0.9141	0.083
C31	0.8880(3)	0.2778(13)	0.8154(3)	0.0314(15)
C32	0.8617(3)	0.2133(13)	0.8726(3)	0.0398(17)
H32	0.8182	0.3111	0.8779	0.048
C33	0.8980(3)	0.0093(13)	0.9212(3)	0.0417(17)
H33	0.8793	-0.0358	0.9598	0.050
C34	0.9621(3)	-0.1302(14)	0.9139(3)	0.0426(18)
H34	0.9872	-0.2718	0.9474	0.051
C35	0.9898(3)	-0.0644(13)	0.8579(3)	0.0407(17)
H35	1.0340	-0.1589	0.8532	0.049
C36	0.9523(3)	0.1406(13)	0.8089(3)	0.0356(17)
H36	0.9711	0.1867	0.7704	0.043

Table S 10: Hydrogen coordinates and isotropic displacement parameters (Å^2) for **8**$_{\mathbf{OMe}}$.

Atom	x	y	z	U_{eq}
H12	0.6709	1.3702	0.5445	0.052
H13	0.7601	1.2586	0.4853	0.058
H14	0.8592	0.9329	0.5348	0.056
H15	0.8694	0.7075	0.6425	0.052
H22	0.7208	0.7065	0.8520	0.051
H23	0.6532	0.7514	0.9334	0.054
H25	0.5143	1.3362	0.8088	0.052
H26	0.5822	1.2943	0.7269	0.048
H28A	0.4537	1.2270	0.9567	0.083
H28B	0.4366	1.1911	0.8733	0.083
H28C	0.4920	1.4432	0.9141	0.083
H32	0.8182	0.3111	0.8779	0.048
H33	0.8793	-0.0358	0.9598	0.050
H34	0.9872	-0.2718	0.9474	0.051
H35	1.0340	-0.1589	0.8532	0.049
H36	0.9711	0.1867	0.7704	0.043

Table S 11: Anisotropic displacement parameters (Å^2) for **8**$_{\mathbf{OMe}}$. The anisotropic displacement factor exponent takes the form: -2 pi^2 (h^2 a^{*2} U_{11} + ... + 2 h k a^* b^* U_{12})

Atom	U_{11}	U_{22}	U_{33}	U_{23}	U_{13}	U_{12}
O1	0.035(3)	0.041(3)	0.034(3)	0.004(2)	0.009(2)	0.003(2)
C2	0.028(4)	0.034(4)	0.030(3)	0.003(3)	0.002(3)	-0.007(3)
C3	0.029(4)	0.034(4)	0.030(4)	0.001(3)	0.005(3)	-0.003(3)
N4	0.032(3)	0.035(3)	0.035(3)	-0.002(3)	0.004(3)	-0.002(2)
N5	0.039(3)	0.034(3)	0.037(3)	-0.002(3)	0.011(3)	0.000(3)
C11	0.032(4)	0.043(5)	0.040(4)	-0.003(3)	0.013(3)	-0.008(3)
C12	0.048(4)	0.045(5)	0.042(4)	0.001(3)	0.020(4)	0.002(4)
C13	0.061(5)	0.053(5)	0.038(4)	-0.006(4)	0.024(4)	-0.004(4)
C14	0.053(5)	0.044(5)	0.051(4)	-0.008(4)	0.026(4)	-0.009(3)
C15	0.045(4)	0.037(5)	0.050(4)	-0.008(3)	0.019(4)	-0.002(3)
C16	0.030(4)	0.039(4)	0.030(4)	-0.011(3)	0.005(3)	-0.008(3)
C21	0.029(4)	0.033(4)	0.037(4)	-0.002(3)	0.010(3)	-0.006(3)
C22	0.036(4)	0.049(5)	0.042(4)	0.003(3)	0.012(3)	0.006(3)
C23	0.046(4)	0.056(5)	0.037(4)	0.005(4)	0.016(3)	0.004(3)
C24	0.037(4)	0.047(5)	0.037(4)	-0.006(3)	0.016(4)	-0.006(3)
C25	0.033(4)	0.050(5)	0.049(4)	0.009(4)	0.014(3)	0.008(3)
C26	0.042(4)	0.045(5)	0.033(4)	0.001(3)	0.012(3)	0.004(3)
O28	0.051(3)	0.063(4)	0.041(3)	0.007(3)	0.020(2)	0.008(2)
C28	0.052(5)	0.074(6)	0.047(4)	-0.001(4)	0.026(4)	0.005(4)
C31	0.032(4)	0.028(4)	0.034(4)	-0.003(3)	0.008(3)	-0.002(3)
C32	0.040(4)	0.043(5)	0.037(4)	-0.002(3)	0.013(3)	0.004(3)
C33	0.048(4)	0.041(5)	0.036(4)	0.005(3)	0.013(4)	0.003(3)
C34	0.043(4)	0.037(5)	0.044(4)	0.006(3)	0.007(3)	-0.003(3)
C35	0.036(4)	0.034(4)	0.051(4)	-0.003(3)	0.012(3)	0.002(3)
C36	0.036(4)	0.035(4)	0.038(4)	-0.004(3)	0.014(3)	-0.004(3)

Table S 12: Bond lengths (Å) and angles (deg) for **8**$_{\mathbf{OMe}}$.

O1-C2	1.386(6)	C25-C26	1.385(7)
O1-C11	1.395(6)	C25-H25	0.9500
C2-C3	1.368(7)	C26-H26	0.9500
C2-C21	1.452(7)	O28-C28	1.443(6)
C3-N4	1.404(7)	C28-H28A	0.9800
C3-C16	1.438(7)	C28-H28B	0.9800
N4-N5	1.283(6)	C28-H28C	0.9800
N5-C31	1.431(7)	C31-C36	1.378(7)
C11-C16	1.376(8)	C31-C32	1.390(7)
C11-C12	1.377(8)	C32-C33	1.374(8)
C12-C13	1.367(7)	C32-H32	0.9500
C12-H12	0.9500	C33-C34	1.385(7)
C13-C14	1.402(8)	C33-H33	0.9500
C13-H13	0.9500	C34-C35	1.385(7)
C14-C15	1.387(8)	C34-H34	0.9500
C14-H14	0.9500	C35-C36	1.387(8)
C15-C16	1.394(8)	C35-H35	0.9500
C15-H15	0.9500	C36-H36	0.9500
C21-C26	1.388(7)	C2-O1-C11	106.5(5)
C21-C22	1.391(8)	C3-C2-O1	109.7(5)
C22-C23	1.376(7)	C3-C2-C21	135.3(6)
C22-H22	0.9500	O1-C2-C21	115.0(5)
C23-C24	1.374(8)	C2-C3-N4	121.0(5)
C23-H23	0.9500	C2-C3-C16	107.8(5)
C24-C25	1.370(8)	N4-C3-C16	131.2(6)
C24-O28	1.376(6)	N5-N4-C3	114.3(5)

N4-N5-C31	111.6(5)
C16-C11-C12	125.3(6)
C16-C11-O1	110.4(5)
C12-C11-O1	124.3(6)
C13-C12-C11	116.7(6)
C13-C12-H12	121.6
C11-C12-H12	121.6
C12-C13-C14	120.4(6)
C12-C13-H13	119.8
C14-C13-H13	119.8
C15-C14-C13	121.3(6)
C15-C14-H14	119.3
C13-C14-H14	119.3
C14-C15-C16	118.9(6)
C14-C15-H15	120.5
C16-C15-H15	120.5
C11-C16-C15	117.3(6)
C11-C16-C3	105.6(5)
C15-C16-C3	137.0(6)
C26-C21-C22	117.9(6)
C26-C21-C2	119.6(6)
C22-C21-C2	122.5(6)
C23-C22-C21	121.2(6)
C23-C22-H22	119.4
C21-C22-H22	119.4
C24-C23-C22	119.9(6)
C24-C23-H23	120.1
C22-C23-H23	120.1
C25-C24-C23	120.3(6)
C25-C24-O28	124.3(6)
C23-C24-O28	115.4(6)
C24-C25-C26	119.9(6)
C24-C25-H25	120.1
C26-C25-H25	120.1
C25-C26-C21	120.9(6)
C25-C26-H26	119.5
C21-C26-H26	119.5
C24-O28-C28	117.2(5)
O28-C28-H28A	109.5
O28-C28-H28B	109.5
H28A-C28-H28B	109.5
O28-C28-H28C	109.5
H28A-C28-H28C	109.5
H28B-C28-H28C	109.5
C36-C31-C32	119.5(6)
C36-C31-N5	115.7(5)
C32-C31-N5	124.8(5)
C33-C32-C31	120.5(6)
C33-C32-H32	119.7
C31-C32-H32	119.7
C32-C33-C34	119.7(6)
C32-C33-H33	120.1
C34-C33-H33	120.1
C35-C34-C33	120.4(6)
C35-C34-H34	119.8
C33-C34-H34	119.8
C34-C35-C36	119.4(6)
C34-C35-H35	120.3
C36-C35-H35	120.3
C31-C36-C35	120.5(6)
C31-C36-H36	119.8
C35-C36-H36	119.8

Short experimental description:

orange crystal (plank), dimensions 0.142 x 0.050 x 0.047 mm^3, crystal system monoclinic, space group P2$_1$/c, Z=4, a=18.331(5) Å, b=4.6232(14) Å, c=19.854(6) Å, alpha=90 deg, beta=107.210(8) deg, gamma=90 deg, V=1607.3(8) Å^3, rho=1.357 g/cm^3, T=200(2) K, Theta$_{max}$= 19.766 deg, radiation MoKα, lambda=0.71073 Å, 0.5 deg omega-scans with CCD area detector, covering the asymmetric unit in reciprocal space with a mean redundancy of 3.68 and a completeness of 99.9% to a resolution of 1.05 Å,[33] 5655 reflections measured, 1458 unique (R(int)=0.1032), 861 observed ($I > 2\sigma(I)$), intensities were corrected for Lorentz and polarization effects, an empirical scaling and absorption correction was applied using SADABS[34] based on the Laue symmetry of the reciprocal space, mu=0.09mm^{-1}, T$_{min}$=0.84, T$_{max}$=0.96, structure solved with SHELXT-2014 (Sheldrick 2014)[35] and refined against F^2 with a Full-matrix least-squares algorithm using the SHELXL-2018/3 (Sheldrick, 2018) software,[36] 227 parameters refined, hydrogen atoms were treated using appropriate riding models, goodness of fit 0.98 for observed reflections, final residual values R1(F)=0.058, wR(F^2)=0.124 for observed reflections, residual electron density -0.24 to 0.20 eÅ^{-3}.
CCDC 1915769 contains the supplementary crystallographic data for this paper. These data can be obtained free of charge from The Cambridge Crystallographic Data Centre *via* https://www.ccdc.cam.ac.uk/structures/.

2.2.1.3) (2-(*p*-Tolyl)benzofuran-3-yl)(triphenyl-λ^5-phosphanyl) gold(I)

A suitable crystal of compound **9** was mounted on top of a cryoloop and transferred into the cold (100 K) nitrogen stream of a Bruker D8 Venture diffractometer. Data collection and reduction was done using the Bruker software suite APEX3.[37] The final unit cell was obtained from the xyz centroids of 9673 reflections after integration. A multiscan absorption correction was applied, based on the intensities of symmetry-related reflections measured at different angular settings (*SADABS*).[37] The structures were solved by direct methods using *SHELXT,*[35] and refinement of the structure was performed using *SHELXL*.[36] The hydrogen atoms were generated by geometrical considerations, constrained to idealized geometries and allowed to ride on their carrier atoms with an isotropic displacement parameter related to the equivalent displacement parameter of their carrier atoms. Refinement was done as an inversion twin (twin, basf) and the dataset was cut off at 0.77 Å. EADP was applied for C2 based on C1 and one reflection is omitted. Crystal data and details on data collection and refinement are presented in **Table S 13**.

CCDC 1915734 contains the supplementary crystallographic data for this paper. These data can be obtained free of charge from The Cambridge Crystallographic Data Centre *via* https://www.ccdc.cam.ac.uk/structures/.

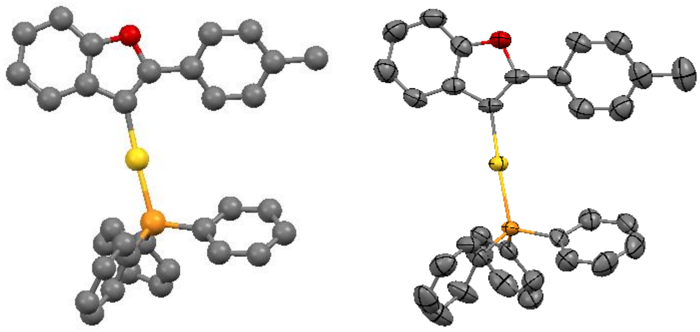

Table S 13: Crystallographic data for compound **9**.

chem formula	$C_{33}H_{26}AuOP$
M_r	666.47
cryst syst	orthorhombic
color, habit	colorless, needle
size (mm)	0.475 x 0.154 x 0.142
space group	$P2_12_12_1$
a (Å)	15.6906(11)
b (Å)	6.6741(5)
c (Å)	24.8603(17)
β (°)	90
V (Å^3)	2603.4(3)
Z	4
ρ_{calc}, g.cm^{-3}	1.700
Radiation [Å]	Mo K$_\alpha$ 0.71073
μ(Mo K$_\alpha$), mm^{-1}	5.737
F(000)	1304
temp (K)	100(2)
θ range (°)	3.07 – 27.57
data collected (h,k,l)	-8:8; -20:20; -32:32
no. of rflns collected	133480
no. of indpndt reflns	5980
observed reflns $F_o \geq 2.0\ \sigma(F_o)$	5920
R(F) (%)	1.67
wR(F^2) (%)	4.23
GooF	1.222
weighting a,b	0.154, 3.2811
params refined	321
min, max resid dens	0.681, -1.315

2.3) Cartesian Coordinates

Donor-Acceptor Complex (singlet ground state)

$E_{\text{TPSS-D3(BJ)/def2-SVP/PCM(MeCN)}}$ =

-2165.68277547

$E_{\text{CAM-B3LYP-D3(BJ)/def2-SVPD/PCM(MeCN)}}$ =

-2164.35075069

Excited singlet state energy:

$E_{\text{CAM-B3LYP-D3(BJ)/def2-SVPD/PCM(MeCN)}}$ =

-2164.27771312

Triplet state energy:

$E_{\text{CAM-B3LYP-D3(BJ)/def2-SVPD/PCM(MeCN)}}$ =

-2164.30349151

C	-2.652640000	-4.579519000	-1.059965000
C	-1.819134000	-3.454633000	-1.044262000
C	-2.411203000	-2.172750000	-1.073071000
C	-3.826509000	-2.081167000	-1.119629000
C	-4.677474000	-3.187806000	-1.142263000
C	-4.060976000	-4.449202000	-1.109370000
H	-4.684340000	-5.349303000	-1.120224000
H	-5.764728000	-3.074545000	-1.175195000
O	-4.207500000	-0.768624000	-1.106711000
C	-3.027871000	-0.011614000	-1.035459000
C	-1.895136000	-0.815423000	-1.020985000
Au	0.064136000	-0.305084000	-0.710874000
P	2.290089000	0.180140000	-0.182212000
C	3.536130000	-0.319729000	-1.422548000
C	3.196572000	-0.204286000	-2.785978000
C	4.135390000	-0.536182000	-3.771468000
C	5.410873000	-0.991790000	-3.401611000
C	5.748523000	-1.115689000	-2.044949000
C	4.815651000	-0.780852000	-1.053350000
H	5.079305000	-0.884018000	0.004182000
H	6.741242000	-1.475390000	-1.755962000
H	6.141435000	-1.256742000	-4.172763000
H	3.868234000	-0.446522000	-4.829206000
H	2.195435000	0.140489000	-3.068666000
C	2.616862000	1.943763000	0.183416000
C	3.920046000	2.478084000	0.139952000
C	4.132668000	3.824906000	0.463848000
C	3.052100000	4.642876000	0.831904000
C	1.752664000	4.114909000	0.873023000
C	1.534467000	2.769775000	0.545832000
H	0.520979000	2.356693000	0.564607000
H	0.905823000	4.749838000	1.152668000
H	3.223514000	5.694960000	1.081405000
H	5.145836000	4.237705000	0.426319000
H	4.765211000	1.846002000	-0.150670000
C	2.738605000	-0.722285000	1.350281000
C	2.987305000	-0.053559000	2.563462000
C	3.215084000	-0.791456000	3.736488000
C	3.205216000	-2.192603000	3.701933000
C	2.966563000	-2.863218000	2.489762000
C	2.724707000	-2.133749000	1.318658000
H	2.523641000	-2.659376000	0.378516000
H	2.963974000	-3.957259000	2.457802000
H	3.384672000	-2.765226000	4.617312000
H	3.403858000	-0.265365000	4.677590000
H	2.999352000	1.040404000	2.593836000
C	-3.232663000	1.422348000	-0.882030000
C	-2.139861000	2.323038000	-0.888526000

C	-2.327312000	3.684153000	-0.651248000
C	-3.613512000	4.216094000	-0.406776000
C	-4.703011000	3.323242000	-0.422670000
C	-4.524228000	1.954771000	-0.656059000
H	-5.385528000	1.281515000	-0.647681000
H	-5.713333000	3.706933000	-0.241197000
C	-3.803443000	5.691509000	-0.147413000
H	-3.484076000	6.290561000	-1.019988000
H	-3.192746000	6.024881000	0.711214000
H	-4.858136000	5.929989000	0.064876000
H	-1.458652000	4.352412000	-0.657745000
H	-1.133599000	1.932252000	-1.080276000
H	-0.729149000	-3.558664000	-1.006592000
H	-2.211174000	-5.581300000	-1.034027000
C	-1.509124000	-1.306202000	2.299324000
N	-0.794732000	-2.465260000	2.301802000
N	-0.172440000	-3.402592000	2.291158000
C	-2.910262000	-1.371555000	2.091640000
C	-3.607936000	-0.168974000	2.063668000
C	-2.929623000	1.054985000	2.224024000
C	-1.537813000	1.092854000	2.417811000
C	-0.797044000	-0.086036000	2.448911000
H	0.282849000	-0.094661000	2.610137000
H	-1.026343000	2.050284000	2.541813000
H	-3.494352000	1.990498000	2.191059000
H	-4.687811000	-0.180796000	1.898565000
H	-3.405195000	-2.334926000	1.957648000

Donor-Acceptor Complex (triplet state)

$E_{TPSS-D3(BJ)/def2-SVP/PCM(MeCN)}$ =

-2165.65478578

$E_{CAM-B3LYP-D3(BJ)/def2-SVPD/PCM(MeCN)}$ =

-2164.32967585

C	-2.786413000	-4.666636000	-0.974034000
C	-1.901137000	-3.589627000	-0.940378000
C	-2.439378000	-2.276380000	-0.988289000
C	-3.849809000	-2.114306000	-1.066804000
C	-4.751217000	-3.166717000	-1.100534000
C	-4.185017000	-4.458488000	-1.051858000
H	-4.851836000	-5.326018000	-1.074176000
H	-5.830498000	-3.008561000	-1.158342000
O	-4.163352000	-0.774009000	-1.092456000
C	-2.973877000	-0.086117000	-1.022185000
C	-1.847772000	-0.974580000	-0.955767000
Au	0.122413000	-0.533808000	-0.645220000
P	2.330825000	0.033504000	-0.115368000
C	3.617255000	-0.781556000	-1.122482000
C	3.335119000	-1.066808000	-2.473917000
C	4.316486000	-1.654441000	-3.282908000
C	5.575244000	-1.966825000	-2.745245000
C	5.854730000	-1.690768000	-1.397660000
C	4.879751000	-1.097886000	-0.583487000
H	5.096915000	-0.883929000	0.468009000
H	6.834692000	-1.938502000	-0.977421000
H	6.338829000	-2.431922000	-3.377068000
H	4.095742000	-1.875143000	-4.332058000
H	2.347242000	-0.830607000	-2.885484000

C	2.624615000	1.833727000	-0.277144000
C	3.745398000	2.349520000	-0.953140000
C	3.924705000	3.738100000	-1.049152000
C	2.993784000	4.612369000	-0.469967000
C	1.874904000	4.099358000	0.207428000
C	1.685319000	2.715500000	0.299159000
H	0.808638000	2.319250000	0.822321000
H	1.146532000	4.778456000	0.662083000
H	3.137413000	5.694856000	-0.546829000
H	4.796724000	4.135271000	-1.578405000
H	4.474925000	1.669709000	-1.403929000
C	2.718561000	-0.365250000	1.627170000
C	3.419621000	0.528757000	2.459399000
C	3.684619000	0.177515000	3.791086000
C	3.254340000	-1.060290000	4.293133000
C	2.556080000	-1.952555000	3.463837000
C	2.283533000	-1.607154000	2.134647000
H	1.721543000	-2.293566000	1.493211000
H	2.209989000	-2.914170000	3.855671000
H	3.458403000	-1.328103000	5.334881000
H	4.227182000	0.874765000	4.437440000
H	3.751814000	1.496105000	2.069958000
C	-3.072084000	1.341578000	-0.981213000
C	-1.907056000	2.159378000	-0.963608000
C	-2.014557000	3.540757000	-0.870208000
C	-3.278999000	4.170893000	-0.789928000
C	-4.440436000	3.356714000	-0.827625000
C	-4.348385000	1.975403000	-0.923616000
H	-5.250842000	1.360183000	-0.941012000
H	-5.426505000	3.829121000	-0.775683000
C	-3.392544000	5.661900000	-0.640858000
H	-2.492655000	6.176252000	-1.013650000
H	-3.506195000	5.921386000	0.429899000
H	-4.281391000	6.051616000	-1.164056000
H	-1.106386000	4.151272000	-0.858383000
H	-0.922253000	1.683914000	-1.024994000
H	-0.819256000	-3.735768000	-0.875595000
H	-2.402983000	-5.690176000	-0.936779000
C	-1.798265000	-0.786625000	2.342670000
N	-1.056536000	-2.030784000	2.328834000
N	-1.510116000	-3.127601000	2.234161000
C	-3.198442000	-0.760948000	2.201480000
C	-3.852547000	0.474160000	2.198853000
C	-3.115310000	1.664746000	2.332583000
C	-1.719294000	1.624367000	2.477944000
C	-1.051348000	0.393134000	2.485952000
H	0.034064000	0.325164000	2.602271000
H	-1.153164000	2.554454000	2.584961000
H	-3.632928000	2.628608000	2.314912000
H	-4.939670000	0.513962000	2.079506000
H	-3.744755000	-1.702340000	2.090315000

C	-3.257409000	-4.767874000	-0.019743000
C	-2.360175000	-3.692837000	-0.021835000
C	-2.875762000	-2.377770000	-0.020858000
C	-4.283932000	-2.205397000	-0.016383000
C	-5.198367000	-3.261287000	-0.014450000
C	-4.656866000	-4.556843000	-0.016263000
H	-5.331727000	-5.419348000	-0.014758000
H	-6.277822000	-3.084158000	-0.011419000
O	-4.588546000	-0.873902000	-0.014968000
C	-3.365706000	-0.183220000	-0.019298000
C	-2.281370000	-1.051224000	-0.021833000
Au	-0.279191000	-0.611362000	-0.009874000
P	1.983055000	-0.014848000	0.009151000
C	2.932268000	-0.565282000	-1.457110000
C	2.289717000	-0.534609000	-2.712315000
C	2.987494000	-0.913239000	-3.866316000
C	4.323726000	-1.335122000	-3.772978000
C	4.962172000	-1.376071000	-2.524185000
C	4.271280000	-0.991090000	-1.365819000
H	4.771345000	-1.023248000	-0.392648000
H	6.002479000	-1.708850000	-2.449205000
H	4.866038000	-1.637412000	-4.674786000
H	2.485423000	-0.886223000	-4.838752000
H	1.243262000	-0.215648000	-2.780025000
C	2.178901000	1.808148000	0.046748000
C	3.112544000	2.482291000	-0.762457000
C	3.214085000	3.880229000	-0.696335000
C	2.389541000	4.607751000	0.174642000
C	1.457911000	3.937302000	0.984493000
C	1.348321000	2.542765000	0.919155000
H	0.613851000	2.020250000	1.542406000
H	0.809553000	4.501835000	1.662289000
H	2.469160000	5.698692000	0.220611000
H	3.939654000	4.400886000	-1.329619000
H	3.755267000	1.917148000	-1.444743000
C	2.929719000	-0.625396000	1.452146000
C	3.922460000	0.154941000	2.075845000
C	4.641878000	-0.367385000	3.160500000
C	4.376185000	-1.665213000	3.623432000
C	3.384917000	-2.444089000	3.004740000
C	2.658397000	-1.925784000	1.924947000
H	1.875398000	-2.525564000	1.447080000
H	3.171830000	-3.454266000	3.368909000
H	4.938468000	-2.069018000	4.471679000
H	5.411532000	0.242224000	3.644852000
H	4.129628000	1.167772000	1.715580000
C	-3.497044000	1.272829000	-0.012600000
C	-2.363231000	2.118370000	-0.081666000
C	-2.495409000	3.506935000	-0.064578000
C	-3.763660000	4.123536000	0.017325000
C	-4.891512000	3.283202000	0.081002000

Au Complex **9**

$E_{\text{TPSS-D3(BJ)/def2-SVP/PCM(MeCN)}}$ =

-1824.88613520

$E_{\text{CAM-B3LYP-D3(BJ)/def2-SVPD/PCM(MeCN)}}$ =

-1823.81462986

Excited singlet state energy:

$E_{\text{CAM-B3LYP-D3(BJ)/def2-SVPD/PCM(MeCN)}}$ =

-1823.67190497

Triplet state energy:

$E_{\text{CAM-B3LYP-D3(BJ)/def2-SVPD/PCM(MeCN)}}$ =

-1823.71303643

C	-4.768153000	1.888146000	0.066847000	
H	-5.662529000	1.261552000	0.120900000	
H	-5.890470000	3.730207000	0.145114000	
C	-3.894338000	5.628769000	0.030729000	
H	-3.498029000	6.070293000	-0.902338000	
H	-3.318448000	6.070962000	0.864148000	
H	-4.946472000	5.939956000	0.136084000	
H	-1.593327000	4.127759000	-0.117193000	
H	-1.365855000	1.667270000	-0.149430000	
H	-1.277443000	-3.860609000	-0.024528000	
H	-2.873637000	-5.793788000	-0.020839000	
C	-0.570613000	0.000165000	0.000202000	PhN_2^+ $E_{\text{TPSS-D3(BJ)/def2-SVP/PCM(MeCN)}}$ = -340.768051002 $E_{\text{CAM-B3LYP-D3(BJ)/def2-SVPD/PCM(MeCN)}}$ = -340.507590903 Excited singlet state energy: $E_{\text{CAM-B3LYP-D3(BJ)/def2-SVPD/PCM(MeCN)}}$ = -340.352044276 Triplet state energy: $E_{\text{CAM-B3LYP-D3(BJ)/def2-SVPD/PCM(MeCN)}}$ = -340.394596969
N	-1.942441000	0.000150000	-0.000043000	
N	-3.062639000	-0.000079000	-0.000227000	
C	0.095335000	-1.250489000	0.000191000	
C	1.487128000	-1.226866000	-0.000064000	
C	2.177107000	-0.000181000	-0.000112000	
C	1.487385000	1.226711000	-0.000035000	
C	0.095626000	1.250629000	0.000192000	
H	-0.472422000	2.182767000	0.000291000	
H	2.039399000	2.169991000	-0.000267000	
H	3.270807000	-0.000288000	-0.000504000	
H	2.038896000	-2.170297000	-0.000096000	
H	-0.472930000	-2.182482000	0.000224000	

2.4) References

[1] A. B. Pangborn, M. A. Giardello, R. H. Grubbs, R. K. Rosen, F. J. Timmers, *Organometallics* **1996**, *15*, 1518-1520.

[2] a) G. R. Fulmer, A. J. M. Miller, N. H. Sherden, H. E. Gottlieb, A. Nudelman, B. M. Stoltz, J. E. Bercaw, K. I. Goldberg, *Organometallics* **2010**, *29*, 2176-2179; b) H. E. Gottlieb, V. Kotlyar, A. Nudelman, *J. Org. Chem.* **1997**, *62*, 7512-7515.

[3] C. C. Le, M. K. Wismer, Z.-C. Shi, R. Zhang, D. V. Conway, G. Li, P. Vachal, I. W. Davies, D. W. C. MacMillan, *ACS Central Science* **2017**, *3*, 647-653.

[4] M. G. Auzias, M. Neuburger, H. A. Wegner, *Synlett* **2010**, *2010*, 2443-2448.

[5] Z. Gonda, F. Béke, O. Tischler, M. Petró, Z. Novák, B. L. Tóth, *Eur. J. Org. Chem.* **2017**, *2017*, 2112-2117.

[6] Y. Nan, H. Miao, Z. Yang, *Org. Lett.* **2000**, *2*, 297-299.

[7] S. Cacchi, G. Fabrizi, L. Moro, *Synlett* **1998**, *1998*, 741-745.

[8] Y. Kondo, F. Shiga, N. Murata, T. Sakamoto, H. Yamanaka, *Tetrahedron* **1994**, *50*, 11803-11812.

[9] W. Erb, A. Hellal, M. Albini, J. Rouden, J. Blanchet, *Chem. Eur. J.* **2014**, *20*, 6608-6612.

[10] a) A. D. Lackner, A. Fürstner, *Angew. Chem. Int. Ed.* **2015**, *54*, 12814-12818; b) A. D. Lackner, A. Fürstner, *Angew. Chem.* **2015**, *127*, 13005-13009.

[11] Z. Y. Tang, Y. Zhang, T. Wang, W. Wang, *Synlett* **2010**, *2010*, 804-808.

[12] T. Yoshito, S. Tetsuya, M. Masahiro, N. Masakatsu, *Bull. Chem. Soc. Jpn.* **1999**, *72*, 2345-2350.

[13] W. Zeng, W. Wu, H. Jiang, L. Huang, Y. Sun, Z. Chen, X. Li, *Chem. Commun.* **2013**, *49*, 6611-6613.

[14] N. T. Hung, M. Hussain, I. Malik, A. Villinger, P. Langer, *Tetrahedron Lett.* **2010**, *51*, 2420-2422.

[15] Z. Xia, O. Khaled, V. Mouriès-Mansuy, C. Ollivier, L. Fensterbank, *J. Org. Chem.* **2016**, *81*, 7182-7190.

[16] A. S. K. Hashmi, T. D. Ramamurthi, F. Rominger, *Adv. Synth. Catal.* **2010**, *352*, 971-975.

[17] M. J. Frisch, G. W. Trucks, H. B. Schlegel, G. E. Scuseria, M. A. Robb, J. R. Cheeseman, G. Scalmani, V. Barone, G. A. Petersson, H. Nakatsuji, X. Li, M. Caricato, A. V. Marenich, J. Bloino, B. G. Janesko, R. Gomperts, B. Mennucci, H. P. Hratchian, J. V. Ortiz, A. F. Izmaylov, J. L. Sonnenberg, Williams, F. Ding, F. Lipparini, F. Egidi, J. Goings, B. Peng, A. Petrone, T. Henderson, D. Ranasinghe, V. G. Zakrzewski, J. Gao, N. Rega, G. Zheng, W. Liang, M. Hada, M. T. Ehara, K. , R. Fukuda, J. Hasegawa, M. Ishida, T. Nakajima, Y. Honda, O. Kitao, H. Nakai, T. Vreven, K. Throssell, J. A. Montgomery Jr., J. E. Peralta, F. Ogliaro, M. J. Bearpark, J. J. Heyd, E. N. Brothers, K. N. Kudin, V. N. Staroverov, T. A. Keith, R. Kobayashi, J. Normand, K. Raghavachari, A. P. Rendell, J. C. Burant, S. S. Iyengar, J. Tomasi, M. Cossi, J. M. Millam, M. Klene, C. Adamo, R. Cammi, J. W. Ochterski, R. L. Martin, K. Morokuma, O. Farkas, J. B. Foresman, andD. J. Fox, *Gaussian 16 Rev. B.01,* **2016**, Gaussian, Inc Wallingford, CT.

[18] J. Tao, J. P. Perdew, V. N. Staroverov, G. E. Scuseria, *Phys. Rev. Lett.* **2003**, *91*, 146401.

[19] a) S. Grimme, S. Ehrlich, L. Goerigk, *J. Comp. Chem.* **2011**, *32*, 1456-1465; b) S. Grimme, J. Antony, S. Ehrlich, H. Krieg, *J. Chem. Phys.* **2010**, *132*, 154104.

[20] F. Weigend, R. Ahlrichs, *Phys. Chem. Chem. Phys.* **2005**, *7*, 3297-3305.

[21] a) B. I. Dunlap, *J. Mol. Struct. (Theochem)* **2000**, *529*, 37-40; b) B. I. Dunlap, *J. Chem. Phys.* **1983**, *78*, 3140-3142.

[22] F. Weigend, *Phys. Chem. Chem. Phys.* **2006**, *8*, 1057-1065.

[23] a) M. E. Casida, C. Jamorski, K. C. Casida, D. R. Salahub, *J. Chem. Phys.* **1998**, *108*, 4439-4449; b) R. E. Stratmann, G. E. Scuseria, M. J. Frisch, *J. Chem. Phys.* **1998**, *109*, 8218-8224; c) R. Bauernschmitt, R. Ahlrichs, *Chem. Phys. Lett.* **1996**, *256*, 454-464.

[24] T. Yanai, D. Tew, N. Handy, *Chem. Phys. Lett.* **2004**, *393*, 51-57.

[25] D. Rappoport, F. Furche, *J. Chem. Phys.* **2010**, *133*, 134105.

[26] D. Andrae, U. Haussermann, M. Dolg, H. Stoll, H. Preuss, *Theor. Chim. Acta* **1990**, *77*, 123-141.

[27] a) G. Scalmani, M. J. Frisch, B. Mennucci, J. Tomasi, R. Cammi, V. Barone, *J. Chem. Phys.* **2006**, *124*, 094107; b) J. Tomasi, B. Mennucci, R. Cammi, *Chem. Rev.* **2005**, *105*, 2999-3094.

[28] a) B. P. Pritchard, D. Altarawy, B. Didier, T. D. Gibson, T. L. Windus, **2019**, *Manuscript in Preparation*; b) K. L. Schuchardt, B. T. Didier, T. Elsethagen, L. Sun, V. Gurumoorthi, J. Chase, J. Li, T. L. J. Windus, *Chem. Inf. Model.* **2007**, *47(3)*, 1045-1052; c) D. Feller, *J. Comp. Chem.* **1996**, *17(13)*, 1571-1586; d) https://www.basissetexchange.org/.

[29] https://www.chemcraftprog.com, Chemcraft - graphical software for visualization of quantum chemistry computations.

[30] a) P. Pracht, S. Grimme, **2019**, *Manuscript in preparation*; b) S. Grimme, *J. Chem. Theory Comput.* **2019**, *15*, 2847−2862; c) S. Grimme, C. Bannwarth, S. Dohm, A. Hansen, J. Pisarek, P. Pracht, J. Seibert, F. Neese, *Angew. Chem. Int. Ed.* **2017**, *56*, 14763–14769; d) S. Grimme, C. Bannwarth, S. Dohm, A. Hansen, J. Pisarek, P. Pracht, J. Seibert, F. Neese, *Angew. Chem.* **2017**, *129*, 14958-14964.

[31] C. Bannwarth, S. Ehlert, S. Grimme, *J. Chem. Theory Comput.* **2019**, *15 (3)*, 1652–1671.

[32] A. Dreuw, M. Head-Gordon, *Chem. Rev.* **2005**, *105*, 4009-4037.

[33] Bruker, *APEX, APEX2, SMART, SAINT, SAINT-Plus* **2007**, Bruker AXS Inc., Madison, Wisconsin, USA.

[34] L. Krause, R. Herbst-Irmer, G. M. Sheldrick, D. Stalke, *Journal of Applied Crystallography* **2015**, *48*, 3-10.

[35] G. Sheldrick, *Acta Crystallographica Section A* **2015**, *71*, 3-8.

[36] G. Sheldrick, *Acta Crystallographica Section C* **2015**, *71*, 3-8.

[37] Bruker, *APEX3, Saint and SADABS.* **2016**, Bruker AXS Inc., Madison, Wisconsin, USA.